Electrochemical methods for determining the mechanism of spontaneous adenosine release

Scott T. Lee

Forsyth, Montana

Bachelor of Science in Chemistry, Forensics Emphasis

Boise State University, 2012

A Dissertation presented to the Graduate Faculty

of the University of Virginia in Candidacy for the

Degree of Doctor of Philosophy

Department of Chemistry

University of Virginia, **May 2018**

. _____ .

. _____ .

. _____ .

. _____ .

. _____ .

Electrochemical methods for determining the mechanism of spontaneous adenosine release

Abstract:

Adenosine is a neuromodulator and neuroprotective agent in the central nervous system. Fast-scan cyclic voltammetry (FSCV) is a method of measuring rapid changes in adenosine concentration in real-time, making it useful for neuroscience research. Spontaneous, transient adenosine is a new form of adenosine signaling discovered in the brain that is unstimulated and has recently been characterized with FSCV. Research on adenosine transients has been focused on how it is formed, how it is regulated, what receptor it act at, and what function it serves. This thesis will cover the characterization of adenosine transients using FSCV to measure these events in brain slices.

The background of adenosine will be covered in Chapter 1. This chapter will cover the formation, regulation, and functions of adenosine in the brain. Electrochemical techniques used in neuroscience research will be covered as well, with an emphasis on FSCV, but covering biosensors and adenosine specific research in the FSCV field, particularly using brain slices as an experimental platform. Chapter 2 will address a known interferent of adenosine with FSCV, histamine. There are conflicting views on histamine oxidation and this chapter will explore the electrochemical behavior of histamine and investigate the oxidation product of histamine using spectroscopic techniques.

Chapters 3-4 will be focused on measuring adenosine transients in brain slices. Chapter 3 will demonstrate that brain slices are a viable method to measure transients and that the frequency, concentration, and duration of adenosine transients are comparable to what has been observed *in vivo*. This chapter will also investigate regional differences in adenosine transients by exploring the prefrontal cortex, thalamus, and hippocampus. Chapter 4 will investigate the release mechanism of adenosine transients, finding that transients are neither activity dependent nor are they released through pannexin 1 channels. Finally, Chapter 5 will present the final conclusions of this research and describe the future of transient adenosine research, with a focus on how determining the mechanism of transient release will allow for a more directed approach to researching the function of adenosine as a neuromodulator and neuroprotective agent.

This thesis provides deeper understanding into the characteristics of spontaneous, transient adenosine. It provides insight into circumventing problems with interferents such as histamine. It also demonstrates regional differences in rapid adenosine signaling and rules out some of the possible mechanisms of formation. A stronger understanding of spontaneous, transient adenosine will help researchers investigate alternative therapeutic approaches to neuromodulation and neuroprotection.

Table of Contents

List of Figures:

List of Tables

Acknowledgments:

I would like to thank Dr. B. Jill Venton for her years of patience, guidance, and good humor as I pursued my degree. I would also like to thank everyone in the Venton lab for their support and insight. I've learned so much from all of you. I'd like to specifically thank Dr. Chris Jacobs for training me on flow cell construction, Dr. Michael Nguyen for training me on the analysis of adenosine transients, and most significantly, Dr. Ashley Ross for training me on brain slice collection and the fundamentals of FSCV. Special thanks to those I collaborated with, Asa Nichols and Dr. Charles Machan for performing the histamine spectroscopy experiments, and Chris Medina and Dr. Kodi Ravichandran for providing the PANX1 KO mice.

I'd like to thank my friends and colleagues in Charlottesville for their constant encouragement and for being my go-to escape after a long week. Thanks to my friends back in Montana and Idaho for the support they've sent over the years. Most importantly, I'd like to thank my family. Thanks to my parents, Bob and Marlys Lee, for never letting me have it too easy, but supported me every step of the way. Thanks to my little sister, Kristina, who is a constant source of inspiration. I'm so proud of the heights to which you've risen. And thanks to my grandparents, especially my grandmother, Sharon Lee, the first chemist in the family. I believe solving logic problems and crossword puzzles with her when I was in elementary school is what initially fostered my analytical tendencies. I may not have pursued this career path had it not been for her.

Chapter 1

Introduction

I can do all this through him who gives me strength.

– Philippians 4:13

1.1 Adenosine overview

Adenosine is a purine nucleoside and breakdown product of ATP. As such, adenosine is ubiquitous through the body and found anywhere that ATP is used as molecular energy currency. In the brain, adenosine serves primarily as a neuromodulatory agent and changes in extracellular adenosine concentration have been measured over the course of several minutes to hours.[1–3] Electrochemical techniques have allowed for real-time measurements of adenosine to detect fast changes in concentration for stimulated release.[4–6] Recently, a spontaneous, transient form of adenosine release has been discovered in spinal column slices and characterized the most in the rat brain *in vivo*.[7–9] Measuring these transients in slices complements the work performed *in vivo* by overcoming pharmacological obstacles such as toxicity and blood-brain barrier permeability. This allows for experiments that wouldn't normally be possible with *in vivo* test subjects and permits the experimenter more precision in pharmacological dosing and electrode placement. A full understanding of the mechanisms of these adenosine transients can help us understand and potentially treat acute brain conditions such as ischemia, hypoxia, or epilepsy.[10,11]

1.1.1 Adenosine in the central nervous system

Adenosine serves two primary roles in the central nervous system, neuroprotection and neuromodulation. As a neuromodulator, adenosine has been investigated in a multitude of physiological and psychological disorders. Neuromodulation of dopamine draws connections to Parkinson's disease, schizophrenia, and addiction.[12–14]

Similarly, adenosine modulation of glutamate has been investigated in combatting excitotoxic damage and modulation of serotonin links adenosine to depression.[15,16] Adenosine can also bind to A_{2A} receptors on blood vessels, which leads to vasodilation. The increase in blood flow, as well as the prevention of glutamatergic overstimulation are the 2 primary actions of adenosine as a neuroprotective agent. Designing pharmacological approaches to manipulating the neuromodulatory and neuroprotective activity of adenosine require an understanding of how adenosine is generated in the extracellular space, where it can bind to, and how it can be removed from the extracellular space.

1.1.1.1 Adenosine formation

Adenosine can come from multiple sources, both intracellularly and extracellularly. In both cases, adenosine is primarily created from the breakdown of adenosine triphosphate (ATP). Intracellularly, ATP can break down to ADP, AMP, or cAMP, each of which can be further metabolized to adenosine.[17,18] Adenosine can then be transported out of the cell through exocytosis, nucleoside transporters, and possibly through connexins and pannexins. Connexins are channel proteins that can form a gap junction, creating a channel directly connecting the intracellular spaces of different cells.[19] Pannexin channels are similarly structured proteins that transport ATP to the extracellular space. While it is currently unknown if adenosine can path through pannexin channels, ATP flux through these channels has been heavily studied.[20]

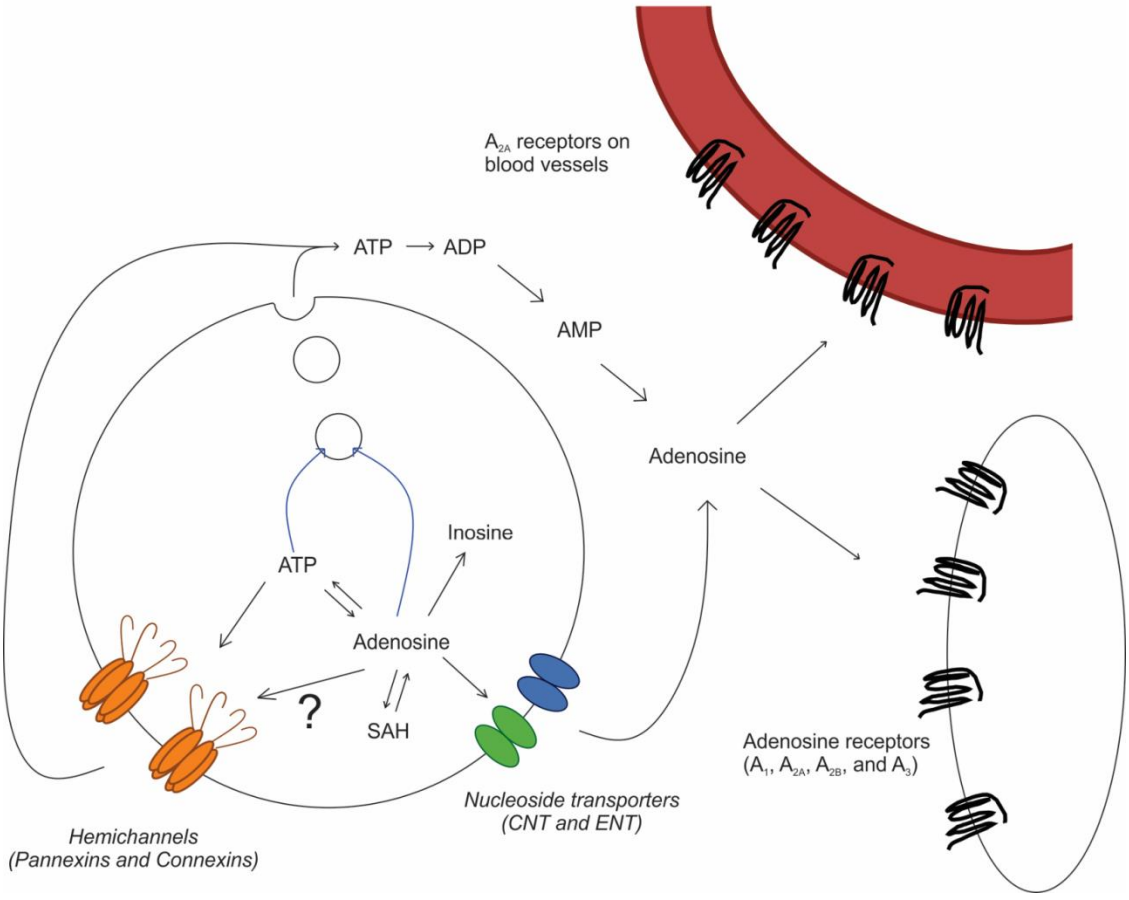

Figure 1.1 Adenosine formation Adenosine can be generated through several pathways and can act at adenosine receptors on different cells as well as A_2 receptors on blood vessels

In the extracellular space, ATP rapidly breaks down to adenosine through a 2-step enzymatic process. First, ATP is broken down to AMP through ecto-ATPase and is subsequently metabolized by ecto-5'-nucleotidase (NT5E) and prostatic acid phosphatase (PAP).[7] This metabolic pathway is very fast, so ATP doesn't typically last long in the extracellular space before being broken down to adenosine. The speed of this breakdown process is necessary as well because ATP is known to have damaging effects in the extracellular space whereas adenosine has more protective functions.[21]

1.1.1.2 Adenosine receptors

There are four different adenosine receptors throughout the body, A_1, A_{2A}, A_{2B}, and A_3. They are G-protein coupled receptors that regulate the generation of intracellular cAMP, thereby indirectly impacting cell excitability. A_1 and A_3 are inhibitory receptors, downregulating cAMP formation, whereas A_{2A} and A_{2B} are excitatory.[12,22] A_1 is the most heavily expressed receptor in the brain with moderate levels of A_{2A} expression. A_{2B} and A_3 are sparsely expressed and only in a few brain regions. A_{2A} receptors are also expressed on blood vessels and cause vasodilation when activated.[23] Adenosine has the strongest affinity for A_1 receptors with a dissociation constant (K_d) of 73 nM whereas it has a lower affinity for A_{2A} at 150 nM.[24] A_3 receptors are weakly expressed in the brain and are more heavily expressed in the spleen, lungs, and reproductive organs of the rat.[25]

1.1.1.3 Adenosine transporters

There are two classes of transporters capable of regulating adenosine reuptake. Concentrative nucleoside transporters (CNTs) uptake adenosine and the other nucleosides using cation gradients.[26] Equilibrative nucleoside transporters (ENTs) are energy dependent, bidirectional transporters. Adenosine is known to be transported by CNTs 1-3 and ENTs 1-4 with ENT4 acting as the only transporter specific to adenosine, although with a low affinity (0.78 mM).[26] ENT-mediated adenosine release is a Ca^{2+} dependent process.[27] Inhibition of ENT1 and ENT2 has been shown to decrease the amount of electrically stimulated adenosine release by 40%.[28]

1.1.1.4 Pannexin channels

A more recently discovered class of channels are pannexin channels. They are related to gap junction proteins, like connexin channels, but only connect the intracellular space to the extracellular space as opposed. There are 3 different pannexin channels (PANX1-3), the most prevalent of which is PANX1, though PANX2 is expressed almost exclusively in the brain.[29,30] PANX3 has only been found if a few types of tissue, including bone, skin, and skeletal muscle.[31] There are many different molecules that may pass through pannexin channels, the list of which continues to grow.[32] They are permeable to cations, anions, and small molecules, though the most heavily studied molecule of interest with respect to pannexin permeability is ATP.[20] ATP is of particular interest as pannexin channels open during ischemia and epileptic activity.[33,34]

Pannexin channels are activated by several different mechanisms including mechanical stimulation, high levels of extracellular potassium or intracellular calcium, or upstream signaling pathways such as NMDA receptors as a component of the apoptosis cellular pathway. There are still many gaps in the knowledge of how exactly the signaling pathways are connected. One theory is that NMDA signals NO productions during ischemia which can open pannexin channels at elevated levels.[35] Another view is that caspases are signaled by NMDAR activation which subsequently cleave the C-terminal tail of the subunits of hexameric pannexin channels.[36] This leads to a conformational change to irreversibly open the pannexin channels. It has been shown that at least two of the C-terminal tails must be cleaved in order to induce an outward flux of ATP and magnitude of that flux increases with an increased number of cleaved tails.[32] However, there are

conflicting views both on how NO functions at pannexin channels and caspase efficacy at maintaining anoxic polarization.[37,38]

Another theory is that NMDARs signal Src family kinases to phosphorylate pannexins into an active state.[39] One possible reason for the confusion and contradictory results regarding the NMDAR and pannexin pathways, beyond the complex array of possible signaling molecules and proteins, is that there is a level of redundancy in neurons for pannexin channels. A PANX1 knockout was unable to prevent neural damage during a stroke in mice and that the knockout of both PANX1 and PANX2 was required to see a significant decrease in cell death.[40] The permeability of pannexins and other hemichannels to ATP make it an intriguing prospect when investigating the mechanisms of adenosine release.

1.1.2 Adenosine function

As a breakdown product of ATP, adenosine is ubiquitous in the body and serves a variety of roles. In the central nervous system, it serves two primary roles, neuromodulation and neuroprotection.

1.1.2.1 Neuromodulation

Adenosine has a major role in modulating the release of other neurotransmitters as well as self-regulating its own release. This is primarily performed through A_1 receptors in the brain as it is the most heavily expressed in the brain and has the strongest affinity for adenosine of the four adenosine receptors. When adenosine binds to A_1 receptors, either presynaptically or postsynaptically, the G-protein signals adenylyl cyclase to shut

off, decreasing the cell excitability.[41] This leads to decreased neurotransmitter release and has shown to be able to impact dopamine[42], glutamate[43], and serotonin.[16]

1.1.2.2 Neuroprotection

The neuroprotective role of adenosine largely falls hand in hand with its neuromodulatory role. Glutamate is an excitatory neurotransmitter; so prolonged, high levels of extracellular glutamate can overstimulate neurons, causing a high influx of Ca^{2+}.[44] This can, in turn, lead to undesirable translocation and activation of intracellular proteins, including kinases and proteases that cause irreparable cell damage and eventually, cell death. Adenosine activation of A_1 receptors can inhibit glutamatergic release and combat this effect.

Adenosine also plays a protective role in its modulation of blood flow. Adenosine can bind to A_{2A} receptors on blood vessels to cause vasodilation, allowing for easier oxygen delivery to the brain.[23] This makes adenosine an interesting target in studying hypoxic and ischemic events in the brain, including stroke.[10] Knockouts of A_1 receptors has also been shown to enhance microglial response implying a neuroinflammatory role for adenosine activity as well.[45] Many of these pathways are well understood over long time courses, but more rapid, transient forms of adenosine signaling have not been as well characterized, leaving questions open as to how impactful brief adenosine signals can be relative to their more tonic counterparts.

1.2 Electrochemical detection of adenosine

There are two primary electrochemical techniques used to detect and quantify adenosine in tissue: fast-scan cyclic voltammetry (FSCV) and amperometry with adenosine specific biosensors. FSCV is a technique that uses a carbon-fiber microelectrode (CMFE) as a sensor to oxidize and reduce electroactive molecules. Unlike traditional cyclic voltammetry that operates with low mV/s to low V/s scan rates, FSCV uses scan rates of a few hundred V/s to as high as 1000 V/s. Between the fast scan rate and the small size of the CFMEs (7 µm diameter, 50-150 µm in length), it takes very little time to charge the capacitive current of the electrode. This large background charging current of a few hundred nAs is very stable, so it may be subtracted out leaving noise levels typically less than 1 nA. As such, this technique does not generally allow for basal level concentration determination, just the measurement of fast changes in the concentration of the analyte in question. However, an adaptation of FSCV called fast-scan controlled adsorption voltammetry (FSCAV) has been developed to find basal level concentrations.[46]

Amperometric detection differs from cyclic voltammetry in that a single potential is held instead of ramping the potential up and down. Any electroactive analyte with an oxidation potential below the chosen potential will oxidize resulting in a current signal. Similar to FSCV, this is useful for real-time, rapid changes in analyte concentration. However, adenosine has a very high oxidation potential (1.3 V vs Ag/AgCl) so the high potential required would make this technique very non-specific.[4] This can be compensated for by using biosensors specific to adenosine. The typical components of an adenosine biosensor include an enzyme cascade of adenosine deaminase, purine

nucleoside phosphorylase, and xanthine oxidase to breakdown adenosine, releasing H_2O_2 in the process.[47] H_2O_2 will then diffuse to the electrode for detection through a polymer layer which repels interfering analytes.

1.2.1 Voltammetry of adenosine

Adenosine has 3 oxidation processes.[4] The first happens at a very high potential, 1.3 V vs Ag/AgCl, and is irreversible. This is a 2-electron process and reduces a water molecule to provide an oxygen atom for the creation of a carbonyl at the C^2 position of the purine structure. This is an irreversible reaction and releases 2 H^+, making the oxidation process pH dependent as well. Once the primary oxidation product has been created, the energy barrier for an oxidation at adenosine's C^8 position drops enough to allow a potential of 0.9 V to oxidize adenosine again. This is the secondary oxidation process for adenosine and similarly requires a water molecule to provide the oxygen to create a carbonyl. Like the primary oxidation, the secondary oxidation is also a 2-electron process that releases 2 H^+ and is irreversible. Both of these oxidation processes leave an

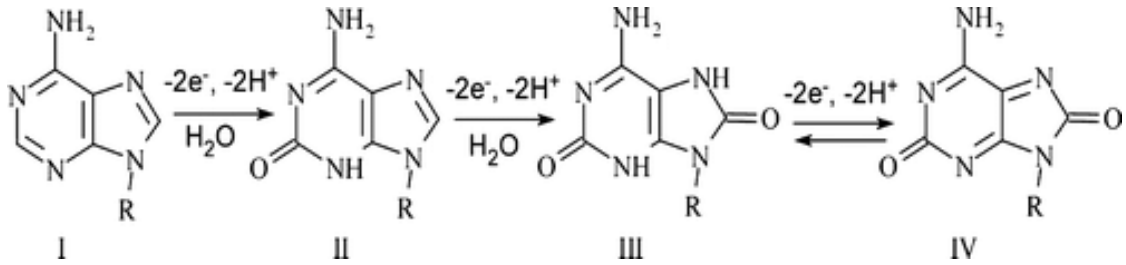

Figure 1.2 3-step oxidation mechanism for adenosine. While the first two steps are irreversible, though seldom detected with FSCV, is reversible. R is a ribose unit. (Reprinted from Swamy and Venton, 2007)

adjacent nitrogen protonated and in the sp^3 state with a double bond connecting C^5 and C^6 of the purine.

In order to regain aromaticity, a tertiary oxidation process may occur after the secondary product has been created. This oxidation occurs at 0.2 V, deprotonating the nitrogen atoms in the 3 and 7 positions and removing 2 more electrons. The electron pair from one of the deprotonated nitrogen atoms push into the ring structure, pushing the double bond in the center of the purine to the other deprotonated nitrogen, forming a more conjugated structure. This oxidation is a reversible process.

1.2.1.1 Fast-scan cyclic voltammetry (FSCV) of adenosine with the triangle waveform

Fast-scan cyclic voltammetry (FSCV) is an electrochemical technique performed with CFMEs. CFMEs are 7 μm in diameter and are usually cut to around 100 μm in length for adenosine detection. The typical waveform used for adenosine detection with FSCV uses a holding potential of -0.4 V. A negative holding potential favors adsorption of neuromolecules as many of them are positively charged.[48] The potential then ramps up at 400 V/s to a switching potential of 1.45V and back down the holding potential at the same rate. The entire scan takes 9.25 ms and the potential is then held at -0.4 V to allow additional adenosine to adsorb to the surface for the next scan. The fast scan rate at such a small electrode causes a large, but stable background current that can be subtracted out from the signal. The necessity of background subtraction makes FSCV very powerful at detecting fast changes in concentration of electroactive analytes, but poor at determining basal level concentrations.

Because of the rapid speed of the voltammetric sweep, oxidation peaks tend to shift from their literature values by about 1 millisecond (0.4 V at 400V/s). As such, the primary oxidation peak for adenosine shifts from 1.3 V on the anodic scan to about 1.35V on the cathodic scan. The oxidation peak would likely be even later in the cathodic scan if there was still a high enough potential at that point in time to continue to oxidize the

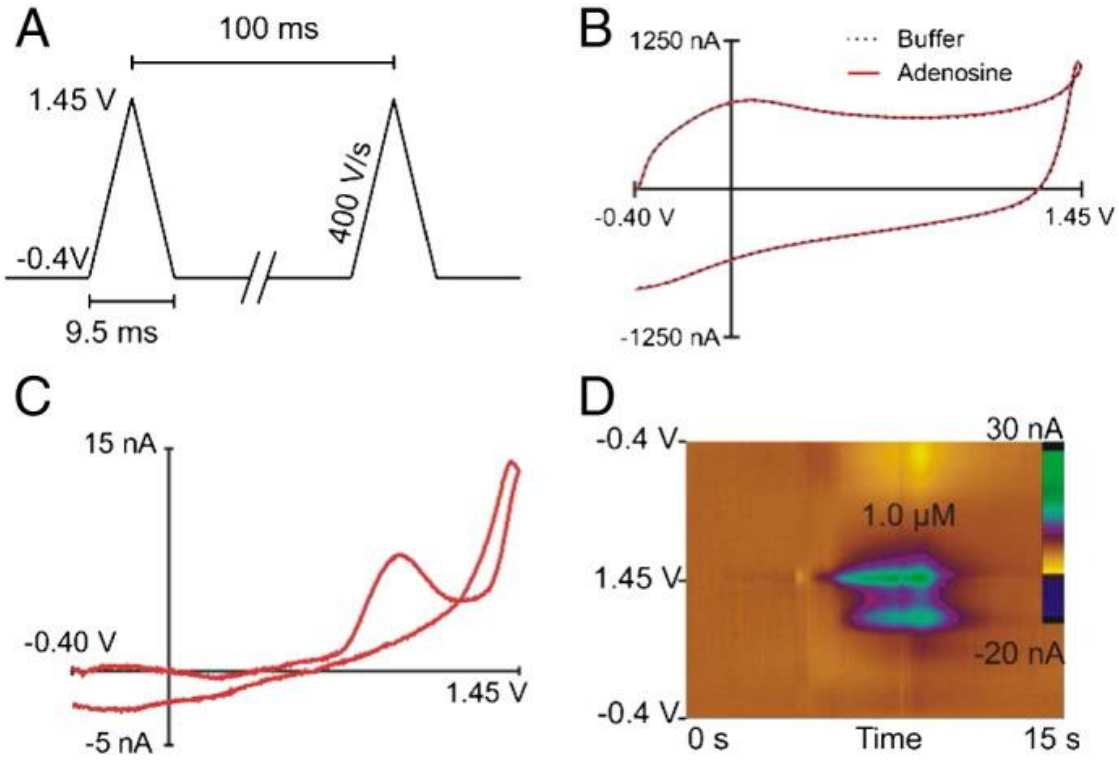

Figure 1.3 FSCV of adenosine (**A**) Waveform for adenosine detection. The potential is held at -0.4 V. ramped up to 1.45 V at 400 V/s and back to -0.4 V with a frequency of 10 Hz. (**B**) The wavefore generates a large, stable background that can be subtracted out to give the (**C**) cyclic voltammogram of adenosine. (**D**) These cyclic voltammograms are plotted as a function of time using a 3D false color plot where time is on the x-axis, potential on the y-axis, and the current in false color. This shows a 5 second plug of 1.0 µM adenosine with the primary peak in the center of the plot and the secondary peak just below it. (Reprinted from Nguyen and Venton, 2015)

adenosine. Similarly, the secondary peak shifts up to 1.2 V, but stays on the anodic side of the scan. Because the primary product is required to undergo the secondary oxidation, the secondary peak won't appear in the first scan with adenosine but will begin to appear in subsequent scans.

The secondary peak is always smaller than the primary peak, about 40% the height. The tertiary oxidation peak is typically only noticeable at higher concentrations. Between scans there is a 90 ms hold time to allow more adenosine to adsorb to the surface of the electrode as a sort of pre-concentration process. During this time a large portion of the oxidation product will desorb from the electrode surface, resulting in the small relative signal from the secondary oxidation process on the subsequent scan.

1.2.1.2 Co-detection of adenosine and O_2 with FSCV

The activity of adenosine as a neuroprotective agent can be investigated by using an altered waveform that can measure both adenosine changes and O_2 changes in tandem. Elevations in extracellular O_2 levels, either long term or acute, are indicative of vasodilation and reflect a physiological response to protect the tissue. O_2 can be reduced to H_2O_2 at -1.2 V with FSCV.[49–51] Co-detection can then be achieved by ramping up to 1.45 V first to oxidize adenosine, then down to -1.4 V to reduce O_2 and back to the holding potential of -0.4 V. This ramp is done at 450 V/s to compensate for the decreased time spent at the holding potential due to the longer duration of this waveform.[52] Increases in adenosine in the extracellular space can cause vasodilation of blood vessels through A_{2A}

receptor activation as described earlier. This process can be characterized by the subsequent increase in O_2 available in the extracellular space.[52]

1.2.1.3 Differentiation of adenosine, ATP, and H_2O_2 with the sawhorse waveform

Several compounds give very similar voltammetric signals to adenosine, notably, ATP, H_2O_2, and histamine. Each of these has its largest oxidation peak at about the same potential as adenosine, but there are a few differences in their electrochemical activity. CFMEs are much less sensitive to ATP than adenosine, so the oxidation peak for ATP tends to be three times smaller.[53] This is even more dramatic with H_2O_2 because of the diffusion controlled nature of peroxide, so CFMEs are about four times more sensitive to adenosine than H_2O_2.[54] Additionally, H_2O_2 does not have a secondary peak like adenosine, so at high concentrations, H_2O_2 is easier to differentiate. Histamine gives both a primary and secondary peak like adenosine and ATP, but the primary oxidation occurs at a

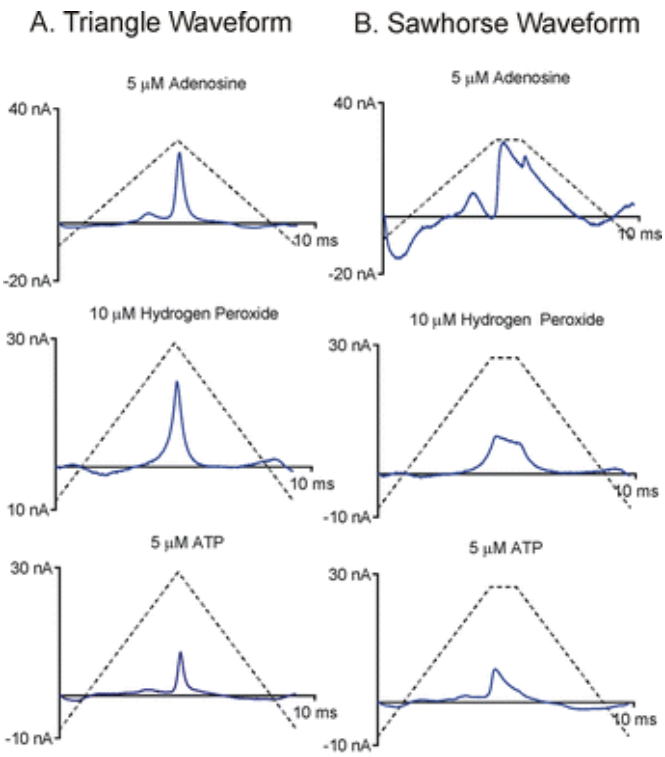

Figure 1.4 Sawhorse waveform can differentiate adenosine, ATP, and H_2O_2. Whereas the primary peaks look similar with the triangle waveform (left), the sawhorse waveform (right) creates an extra shoulder during the primary oxidation of adenosine. (Reprinted from Ross and Venton, 2014)

slightly lower potential for histamine, closer to 1.25 V.[55] But this slight difference still makes it very hard to quantitatively separate the signals of adenosine and histamine.

Using a sawhorse waveform can differentiate adenosine, ATP, and H_2O_2.[54] A sawhorse waveform is only slightly different from the triangle waveform in that there is a 1 ms hold at the switching potential (here, 1.35V). This waveform gives adenosine, ATP, and H_2O_2 all slightly different peak shapes such that they can be differentiated by principal components analysis (PCA). The unique characteristic of the CV of adenosine is an extra shoulder near the end of the oxidation peak just as the cathodic sweep begins. While the CVs of both ATP and H_2O_2 both lack this characteristic, histamine also exhibits this shoulder, so it must be differentiated by alternative means.

1.2.1.4 Histamine interference of adenosine detection with FSCV

Histamine oxidation has been separated out from adenosine oxidation with FSCV before. Chang, *et al.* demonstrated that only scanning up to a potential of 1.3 V will give a strong signal for histamine without oxidizing adenosine.[56] While this is useful for histamine analysis and characterization, it doesn't allow for simultaneous adenosine analysis. The Hashemi group has presented an alternative approach to histamine detection with FSCV. Using an altered waveform that holds at a potential of -0.5 V vs Ag/AgCl, scans down to -0.7 V and up to 1.1 V at 600 V/s before scanning back down to the -0.5 V holding potential. This creates a peak at 0.3 V vs Ag/AgCl with a limit of detection of 1 μM.[57] They attribute the classical oxidation peak of 1.25 V to non-Faradaic

adsorption processes. While they clearly prove pharmacologically that the peak at 0.3 V is due to histamine, they have not been able to prove this mechanistic hypothesis.

In fact, little is known about what the actual oxidation process of histamine even is. There are some theories as to the identity of the histamine oxidation product including an electropolymerization process known for imidazoles.[58] However, due to the known secondary reaction of adenosine, which takes place on the imidazole ring of adenosine, it is likely that histamine undergoes a similar process of carbonyl generation between the two nitrogens.[4,59]

1.2.2 Adenosine biosensors

Adenosine biosensors have the advantage of analyte specificity over CFMEs used in FSCV. The enzyme cascade and polymer layers insure that only adenosine and the subsequent breakdown products of adenosine metabolism (inosine and H_2O_2) can act as interferents.[47] Histamine is no longer an interferent as there is no way for histamine to generate H_2O_2 near the surface of the electrode. However, ATP can be an interferent at these biosensors due the rapid pace at which it can be broken down to adenosine in the extracellular space. This can be combatted by application of sodium polyoxotungstate (POM-1, 100 μM)[60] which inhibits NTPDase's, and therefore prevents ATP, ADP, and AMP from breaking down to adenosine.

Nicholas Dale and Bruno Frenguelli are the primary researchers who work on the design and application of adenosine biosensors. Their original 'Mk-1' biosensor was effective, but had a large diameter (~500 μm).[61] Concerns of tissue damage subsequently

prompted them to improve upon the design to decrease that diameter to less than 100 µm with their 'Mk-2' biosensor.[47]

1.2.3 Rapid adenosine release mechanisms

There are three forms of adenosine release that can be measured in real-time in the brain with FSCV. Adenosine can be electrically stimulated, mechanically stimulated, or it can release spontaneously, without a controlled stimulus provided by the experimenter.

1.2.3.1 Electrical stimulation of adenosine

Adenosine can be evoked by electrical stimulation in the striatum[5] as well as the caudate putamen, nucleus accumbens, hippocampus, and cortex.[62] This adenosine is released using a 300 µA biphasic stimulation, using five 4-ms pulses at a rate of 60 Hz. The mechanism of formation for this form of adenosine can be attributed to activity dependence and comes from both extracellular ATP breakdown and from glutamate receptor activation. However, this glutamate receptor dependence varies between brain region and species.[63,64]

1.2.3.2 Mechanical stimulation of adenosine

Adenosine can also be released by applying mechanical stress or strain on tissue. When the CFME is already inserted in the tissue, lowering the electrode further into the tissue (50 µm) causes a transient spike in adenosine that takes two seconds to two minutes to clear back to baseline.[6] This can also be evoked by using an auxiliary probe such as a pulled glass pipette to prod the tissue near the electrode surface. This technique ensures the signal is not due to the electrode being in a slightly different environment.

Like electrically stimulated adenosine release, this was also found to be an activity dependent form of release as well as originating from the breakdown of extracellular ATP.

1.2.3.3 Spontaneous transient adenosine

Spontaneous, transient adenosine was first found by Zylka and Wightman in mouse spinal cord slices.[7] They occurred at irregular intervals, averaging about one every 3 minutes, lasted less than 2 seconds each, and had an average peak concentration around 500 nM. Unlike with electrical or mechanical stimulation, spontaneous transient adenosine occurs without any controlled source of stimulus by the experimenter. An electrode is inserted into the tissue and the events happen sporadically. Later, transients were discovered in the anesthetized rat brain *in vivo* in both the caudate-putamen and the prefrontal cortex (PFC).[8] Whereas transient adenosine events were more frequent in the brain than in spinal cord slices, they also had smaller average event concentrations, 170 nM in the caudate-putamen and 190 nM in the PFC.

Zylka found in the spinal cord slices that transients appeared to originate from hydrolyzed nucleotides as lower frequencies of transients were observed in NT5E and PAP knockout mice. There was also a lower frequency observed in wild-type mice when slices were deprived of Ca^{2+} suggesting an activity dependent form of release. Nguyen et. al. found that transients were also A_1 receptor dependent, increasing in frequency when the A_1 pathway was inhibited with 8-cyclopentyl-1,3-dipropylxanthine (DPCPX). Transient adenosine found *in vivo* was also found to be cleared from the extracellular space by a combination of mechanisms.[9] ENT1 was inhibited with nitrobenzylthioinosine (NBTI),

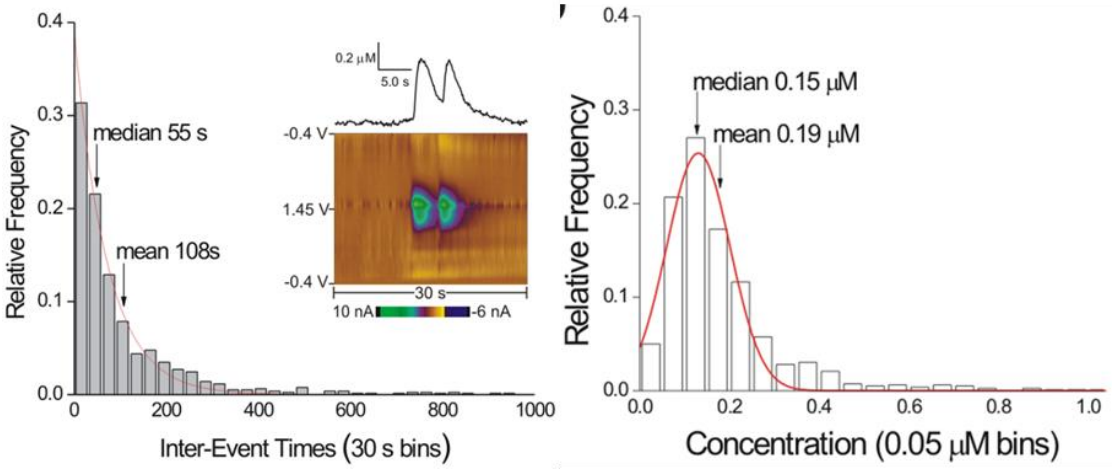

Figure 1.5: Spontaneous, transient adenosine events in the prefrontal cortex occurred on average more than once every two minutes (left) and had an average concentration of 190 nM. (Reprinted from Nguyen, et. al. 2014)

adenosine kinase was inhibited with 5-(3-bromophenyl)-7-[6-(4-morpholinyl)-3-pyrido[2,3-d]byrimidin-4-amine dihydrochloride (ABT-702), and adenosine deaminase was inhibited with erythro-9-(2-hydroxy-3-nonyl)adenine (EHNA). Inhibition of the transporter and both metabolic enzymes each showed a significant decrease in the decay rate of adenosine transients suggestion each of these is responsible for clearing transients. Interestingly, there was not an additive effect of these three pathways when inhibited in unison and clearance was still fast enough to suggest some other source of clearance outside of just diffusion.

Because basal adenosine changes are associate with both neuroprotective and neuromodulatory activity, spontaneous adenosine is believed to have a similar role in a more acute manner. Spontaneous adenosine transients correlated strongly with brief increases in extracellular oxygen.[65] Adenosine can bind to A_{2A} receptors on blood vessels,

causing vasodilation and increasing the availability of oxygen to the brain. The temporal correlation of adenosine transients with oxygen transients suggests a neuroprotective action of transient adenosine. In brain slices, exogenously puffing a solution of adenosine to simulate an adenosine transient decreased the amount of stimulated dopamine released by 54%, as long as the electrical stimulation occurred within a few seconds of the adenosine event.[42] The fact that an adenosine transient can modulate a dopamine event that occurs two seconds later but not modulate a dopamine event ten seconds later indicates an acute neuromodulatory role for spontaneous, transient adenosine.

1.3 Adenosine pathways modeled in brain slices

As described before, there are a multitude of pathways by which adenosine can end up in the extracellular space. It can be released by exocytosis, it can be transported by ENTs and CNTs, and though it is currently unknown, it may be able to pass through hemichannels such as pannexins or connexins.[63,66] In each of these pathways, adenosine could actually be released as ATP that is initially expelled from the cell, then rapidly metabolized to adenosine by ectonucleotidases.[67–69] Studying adenosine signaling can be complicated even further when more than one of these pathways are contributing to the release or accumulation of adenosine or ATP.[70] Brain slices make a good model for helping to elucidate these pathways. Precise concentrations of drugs to treat these pathways can be delivered directly to the tissue without worrying about blood-brain barrier permeability or drug metabolism prior to reaching the brain. In addition, the wide variety

of pathways that could be tested in tandem or in series easier as a simple washout step, a technique which is not feasible *in vivo*.

1.3.1 Adenosine measurements in hypoxia and ischemia

As stated before, analysis of adenosine and ATP with biosensors has been largely pioneered by Nicholas Dale and Bruno Frenguelli. They are interested in the dynamics of purine release in the brain under harmful conditions such as hypoxia or glutamate excitotoxicity. The first iteration of the biosensors, referred to as the 'Mk-1', was too large to insert into the tissue.[71] Therefore, only surface measurements were made with that model. The design was later improved with the 'Mk-2' which consists of the same enzyme cascade (adenosine deaminase, nucleoside phosphorylase, and xanthine oxidase) on platinum and platinum/iridium (90/10) wires.[47] The final diameter of the 'Mk-2' is less than 50 μm. In their studies, they demonstrated that adenosine release occurs simultaneously with the depression of glutamatergic signaling in the hippocampus of the rat.[10] Moreover, adenosine release decreases after repeated hypoxic events are imposed on the tissue.[61] An intriguing finding was the generation of a large increase in adenosine release upon returning hypoxic tissue back to a normoxic environment. This phenomenon, referred to as the post-hypoxic purine efflux (PPE), reaches a peak adenosine concentration of 22.7 ± 1.6 μM.[72,73] The source of the adenosine measured during the PPE was not from ATP metabolism, suggesting direct release of adenosine itself, though ATP also gets released to a lesser degree and later than adenosine. Additionally, this PPE was independent of glutamate receptor activation as purine release

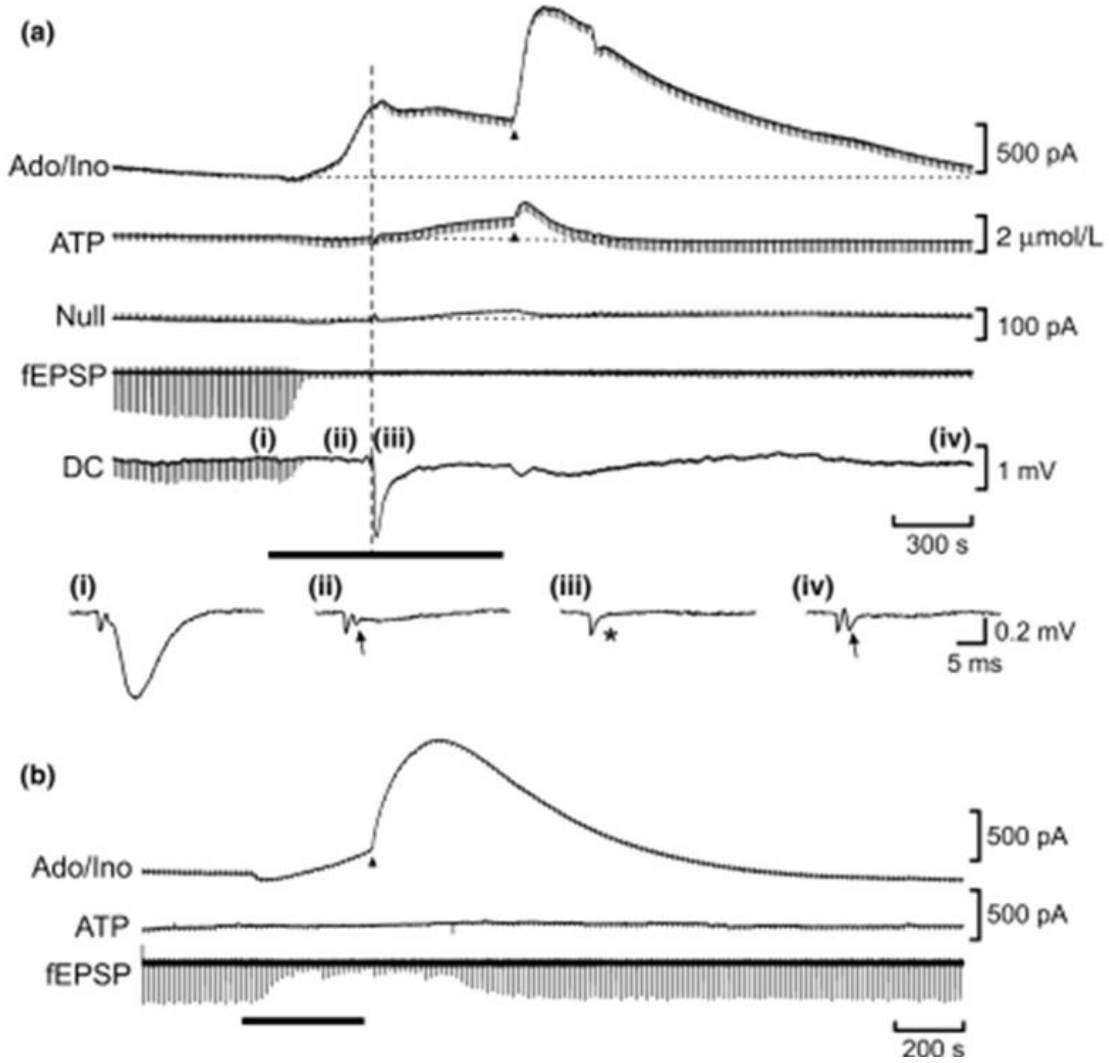

Figure 1.6: ATP and adenosine release during ischemia (**a**) Imposing an ischemic environment (black bar) to rat hippocampal slices causes a rise in adenosine signal. Once adenosine signal plateaus, the ATP signal begins to increase at the same time that the anoxic depolarization occurs as indicated by the extracellular DC trace (dotted line). Reoxygenation induces the PPE (black triangle). (**b**) A shorter ischemic event that doesn't trigger anoxic depolarization gives no ATP signal, even during the PPE. (Reprinted from Frenguelli, et al. 2007)

did not decrease in the presence of glutamate antagonist, kynurenic acid.[73] They followed up by studying the changes of adenosine and ATP during hypoxic anoxic depolarization.[73]

Within a couple minutes of hypoxic onset, adenosine signal began to rise to a maximum of

8.9 µM before plateauing off into a very slow decline. Within a minute of reoxygenation, the PPE occurred, indicated by the adenosine signal spiking dramatically to 22.7 µM before gradually returning to baseline over the next 20 minutes. ATP, however, only began to rise during the spreading depression once the adenosine signal plateaued and rose very gradually to a maximum of 0.7 µM. Reoxygenation saw ATP also spike up quickly as a part of the PPE, though only to 1.8 µM, and rapidly returned to baseline in about 5 minutes. Shorter periods of ischemia induced an adenosine signal with no discernable ATP signal. These differences in time course as well as the lack of correlation between ATP and adenosine signals under different pharmacological treatments indicate that that the adenosine release under hypoxic spreading depression does not result from the breakdown ATP in the extracellular space. For instance, ecto-ATPases were inhibited with ARL 67156 and while this decreased the basal concentration of adenosine, it made no impact on the net adenosine release during hypoxia.[74] It also gave no indication that ATP was present during the early stage of hypoxia where only adenosine had been seen under control conditions.

Although the exact mechanism of release of adenosine and ATP during ischemic events were not determined, they did rule out gap junction hemichannels by treatment with carbenoxolone, activity dependence by treatment with TTX and Ca^{2+}-free artificial cerebral spinal fluid (aCSF), and ENT1 and ENT2 by treatment with inhibitors dipyridamole and NBTI. Though the mechanism was unsolved by them, there is evidence that astrocytes are the primary contributors to adenosine release during hypoxic conditions.[75]

1.3.2 Measuring adenosine in epileptic slices

Epileptic events in hippocampal slices, as well as seizures *in vivo,* have been shown to be triggered by Group I metabotropic glutamate receptor (mGluR) activation.[76–78] Adenosine is responsible for modulating glutamate activity and can dampen the severity of seizures.[79] (*S*)-3,5-Dihydroxyphenylglycine (DHPG) can activate mGluRs, causing neurons to undergo burst firing.[34] This is followed by a long lasting rise in extracellular adenosine concentration that activates A_1 receptors to inhibit this glutamateric signaling.

1.4 The field of rapid adenosine signaling and remaining uncertainties

With the various mechanisms of adenosine release, reuptake, binding sites, and both upstream and downstream regulation thereof, the pathway of adenosine signaling is incredibly convoluted. This is only exacerbated by the evidence that multiple routes through this pathway may be taken in tandem, resulting in some level of redundancy. For instance, electrically stimulated adenosine release was found to be abolished by TTX, indicating activity dependence, but could still be triggered by glutamate application, even in the presence of TTX.[28] Whereas some of this signal was due to direct adenosine release through ENTs, a portion was from the rapid metabolism of ATP that had been released via exocytosis.

The capabilities of real-time electrochemical techniques, such as FSCV and amperometric biosensors, have helped elucidate the mechanisms of rapid adenosine signaling in the brain. Between stimulated release, mechanosensitive release, and spontaneous, transient release, the fast time course of adenosine and the underlying

pathways have begun to be explained. Rapid events acutely cause neuromodulatory and neuroprotective effects. In the brain, A_1 receptors are a large factor in self-regulation of fast adenosine release. Additionally, metabolic and reuptake processes have been shown to play a role in the clearance of rapid adenosine events. However, much more work is needed to fill in uncertainties in these pathways. Most of the aforementioned work was performed *in vivo*. Brain slice experiments complement the *in vivo* work as these techniques avoid obstacles such as toxicity and blood-brain barrier permeability. In this thesis, I use brain slice experiments to demonstrate how the characteristics of spontaneous, transient adenosine differs between brain regions and I pursue the controlling mechanism for their release.

In this thesis I start by investigating the oxidation mechanism of histamine, a known interferent of adenosine with FSCV, and demonstrate a new approach to separating the signals of the two analytes by manipulating the waveform (Chapter 2). I then look into how spontaneous, transient adenosine varies between three distinct brain regions in rat brain slices, the prefrontal cortex, the thalamus, and the CA1 region of the hippocampus and found significant differences in the frequency, concentration, and duration of adenosine transients (Chapter 3). I then investigated some of the possible mechanism of spontaneous transient adenosine release, primarily activity dependence of adenosine transients via inhibition of Na^+ channels with tetrodotoxin and inhibition of pannexin channels via direct inhibition, indirect activation, and genetically modified mice (Chapter 4). I then propose future experiments to address some of the remaining

uncertainties in the field of transient adenosine and give an overview of the current state of adenosine research with FSCV (Chapter 5).

References

(1) Lloyd, H. G.; Fredholm, B. B. *Neurochem. Int.* 1995, *26* (4), 387–395.

(2) Pazzagli, M.; Pedata, F.; Pepeu, G. *Eur. J. Pharmacol.* 1993, *234* (1), 61–65.

(3) Cui, M.; Bai, X.; Li, T.; Chen, F.; Dong, Q.; Zhao, Y.; Liu, X. *PLoS One* 2013, *8* (2), e57065.

(4) Swamy, B. E. K.; Venton, B. J. *Anal. Chem.* 2007, *79* (2), 744–750.

(5) Pajski, M. L.; Venton, B. J. *ACS Chem. Neurosci.* 2010, *1* (12), 775–787.

(6) Ross, A. E.; Nguyen, M. D.; Privman, E.; Venton, B. J. *J. Neurochem.* 2014, *130* (1), 50–60.

(7) Street, S. E.; Walsh, P. L.; Sowa, N. A.; Taylor-Blake, B.; Guillot, T. S.; Vihko, P.; Wightman, R. M.; Zylka, M. J. *Mol. Pain* 2011, *7* (27), 80.

(8) Nguyen, M. D.; Lee, S. T.; Ross, A. E.; Ryals, M.; Choudhry, V. I.; Venton, B. J. *PLoS One* 2014, *9* (1), e87165.

(9) Nguyen, M. D.; Ross, A. E.; Ryals, M.; Lee, S. T.; Venton, B. J. *Pharmacol. Res. Perspect.* 2015, *3* (6), e00189.

(10) Dale, N.; Pearson, T.; Frenguelli, B. G. *J. Physiol.* 2000, *526 Pt 1*, 143–155.

(11) Frenguelli, B. G.; Wall, M. J. *J. Neurosci. Methods* 2016, *260*, 202–214.

(12) Stockwell, J.; Jakova, E.; Cayabyab, F. S. *Molecules* 2017, *22* (4), 676.

(13) Rial, D.; Lara, D. R.; Cunha, R. A. *Int. Rev. Neurobiol.* 2014, *119*, 395–449.

(14) Shen, H. Y.; Chen, J. F. *Curr Neuropharmacol* 2009, *7* (3), 195–206.

(15) Dunwiddie, T. V; Hoffer, B. J. *Br J Pharmacol* 1980, *69* (1), 59–68.

(16) Okada, M.; Nutt, D. J.; Murakami, T.; Zhu, G.; Kamata, a; Kawata, Y.; Kaneko, S. *J Neurosci* 2001, *21* (2), 628–640.

(17) Boison, D. *Pharmacol. Rev.* 2013, *65* (3), 906–943.

(18) Lapa, R.; José, S.; Júnior, M.; Cerutti, M. L.; Roberto, A.; Santos, S. *Pharmacol. Ther.* 2014, 85–130.

(19) Maes, M.; Decrock, E.; Cogliati, B.; Oliveira, A. G.; Marques, P. E.; Dagli, M. L. Z.; Menezes, G. B.; Mennecier, G.; Leybaert, L.; Vanhaecke, T.; Rogiers, V.; Vinken, M. *Frontiers in Physiology*. 2014.

(20) Heinrich, A.; Andó, R.; Túri, G.; Rózsa, B.; Sperlágh, B. *Br. J. Pharmacol.* 2012, *167* (5), 1003–1020.

(21) Gandelman, M.; Peluffo, H.; Beckman, J. S.; Cassina, P.; Barbeito, L. *J. Neuroinflammation* 2010, *7* (1), 33.

(22) Rebola, N.; Coelho, J. E.; Costenla, A. R.; Lopes, L. V.; Parada, A.; Oliveira, C. R.; Soares-da-Silva, P.; de Mendonca, A.; Cunha, R. A. *Eur. J. Neurosci.* 2003, *18* (4), 820–828.

(23) Belardinelli, L.; Shryock, J. C.; Snowdy, S.; Zhang, Y.; Monopoli, A.; Lozza, G.; Ongini, E.; Olsson, R. A.; Dennis, D. M. *J. Pharmacol. Exp. Ther.* 1998, *284* (3), 1066–1073.

(24) Fredholm, B. B.; IJzerman, A. P.; Jacobson, K. A.; Linden, J.; Mu, C. E.; Müller, C. E. *Pharmacol. Rev.* 2011, *63* (1), 1–34.

(25) Dixon, a K.; Gubitz, a K.; Sirinathsinghji, D. J.; Richardson, P. J.; Freeman, T. C. *Br. J. Pharmacol.* 1996, *118* (6), 1461–1468.

(26) Young, J. D.; Yao, S. Y. M.; Baldwin, J. M.; Cass, C. E.; Baldwin, S. A. *Mol. Aspects Med.* 2013, *34* (2–3), 529–547.

(27) Zamzow, C. R.; Bose, R.; Parkinson, F. E. *Can J Physiol Pharmacol* 2009, *87* (10), 850–858.

(28) Wall, M. J.; Dale, N. *J. Physiol.* 2013, *591* (Pt 16), 3853–3871.

(29) Bruzzone, R.; Hormuzdi, S. G.; Barbe, M. T.; Herb, A.; Monyer, H. *Proc. Natl. Acad. Sci.* 2003, *100* (23), 13644–13649.

(30) Wicki-Stordeur, L. E.; Boyce, A. K. J.; Swayne, L. A. *Cell Commun. Adhes.* 2013, *20* (3–4), 73–79.

(31) Bond, S. R.; Lau, A.; Penuela, S.; Sampaio, A. V.; Underhill, T. M.; Laird, D. W.; Naus, C. C. *J. Bone Miner. Res.* 2011, *26* (12), 2911–2922.

(32) Chiu, Y.-H.; Jin, X.; Medina, C. B.; Leonhardt, S. A.; Kiessling, V.; Bennett, B. C.; Shu, S.; Tamm, L. K.; Yeager, M.; Ravichandran, K. S.; Bayliss, D. A. *Nat. Commun.* 2017, *8*, 14324.

(33) Kim, Y.; Davidson, J. O.; Green, C. R.; Nicholson, L. F. B.; O'Carroll, S. J.; Zhang, J. *Biochimica et Biophysica Acta - Biomembranes*. 2018, pp 224–236.

(34) Lopatář, J.; Dale, N.; Frenguelli, B. G. *Neuropharmacology* 2015, *93*, 219–228.

(35) Nakamura, T.; Tu, S.; Akhtar, M. W.; Sunico, C. R.; Okamoto, S. ichi; Lipton, S. A. *Neuron*. 2013, pp 596–614.

(36) Chekeni, F. B.; Elliott, M. R.; Sandilos, J. K.; Walk, S. F.; Kinchen, J. M.; Lazarowski, E. R.; Armstrong, A. J.; Penuela, S.; Laird, D. W.; Salvesen, G. S.; Isakson, B. E.; Bayliss, D. A.; Ravichandran, K. S. *Nature* 2010, *467* (7317), 863–867.

(37) Lohman, A. W.; Weaver, J. L.; Billaud, M.; Sandilos, J. K.; Griffiths, R.; Straub, A. C.; Penuela, S.; Leitinger, N.; Laird, D. W.; Bayliss, D. A.; Isakson, B. E. *J. Biol. Chem.* 2012, *287* (47), 39602–39612.

(38) Zhang, L.; Deng, T.; Sun, Y.; Liu, K.; Yang, Y.; Zheng, X. *J. Neurosci. Res.* 2008, *86* (10), 2281–2291.

(39) Weilinger, N. L.; Tang, P. L.; Thompson, R. J. *J. Neurosci.* 2012, *32* (36), 12579–12588.

(40) Bargiotas, P.; Krenz, A.; Monyer, H.; Schwaninger, M. *Channels* 2012, *6* (6), 453–456.

(41) Cunha, R. A. *Purinergic Signalling*. 2005, pp 111–134.

(42) Ross, A. E.; Venton, B. J. *J. Neurochem.* 2015, *132* (1), 51–60.

(43) Poli, A.; Lucchi, R.; Vibio, M.; Barnabei, O. *J Neurochem* 1991, *57* (1), 298–306.

(44) Manev, H.; Favaron, M.; Guidotti, a; Costa, E. *Mol. Pharmacol.* 1989, *36* (1), 106–112.

(45) Haselkorn, M. L.; Shellington, D. K.; Jackson, E. K.; Vagni, V. A.; Janesko-Feldman, K.; Dubey, R. K.; Gillespie, D. G.; Cheng, D.; Bell, M. J.; Jenkins, L. W.; Homanics, G. E.; Schnermann, J.; Kochanek, P. M. *J Neurotrauma* 2010, *27* (5), 901–910.

(46) Atcherley, C. W.; Laude, N. D.; Parent, K. L.; Heien, M. L. *Langmuir* 2013, *29* (48), 14885–14892.

(47) Llaudet, E.; Botting, N. P.; Crayston, J. A.; Dale, N. *Biosens. Bioelectron.* 2003, *18* (1), 43–52.

(48) Bath, B. D.; Michael, D. J.; Trafton, B. J.; Joseph, J. D.; Runnels, P. L.; Wightman, R. M. *Anal. Chem.* 2000, *72* (24), 5994–6002.

(49) Zimmerman, J. B.; Wightman, R. M. *Anal. Chem.* 1991, *63* (1), 24–28.

(50) Venton, B. J.; Michael, D. J.; Wightman, R. M. *J. Neurochem.* 2003, *84* (2), 373–381.

(51) Zachek, M. K.; Takmakov, P.; Moody, B.; Wightman, R. M.; McCarty, G. S. *Anal. Chem.* 2009, *81* (15), 6258–6265.

(52) Wang, Y.; Venton, B. J. *J. Neurochem.* 2017, *140* (1), 13–23.

(53) Ross, A. E.; Venton, B. J. *Analyst* 2012, *137* (13), 3045–3051.

(54) Ross, A. E.; Venton, B. J. *Anal. Chem.* 2014, *86* (15), 7486–7493.

(55) Chang, S.-Y.; Jay, T.; Muñoz, J.; Kim, I.; Lee, K. H. *Analyst* 2012, *137* (9), 2158.

(56) Chang, S.-Y.; Jay, T.; Muñoz, J.; Kim, I.; Lee, K. H. *Analyst* 2012, *137* (9), 2158.

(57) Samaranayake, S.; Abdalla, A.; Robke, R.; Wood, K. M.; Zeqja, A.; Hashemi, P. *Analyst* 2015, *140* (11), 3759–3765.

(58) Wang, H. L.; O'Malley, R. M.; Fernandez, J. E. *Macromolecules* 1994, *27* (4), 893–901.

(59) Dryhurst, G. *Electrochemistry of Biological Molecules*; 1977.

(60) Wall, M. J.; Wigmore, G.; Lopatář, J.; Frenguelli, B. G.; Dale, N. *Neuropharmacology* 2008, *55* (7), 1251–1258.

(61) Pearson, T.; Nuritova, F.; Caldwell, D.; Dale, N.; Frenguelli, B. G. *J.Neurosci.* 2001, *21* (7), 2298–2307.

(62) Pajski, M. L.; Venton, B. J. *Purinergic Signal.* 2013, *9* (2), 167–174.

(63) Klyuch, B. P.; Dale, N.; Wall, M. J. *J. Neurosci.* 2012, *32* (11), 3842–3847.

(64) Wall, M. J.; Atterbury, A.; Dale, N. *J. Physiol.* 2007, *582* (Pt 1), 137–151.

(65) Wang, Y.; Venton, B. J. *J. Neurochem.* 2016, 2–4.

(66) Gu, J. G.; Foga, I. O.; Parkinson, F. E.; Geiger, J. D. *J. Neurochem.* 1995, *64* (5), 2105–2110.

(67) WHITE, T. D.; MacDONALD, W. F. *Ann. N. Y. Acad. Sci.* 1990, *603* (1), 287–298.

(68) Jo, Y. H.; Schlichter, R. *Nat. Neurosci.* 1999, *2* (3), 241–245.

(69) Zhang, J. M.; Wang, H. K.; Ye, C. Q.; Ge, W.; Chen, Y.; Jiang, Z. L.; Wu, C. P.; Poo, M. M.; Duan, S. *Neuron* 2003, *40* (5), 971–982.

(70) Cunha, R. A.; Vizi, E. S.; Ribeiro, J. A.; Sebastião, A. M. *J. Neurochem.* 1996, *67* (5), 2180–2187.

(71) Dale, N.; Pearson, T.; Frenguelli, B. G. *J. Physiol.* 2000, *526 Pt 1*, 143–155.

(72) Frenguelli, B. G.; Llaudet, E.; Dale, N. *J. Neurochem.* 2003, *86* (6), 1506–1515.

(73) Frenguelli, B. G.; Wigmore, G.; Llaudet, E.; Dale, N. *J. Neurochem.* 2007, *101* (5), 1400–1413.

(74) Crack, B. E.; Pollard, C. E.; Beukers, M. W.; Roberts, S. M.; Hunt, S. F.; Ingall, A. H.; McKechnie, K. C. W.; IJzerman, A. P.; Leff, P. *Br. J. Pharmacol.* 1995, *114* (2), 475–481.

(75) Martín, E. D.; Fernández, M.; Perea, G.; Pascual, O.; Haydon, P. G.; Araque, A.; Ceña, V. *Glia* 2007, *55* (1), 36–45.

(76) Sayin, U.; Rutecki, P. A. *Epilepsy Res.* 2003, *53* (3), 186–195.

(77) Taylor, G. W.; Merlin, L. R.; Wong, R. K. *J. Neurosci.* 1995, *15* (12), 8039–8052.

(78) Sacaan, A. I.; Schoepp, D. D. *Neurosci. Lett.* 1992, *139* (1), 77–82.

(79) Dale, N.; Frenguelli, B. G. *Curr.Neuropharmacol.* 2009, *7* (3), 160–179.

Chapter 2

Investigating the fundamentals of histamine oxidation for the application of fast-scan cyclic voltammetry.

Success is how high you bounce when you hit bottom

– Gen. George S. Patton

Abstract:

Histamine is an immunological molecule that is also a neurotransmitter which modulates serotonin release and plays a role in the sleep cycle and, in invertebrates, visual transduction. Histamine can be detected electrochemically and the oxidation is thought to occur at a high potential, around 1.2 V vs Ag/AgCl, which could be problematic since other species oxidize at high potentials as well. However, a new detection method with fast-scan cyclic voltammetry (FSCV) for histamine was recently proposed, with an oxidation peak near 0.3 V and a claim that higher potential peaks are non-Faradaic due to adsorption. The oxidation product of histamine at carbon electrodes has not been determined and would provide clarity for developing *in vivo* methods of detection. In this work, we prove through amperometry and spectroelectrochemistry that a potential above 1.0 V is required to observe histamine oxidation. Evidence of fouling suggests the oxidation product to be an electropolymerization product. Additionally, we develop an alternative waveform that can separate the oxidation peaks of histamine and adenosine *in vitro*. Adding a potential hold at 1.25 V allows histamine to oxidize entirely without adenosine oxidation, and a later hold can be incorporated to differentiate the signal of H_2O_2 as well. Whereas mixtures of adenosine, histamine, and H_2O_2 were analyzed with principal components analysis in vitro, the waveform did not function well in tissue, as the potential for histamine shifted to higher potentials. This work shows that high potentials are required for Faradaic reactions for histamine and the advances to combat biofouling and

impedance, along with specialized waveforms, could be a valuable tool for histamine and adenosine measurements with FSCV.

2.1 Introduction:

Histamine is a compound most known for its role in immune response as an inflammatory agent. It also functions as a neurotransmitter and neuromodulator, regulating serotonin release and playing a part in sleep.[1–3] Histaminergic neurons are found in the tuberomammillary nucleus in the hypothalamus and have projections that reach throughout the brain.[3–5] Histamine has been measured in the brain over long periods of time using techniques such as microdialysis coupled to chromatography.[6,7] Using fast-scan cyclic voltammetry, rapid histamine release has been detected that correlates with serotonin release.[8] This suggests that in addition to it immunological role, histamine also may play a role in neurological or psychological disorders.[9] Histamine has also been quantified in the ventral nerve cord of fruit flies using CE-FSCV .[10] In order to detect histaminergic signaling behavior on a rapid time scale, electrochemical methods are a more appropriate approach than separation based techniques.

The traditional FSCV parameters for histamine detection *in vivo* use a triangle waveform, scanning from a holding potential of -0.4 V vs Ag/AgCl to a switching potential of 1.30 V and back down at 400V/s and repeating at a rate of 10 Hz.[11] The voltammogram of histamine is characterized by a strong primary oxidation peak at 1.3 V

on the cathodic scan and a weaker, broad secondary peak at 0.8 V on the anodic scan. A higher switching potential can give larger signals for histamine, but there are other analytes that have similar voltammetric profiles. The primary peak for histamine, which is used to quantify the concentration of a release event, shows up around the same potential as adenosine, ATP, and H_2O_2, when using switching potentials of 1.35 V to 1.50 V.[11,12] The identity of histamine can be confirmed by using pharmacological experiments, blocking histamine receptors and observing changes in the duration and concentration of events. However, pharmacological confirmation requires more animals and more drugs than other possible methods. A more cost-effective approach would be to alter the waveform so that signals can be separated from each other. Previous work shows that using a sawhorse waveform, which holds at the switching potential of 1.35 V vs Ag/AgCl for 1 ms before scanning back to -0.4 V, can differentiate adenosine from ATP and H_2O_2, but did not include histamine.[12] Histamine still gives a very similar signal to adenosine with the sawhorse waveform.

Histamine has been differentiated from adenosine by scanning up to a switching potential of 1.3 V with a triangle waveform, which is enough to oxidize histamine fully, but leaves very little signal for adenosine.[11] This method is useful for histamine detection, but is limited in its applicability for codetection of adenosine.

The Hashemi lab developed a waveform that detects histamine at 0.3 V vs Ag/AgCl.[2] Since shifting the oxidation peak by 1.0 V should not be possible with only a

waveform manipulation, they hypothesize that the oxidation potential of histamine actually is very low and the peak that has been observed near 1.3 V is only an adsorption peak. However, this hypothesis lacks a mechanistic explanation of the redox reaction and evidence that the peak observed with this histamine specific waveform is actually faradaic in nature. Imidazole oxidations require a very high potential to be applied. Almost all prior research states that histamine is no different, in the FSCV field as well as the more traditional electrochemistry fields.[11,13,14] However, there are few studies that have actually looked at the mechanism of histamine oxidation at carbon electrodes.

The oxidation product of histamine at carbon electrodes has not been determined. Wang, O'Malley and Fernandez determined that imidazole electropolymerizes at high potentials forming N-N bonds through a series of 1-electron oxidations. This connects the rings into a long chain polymer, visualized as a brown coating on the electrode surface.[13] However, this electropolymerization was never performed with histamine (**Fig 2.1: Scheme 1**). Alternatively, the oxidation of histamine could resemble the secondary oxidation process of adenosine. The secondary oxidation of adenosine occurs on the imidazole ring generating a carbonyl on the carbon between the 2 nitrogens (**Fig 2.1: Scheme 2**).[15] Both oxidation pathways are feasible with

Scheme 1: Electropolymerization of Histamine

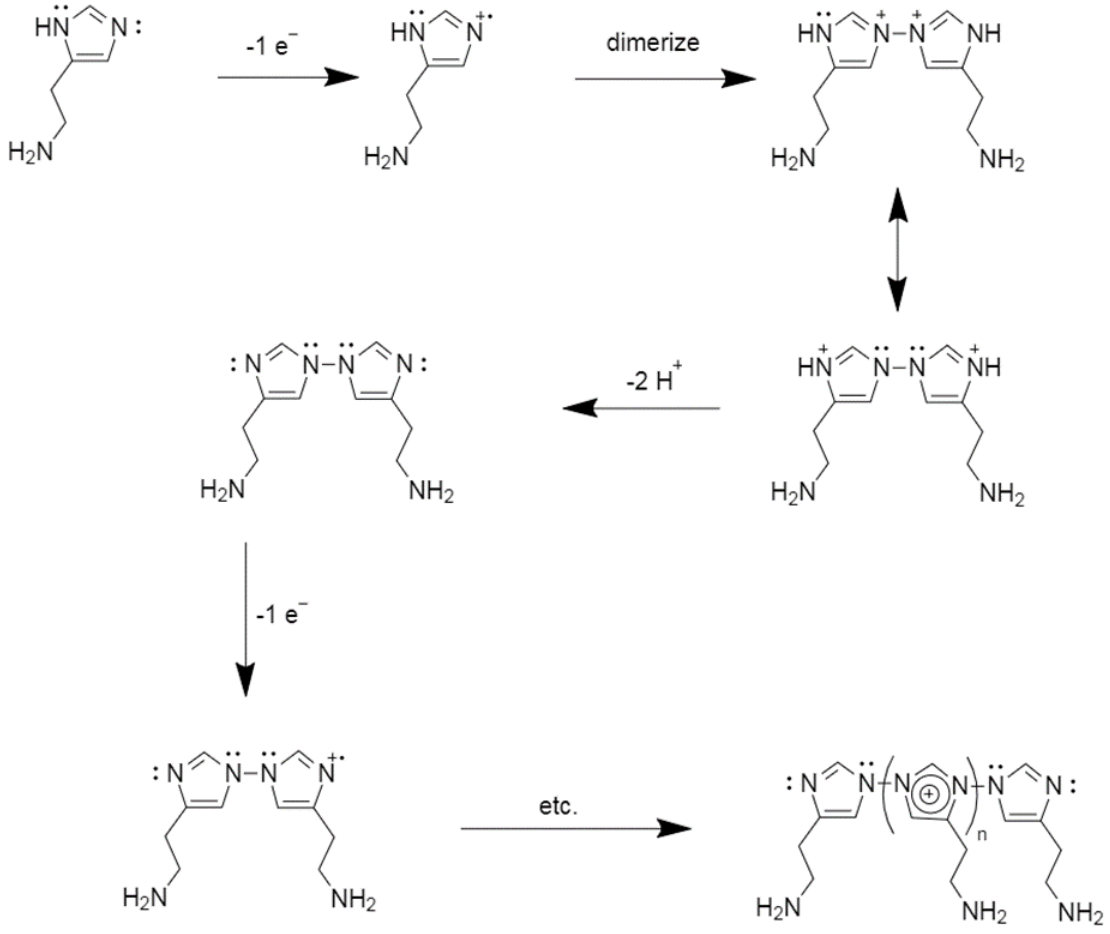

Scheme 2. Carbonyl Formation

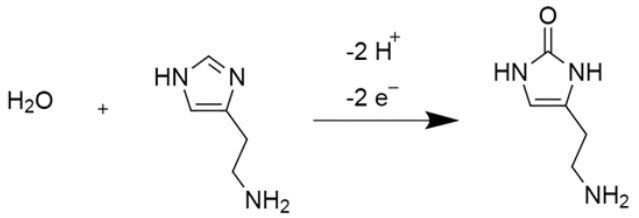

Figure 2.1 Histamine oxidation schemes. **Scheme 1**: Electropolymerization of histamine based on reported reaction of imidazole by Wang, et al. **Scheme 2**: Carbonyl formation in the same manner as the secondary oxidation of adenosine.

histamine but neither has been proven, and both should require a high oxidation potential. The work proposing a 0.3 V oxidation potential did not present any alternative oxidation mechanisms.

In this work, we address this mechanistic question: what is the potential required to oxidize histamine and what is the oxidation mechanism? We use amperometry to determine the minimum potential required to observe histamine oxidation. We also employ infrared spectroelectrochemistry (IR-SEC) to perform a thin-layer oxidation of histamine at different potentials with a subsequent infra-red spectroscopy measurement to look for changes in the molecular structure. We also performed a bulk oxidation of histamine for analysis with ^{13}C NMR to help confirm structure identity. These studies point to the electropolymerization scheme at the imidazole N as the most likely mechanism.

We also investigate how waveform manipulation for FSCV can be used to separate the signals of histamine and adenosine. Traditionally, histamine can be oxidized at a lower potential than adenosine but because of fast scan rates with FSCV, they often still show up at the same potential. This indicates that the electron transfer kinetics of histamine oxidation must be slower than that of adenosine. We demonstrate this subtle difference by developing a new ‘sawtip’ waveform that can separate the oxidation peaks of adenosine and histamine in a quantitative manner. In real tissue, the potentials do shift, making it more difficult to implement. Once the complications of

impedance from the tissue sample matrix can be accounted and corrected for, this waveform could be useful in real brain tissue samples.

2.2 Methods:

2.2.1 IR-SEC

Phosphate buffered saline solutions were made consisting of NaCl (0.0625 M), $NaH_2PO_4 \bullet H_2O$ (0.026 M), and Na_2HPO_4 (0.099 M) in 20 mL of D_2O. Histamine•2HCl (Sigma) was neutralized with a 0.25 M solution of NaOH by dissolving 0.050 g of NaOH in 5 mL of D_2O. 0.3 mL of neutralized histamine was then combined with 0.45 mL of buffered electrolyte to generate a 0.1 M solution of histamine at pH=7. To account for the buffer dilution and addition of extra NaCl from the neutralization reaction, a 0.25 M NaCl solution was made in D_2O for the purpose of referencing the IR-SEC cell.

All IR-SEC experiments were conducted using a custom cell (**Fig 2.2**) based on a previously published design.[16–18] The three-electrode set-up consists of an inner glassy carbon working electrode disk (10 mm diameter), a central circular silver bare metal pseudoreference electrode, and an outer circular glassy carbon counter electrode embedded within a polyether ether ketone (PEEK) block. All data were referenced to an internal $K_4[Fe(CN)_6]$ standard in buffered electrolyte diluted with the NaCl solution described above and converted to Ag/AgCl, obtained by taking a CV with the cell prior to injecting analyte for IR-SEC experiments. IR spectra were collected using a Vertex V80 IR (Bruker). All spectra were processed by subtraction of the solvent blank, and difference

Figure 2.2. Infrared Spectroelectrochemistry cell. The three-electrode set-up consists of an inner glassy carbon working electrode disc (10 mm diameter), a central circular silver metal pseudoreference electrode, and an outer circular glassy carbon counter electrode embedded within a PEEK block.

spectra were obtained by subtracting the spectrum at 0 V vs AgCl/Ag from the stated potential.

2.2.2 Bulk electrolysis of histamine for NMR

A 100 mL solution was made in a volumetric flask consisting of DI H_2O, NaCl (1 M), Na_2HPO_4 (0.61 M), $NaH_2PO_4 \bullet H_2O$ (0.39 M) to give a pH = 7 buffer. Electrolysis was performed on a 20 mL aliquot of the buffer containing 0.1 M histamine dihydrochloride in a Pine H-Cell open to air. The working electrode was a 5 mm glassy carbon rod, with a glassy carbon counter electrode and a 3 M CaCL Ag/AgCl reference electrode. Electrolysis was performed for 27 hours and 0.5 mL was used for ^{13}C NMR, which ran overnight to signal average 32,768 scans. A control ^{13}C NMR of histamine in the same buffer was obtained after 27 hours of incubation in an NMR tube open to air. ^{13}C NMR spectra were obtained on a Varian 600 MHz NMR with a custom D_2O insert.

2.2.3 Amperometry

Amperometry measurements were taken on a Gamry Reference600 Potentiostat using glassy carbon working electrode (CH Instruments Inc.) with a 3 mm diameter, Ag/AgCl reference electrode, and a platinum counter electrode. Working solutions were made in phosphate buffered saline (PBS) consisting of 131.25 mM NaCl, 3.00 mM KCl, 10 mM $NaH_2PO_4 \bullet H_2O$, 1.2 mM $MgCl_2 \bullet 6H_2O$, 2.0 mM anhydrous Na_2SO_4, and 1.2 mM $CaCl_2 \bullet 2H_2O$ at a pH of 7.4. Ten mL solutions of 10 mM dopamine•HCl (Acros) and 10 mM histamine•2HCl were prepared in PBS immediately prior to experimentation. Diffusion effects were minimized by constantly mixing the solution with a magnetic stirrer.

2.2.4 Fast-scan cyclic voltammetry: waveform development

Ten mM stock solutions of adenosine (Acros), ATP disodium salt hydrate (Sigma), histamine, H_2O_2 (Macron) were made in 0.1 M $HClO_4$. Daily samples were prepared by diluted stock solution in the PBS described in the amperometry methods. FSCV was performed using a ChemClamp (Dagan) and data was collecting using the HDCV software, (Mark Wightman, UNC)

The CFMEs used for FSCV are made from T-650 carbon fibers (gift from Cytec Engineering Materials) which are 7 µm in diameter and cut to 50-100 µm in length. To ensure a the capillary is properly sealed around the carbon-fiber, the tips of the CFMEs were epoxied closed with Epon Resin 828 (Miller-Stephenson) and 14% (w/w) 1,3-phenylenediamine hardener (Sigma), dipped in acetone to clean away excess epoxy, and

cured in the oven overnight as described previously.[19] Electrodes were back-filled with 4 M KCl to create the electrical connection between the carbon fiber and the silver wire lead from the headstage. The reference electrode was a Ag/AgCl wire.

Waveform development was performed using flow-injection analysis. The CFME was place in the outflow port of a six-port, stainless steel, HPLC loop injector and the reference electrode was placed in the overflow cup to complete the circuit. Sample was loaded into a 500 µL sample loop and an air actuator controlled the switch between lines to allow a rapid change between PBS and sample. PBS was pumped using a syringe pump at 2 mL/min with 5 second injections of the analytes.

2.2.5 Slice preparation

For slice experiments and post-calibrations, PBS was substituted with artificial cerebral spinal fluid (aCSF): 126 mM NaCl, 2.5 mM KCl, 1.2 mM NaH_2PO_4 monohydrate, 1.2 mM $MgCl_2$ hexahydrate, 25 mM $NaHCO_3$, 11 mM glucose (all from Fisher), 2.4 mM $CaCl_2$ dihydrate, and 15 mM tris (hydroxymethyl) aminomethane (both from Sigma), with added HCL to obtain pH 7.4. All rat experiments were approved of by the Animal Care and Use Committee at the University of Virginia. Male, Sprague-Dawley rats weighing between 250-350 g were purchased from Charles River (Willmington, MA) were housed in a vivarium and given food and water *ad libitum*. Rats were anesthetized with isoflurane in a desiccator and promptly beheaded. The brain was removed in less than 2 minutes and kept in 0-5°C oxygenated aCSF (95% O_2, balance CO_2) for a couple

minutes for recovery. A LeicaVT1000S vibratome was used to collect 400 µm thick coronal slices of the caudate putamen. During collection, slices were transferred to room temperature oxygenated aCSF. Once slicing was complete, the aCSF was warmed to body temperature of 37°C using an IsoTemp 205 water bath (Fisher). During experimentation, a perfusion pump (Watson-Marlo 205U) was used to flow 37° aCSF over the brain slice at 2 mL/min. CFMEs were implanted 50-100 µm into the slice for at least 15 minutes prior to any data collection. Histamine and adenosine were each pressure ejected into the tissue with a Parker Hannifin picospritzer (Picospritzer III). A pulled glass pipette filled with 25 µM adenosine or histamine in aCSF was placed in close proximity to the tip of CFME in the brain slice. The parameters for picospritzing were 20 psi for 300 milliseconds, which resulted in 14 nL volume being delivered to the slice.

2.2.6 Quantitative analysis and statistics

Principal components analysis (PCA), as built into the HDCV Analysis software, was used to determine if an optimized waveform could differentiate the CVs of different analytes from each other. Training sets were created using a range of concentrations for each analyte. The software then extracts the principal components and utilizes principal component regression to quantify the amount of each component present in an unknown sample. The Q-score, which is the sum of squares of residual current for each variable, determined if data could be accepted for analysis. If residual signal went over the Q-score, the sample would be omitted from analysis.

All reported concentrations in this work are reported as the mean ± standard error of the mean (SEM). Statistics were performed in Graphpad Prism 6. Differences in means were considered significant at the 95% confidence level ($p < 0.05$).

2.3 Results

2.3.1 Amperometry of histamine

To test the potential that histamine oxidation can occur, we performed amperometry at different potentials at a glassy carbon electrode. For each amperogram, the potential was held for two minutes to allow the current to stabilize prior to sample injections. There were 6 injections made in each experiment with 1-minute intervals between each injection. The first two injections were 50 µL PBS as a control to demonstrate no change in signal. The third and fourth injections were 50 µL of 10 mM histamine, and the fifth and sixth injections were 50 µL of 10 mM dopamine, which was chosen because the electrochemistry of dopamine is widely understood, and it is a good test compound. Accounting for dilution, an injection of analyte to the working solution resulted in a 49.2 µM increase in the bulk concentration of that analyte. Each subsequent injection would cause the concentration spike to increase by 0.2 µM less than the previous injection. Standard errors between injections are larger than this difference so each injection was considered equivalent for the sake of simplicity.

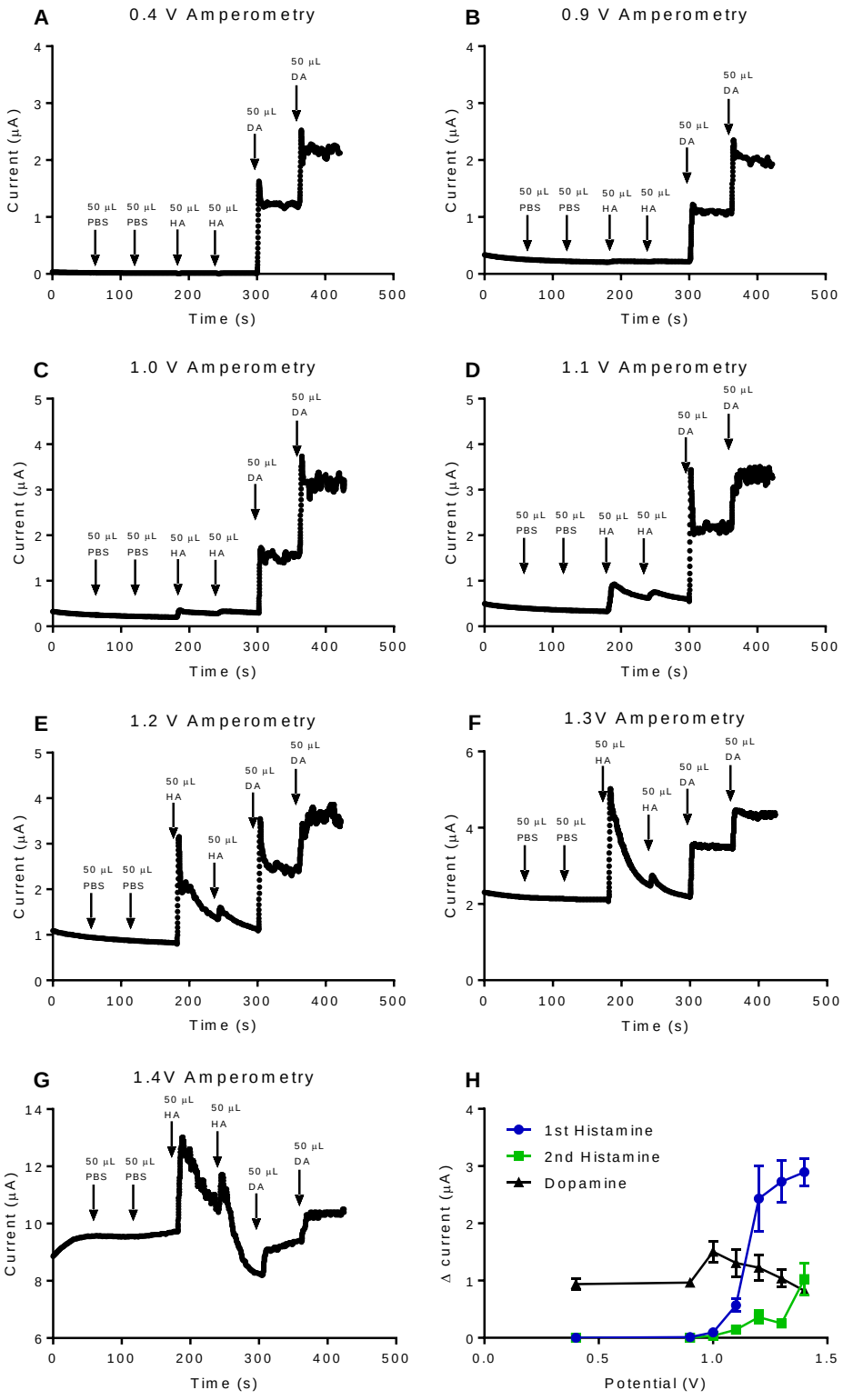
A
0.4 V Amperometry
B
0.9 V Amperometry
C
1.0 V Amperometry
D
1.1 V Amperometry
E
1.2 V Amperometry
F
1.3V Amperometry
G
1.4V Amperometry
H
Current (µA)
Time (s)
50 µL PBS
50 µL HA
50 µL DA
Δ current (µA)
Potential (V)
1st Histamine
2nd Histamine
Dopamine

Figure 2.3: Amperograms of PBS, histamine (HA), and dopamine (DA) using held potentials of (**A**) 0.4 V, (**B**) 0.9 V, (**C**) 1.0 V, (**D**) 1.1 V, (**E**) 1.2 V, (**F**) 1.3 V, and (**G**) 1.4 V. Each injection was 50 uL, either of PBS (control), histamine (10 mM), or dopamine (10 mM). (**F**) Plot of maximum current vs applied potential. There is no noticeable current from histamine using 0.4 V or 0.9 V, but a little bit of current begins to appear for histamine with a 1.0 V hold and this current becomes even more prominent at higher potentials, generating a maximum of about 2.4 ± 0.6 μA of current with potentials of 1.2 V or higher. Dopamine, with a redox potential of 0.2 V vs Ag/AgCl is oxidized for all potentials. Error bars are SEM.

As seen in the amperograms (**Fig. 3**), PBS never causes in any change in current. Using a potential of 0.4 V, there was no signal from histamine, while current increased 1.03 μA for the dopamine injection (**Fig. 2.3A**). Raising the potential to 0.9 V, there was no quantifiable signal observed for histamine (**Fig. 2.3B**). At 1.0 V, the current of the first histamine injection is noticeably larger than the baseline with an increase of 0.10 μA and there was a faint rise in current for the second injection (**Fig. 2.3C**). Additionally, the current from histamine injections slowly fell back to baseline, whereas the dopamine signals stayed steady. With a potential of 1.2 V (**Fig. 2.3E**), the first injection of histamine was significantly larger (ANOVA, $p < 0.0001$ $n = 3$ each) than the dopamine signal with an average current of 2.4 ± 0.6 μA. However, this was only true of the first injection. The first injection was substantially larger than the second (Tukey's post-test, $p < 0.0001$). The second histamine injection generated less current than the first and there was still a drop-off of current toward baseline. Potentials of 1.3 V and 1.4 V showed no further increase in current for histamine on either the first or second injection (**Fig. 2.3F-G**). There was no significant (Tukey's post-test, $p > 0.05$) change in current generated by dopamine oxidation across the entire span of potentials.

These studies show that a minimum potential of about 1.0 V vs Ag/AgCl is required to observe histamine oxidation at a glassy carbon electrode with amperometry. 1.2 V is required to obtain the maximal rate of oxidation. However, the decrease in current with a constant injection of histamine demonstrates some fouling of the electrode by histamine oxidation products. Fouling reduces the number of adsorption sites on the electrode and the response time of the electrode.

2.3.2 Spectroelectrochemical determination of the oxidation product of histamine

Infrared-spectroelectrochemistry (IR-SEC) is a technique where IR active modes are monitored of a compound as it undergoes a redox reaction over time due to a potential applied to an electrode in the electrochemical cell.[16,20,21] To examine histamine oxidation, a 0.1 M solution of histamine, buffered to pH 7, was dissolved in D_2O, as it gave the best resolution in all regions of the infrared spectrum relevant to this chemistry. No changes in the IR spectra were observed until 1.30 V vs Ag/AgCl was applied (**Fig. 2.4A**). At this potential, the IR absorbance band at 3157 cm^{-1} increased in intensity with a longer hold time, indicating a structural change. Increasing the potential to 1.35 V caused further growth in this band; however, no other changes in the IR spectra were noted. Difference spectra normalized to the experimental starting conditions confirm the observed changes (**Fig. 2.4B**). A potential of 1.3 V is required to see any change in this IR peak and the peak can be increased by either oxidizing for more time or at a higher potential of 1.35 V. Control experiments were performed by

stepping to the same potentials in the same solution, but without any histamine (**Fig. 2.4C)**. There are no observable changes in the IR absorbance for any of the potentials; thus, applying these potentials does not cause changes in the surface of glassy carbon electrodes. Whereas 3157 cm^{-1} is high enough to reflect an N-H stretch, previous work has typically assigned this IR peak to the sp^2 C-H stretches on the imidazole ring.[22,23] ^{13}C NMR also demonstrates that no changes in the shifts of the 5 carbon peaks (**Fig. 2.5**). Had a carbonyl formed in the manner of **Scheme 2**, the peak at 138 ppm should have shifted up to about 160 ppm.

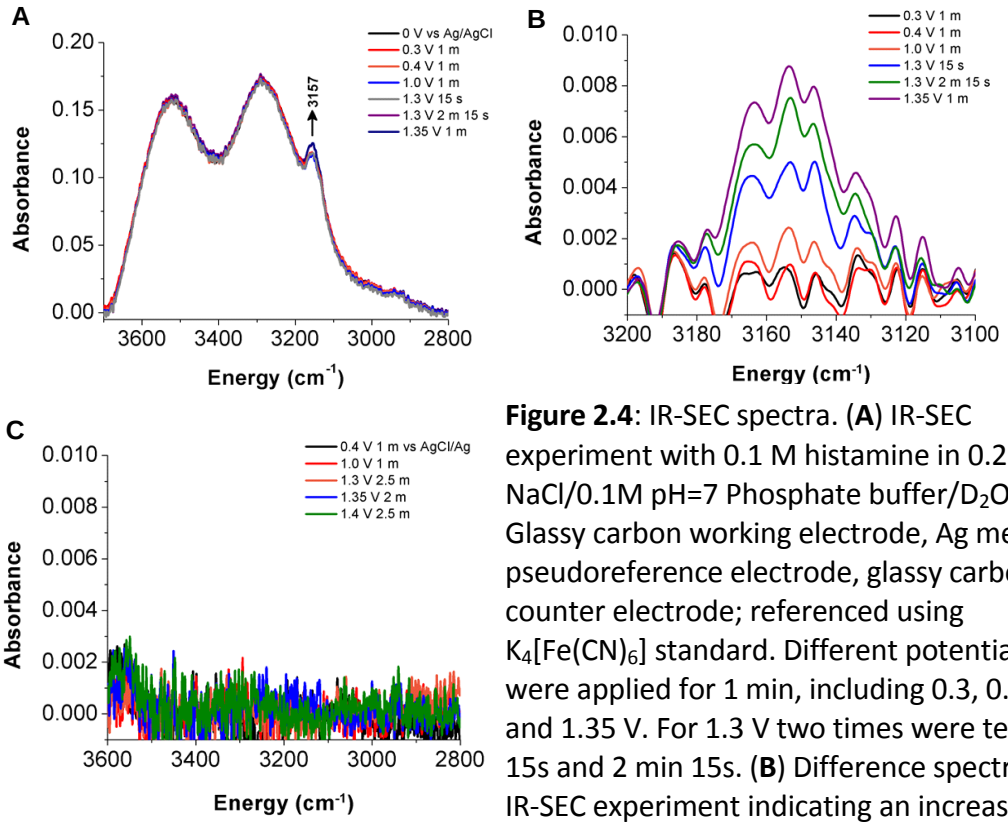

Figure 2.4: IR-SEC spectra. (**A**) IR-SEC experiment with 0.1 M histamine in 0.2 M NaCl/0.1M pH=7 Phosphate buffer/D_2O. Glassy carbon working electrode, Ag metal pseudoreference electrode, glassy carbon counter electrode; referenced using $K_4[Fe(CN)_6]$ standard. Different potentials were applied for 1 min, including 0.3, 0.4, 1.0, and 1.35 V. For 1.3 V two times were tested, 15s and 2 min 15s. (**B**) Difference spectra from IR-SEC experiment indicating an increase in IR absorbance at 3157 cm^{-1} with potentials above 1.3 V vs Ag/AgCl. (**C**) Difference spectra from control experiment shows no change.

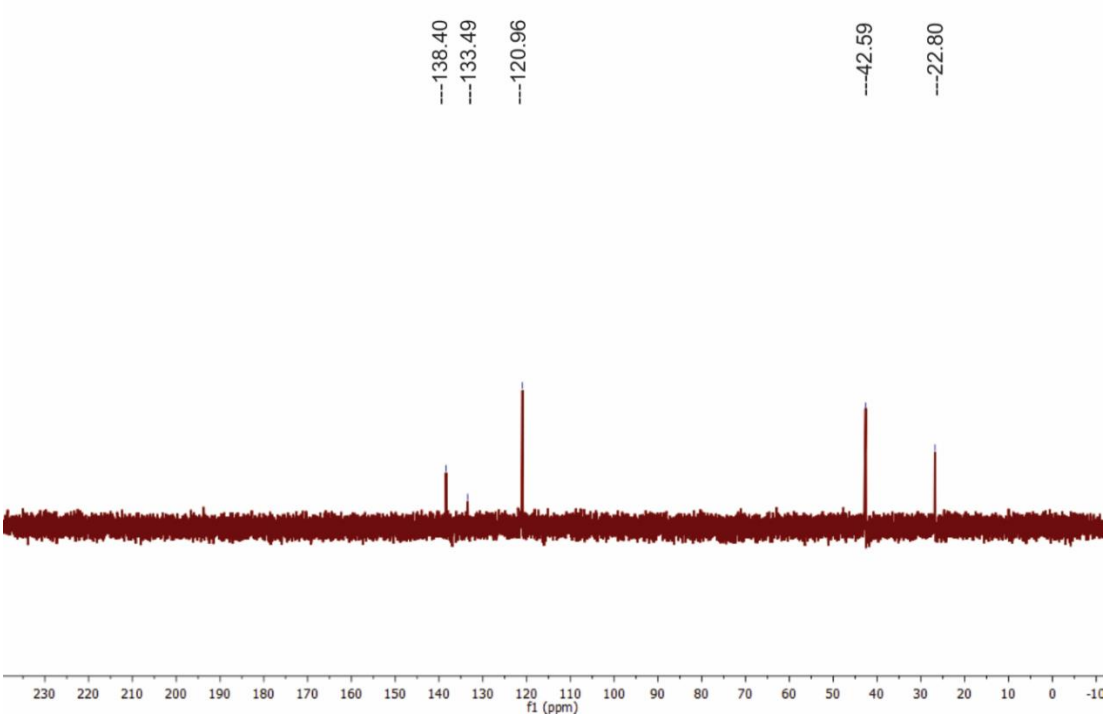

Figure 2.5A: ^{13}C NMR of histamine

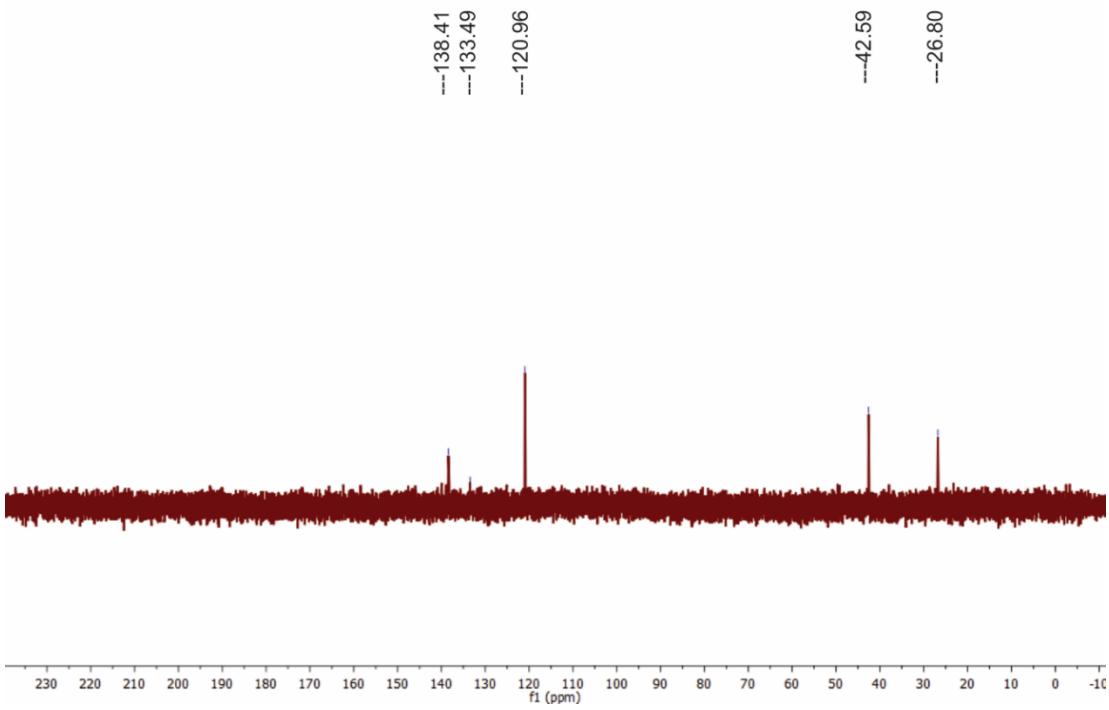

Figure 2.5B: ^{13}C NMR of histamine after 27 hours electrolysis.

2.3.3 Developing a waveform that differentiates histamine and adenosine.

The amperometry and spectroelectrochemistry experiments demonstrate that histamine oxidizes at a high potential of 1.2 V, but there are many other compounds that oxidize at same potentials, including adenosine. Thus, a new waveform was developed to separate the signals of each with FSCV. A standard triangle waveform used in FSCV, with a switching potential of 1.4 V, results in CVs of adenosine and histamine that look very similar.[11] The secondary peak of adenosine is more prominent than that of histamine, but the difference is so small that principal components analysis was unable to confidently differentiate the two. The literature suggests that the oxidation potential of histamine should be slightly lower than that of adenosine.[11,14,15] Chang, et al. determined that a triangle waveform with a switching potential of 1.3 V would oxidize histamine without oxidizing adenosine. Ross and Venton had previously used a sawhorse waveform, that plateaus at the upper potential, to differentiate adenosine and ATP but the waveform did not work as well for differentiating histamine and adenosine.[12] Our hypothesis is that it is possible for histamine to be oxidized at a lower potential than adenosine if the correct potential was used for the plateau. The sawhorse switching potential was increased from 1.15 V to 1.35 V to determine the potential that would generate the strongest histamine oxidation without oxidizing adenosine (**Fig. 2.6**). Neither oxidize with a 1.15 V holding potential, but histamine generates a moderate

oxidation current of 6 nA with 1.2 V and an even stronger current of 10 nA with 1.25 V. Adenosine gives a weak signal at 1.2 V which is more indicative of a small background change rather than a faradaic reaction. At 1.25 V, there is a small Faradaic current for adenosine, but histamine current is much larger. When the switching potential was raised to 1.3 V, adenosine oxidation looked very similar to histamine, both generating around 10 nA of current at approximately the same time during the hold. Adenosine does have a more prominent secondary peak, but it would be difficult to distinguish the two species. Increasing the switching potential to 1.35 V resulted in an even larger adenosine oxidation current and, strangely, decreased the histamine oxidation current down to 6 nA (**Fig. 2.6E**).

On most electrodes, the plateau potential required to see robust histamine oxidation without much adenosine current was 1.25 V. However, there is some deviation between electrodes. Occasionally, an electrode could separate the signals with a plateau at 1.2 V, while another would require the hold to be at 1.3 V. This could be due to impedance of the electrode due to the epoxy step of electrode fabrication. As this did not occur often, the optimized version was the sawtip waveform with a 0.75 ms hold at 1.25 V.

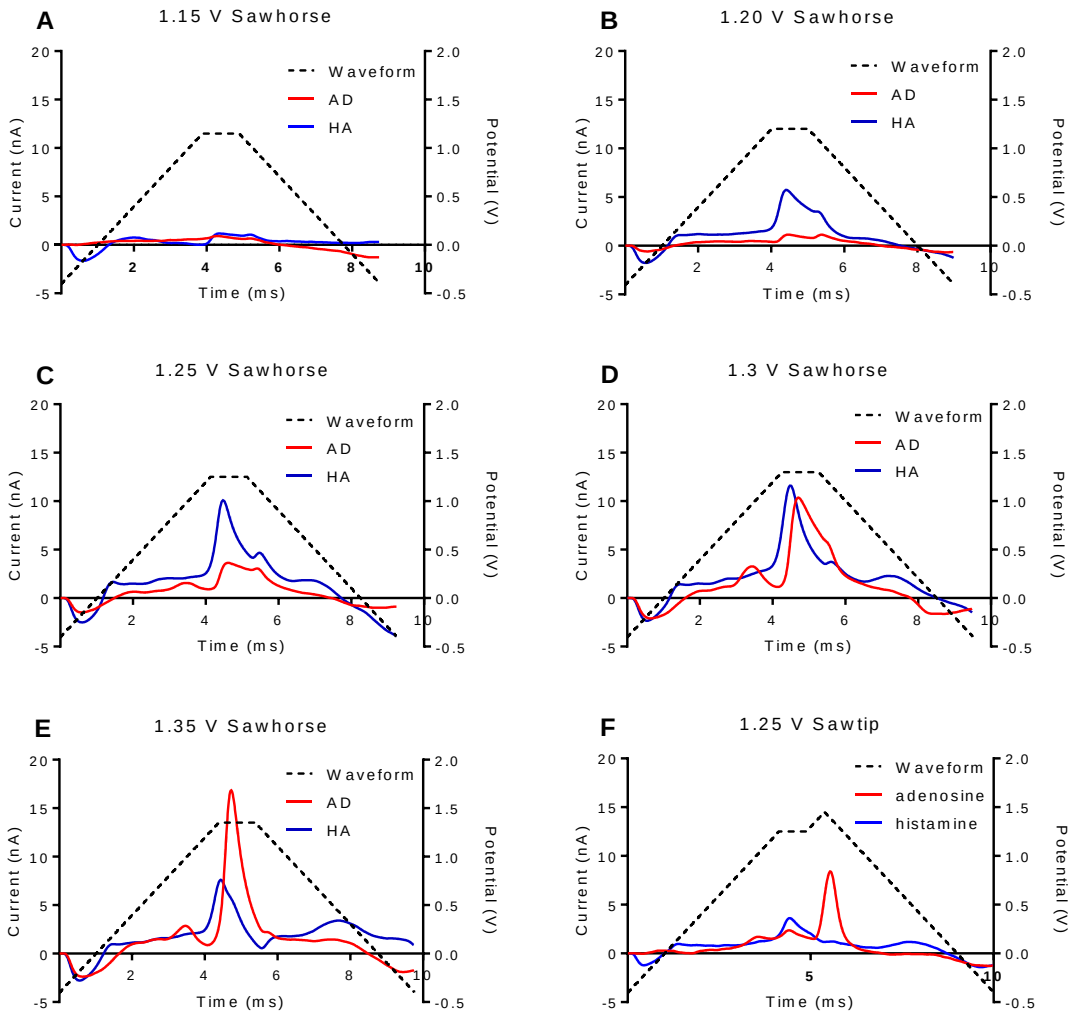

Figure 2.6: Sawhorse waveform demonstrating histamine is more readily oxidized than adenosine with lower switching potentials. Neither oxidize at (**A**) 1.15 V, but histamine oxidizes with (**B**) 1.2 V and (**C**) 1.25 V whereas adenosine is still mostly unreactive. Adenosine begins to oxidize strongly with a (**D**) 1.3 V sawhorse and gives a strong signal with a (**E**) 1.35 V sawhorse. The 1.25 V sawhorse was modified with a triangular switch at 1.45 V to create the (**F**) sawtip waveform that differentiates adenosine and histamine on a different electrode.

The sawhorse waveforms still did not fully allow co-detection of adenosine and histamine. Thus, we designed a waveform with an early plateau to oxidize histamine

that then continued to the switching potential needed for adenosine. We called this a "sawtip" waveform. Due to the generation of a strong current for histamine when using the 1.25 V sawhorse waveform, without seeing much current from adenosine, the first plateau was at 1.25 V. At this plateau, histamine primarily oxidizes, and then the potential is ramped to 1.45 V so as to oxidize adenosine in the usual manner. The full parameters for this "sawtip" waveform have a scan from -0.4 V at 400 V/s up to 1.25 V, where the potential is held for 0.75 ms, and then the potential is ramped up to 1.45 V and then back down to -0.4V at 400 V/s (**Fig. 2.6F**). The repetition frequency of FSCV was kept at 10 Hz and each scan only took 10 ms. The sample sawtip in **Fig. 2.6F** was on a slightly shorter electrode, hence the difference in sensitivity from the from the sawhorse examples.

In Fig. 5F, using the sawtip waveform completely separates the primary peaks of adenosine and histamine. The entirety of the histamine oxidation peak is during the hold at 1.25 V. Almost all of the adenosine signal is on the cathodic scan, as usual. There is a small amount of current for adenosine where histamine oxidizes, but it is faint. Additionally, adenosine still has a strong secondary oxidation peak whereas histamine has no other apparent peaks with this waveform. However, this waveform is not good for separating out ATP or H_2O_2 from the adenosine signal (**Fig. 2.7A**). Therefore, the next step was to create a 'double-hold' waveform. This would allow for the simultaneous separation of histamine signal from adenosine as well as the differentiation of ATP and

H_2O_2 as Ross and Venton did with the sawhorse waveform.[12] The parameters of the 'double-hold' waveform start with the holding potential at -0.4 V, scanning at 400 V/s up to 1.25 V and holding the potential for 0.75 ms, then scanning to 1.35 V where the potential is held for another 0.75 ms. The cathodic sweep then brings the potential back down to -0.4 V again at 400 V/s and this process was repeated at a rate of 10 Hz. **Fig.**

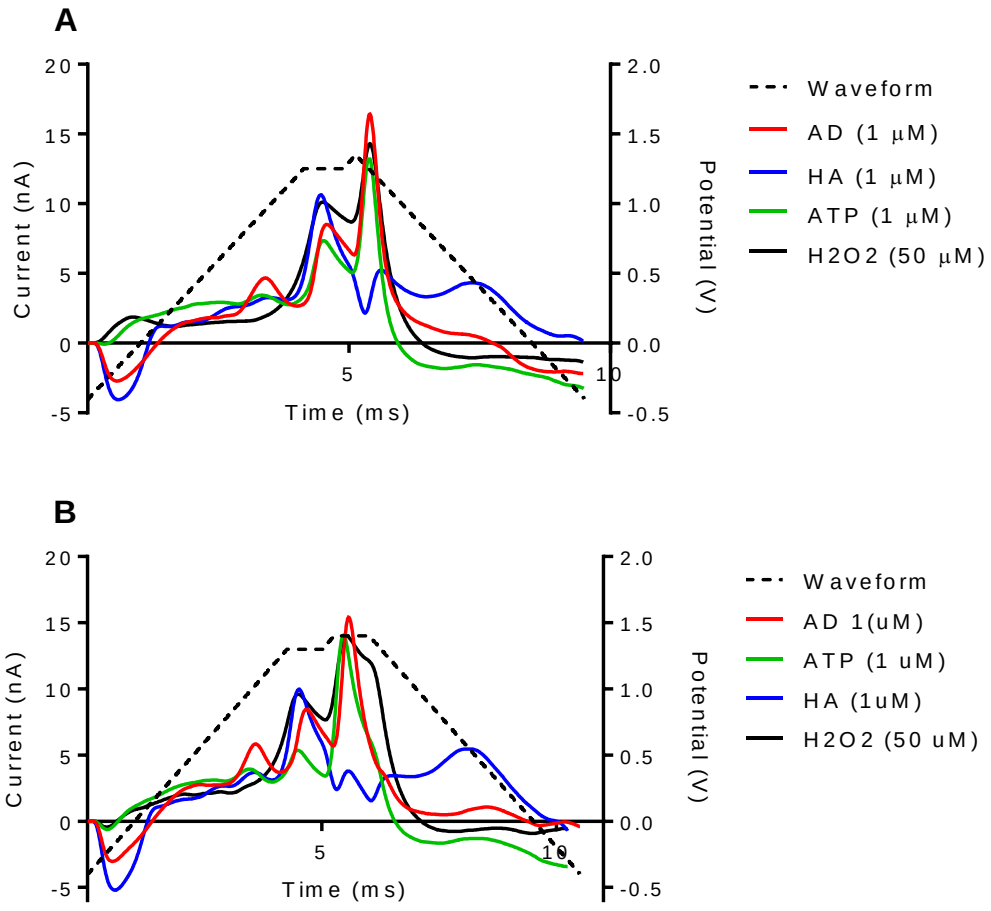

Figure 2.7: Sawtip and double-hold waveforms(**A**) The sawtip waveform oxidizes histamine during the hold at 1.25 V but the voltammograms of adenosine, ATP, and H_2O_2 still look very similar with this waveform. (**B**) Adding a second hold at 1.35 V, akin to the sawhorse waveform, causes the H_2O_2 voltammogram to take on a different shape from adenosine and ATP.

2.7A shows the sawtip waveform with a 1.35 V switching potential. With this waveform, the histamine peak occurs during the hold at 1.25 V whereas the adenosine, ATP, and H_2O_2 look very similar, oxidizing shortly after the switching potential. **Fig. 2.7B** shows that when the sawhorse characteristic is added to the waveform, the broad signal of H_2O_2 looks very different from the narrow peaks of adenosine and ATP. Unfortunately, the adenosine peak and ATP peak are not different from each other with the double-hold waveform. The sawhorse waveform was able to differentiate adenosine and ATP largely due to a "shoulder" peak on the adenosine CV.[12] That characteristic is absent with this waveform. It is possible that there is a discernable difference between these signals that could be determined computationally.

To determine if a computer could differentiate the signals between the analytes using the double-hold waveform we used principal component analysis (PCA) to test mixtures of compounds and predict the concentrations of each analyte. PCA can be used to parse out the subtle differences in the voltammograms of each analyte and has been used to confirm the identity of and quantify neurotransmitters *in vivo*, *in situ*, and *in vitro* with mixtures of analytes.[12,24–28] The first step for each electrode is to make a training set of different concentrations for each analyte: adenosine, histamine (0.1 - 5 µM each), and H_2O_2 (10 – 300 µM). ATP was excluded since it was not sufficiently different than adenosine. A higher range of concentrations is required for H_2O_2 as

CFMEs are less sensitive H_2O_2 compared to most neurotransmitters.[12,29] The resulting voltammograms of different concentrations were used to create a training set for each

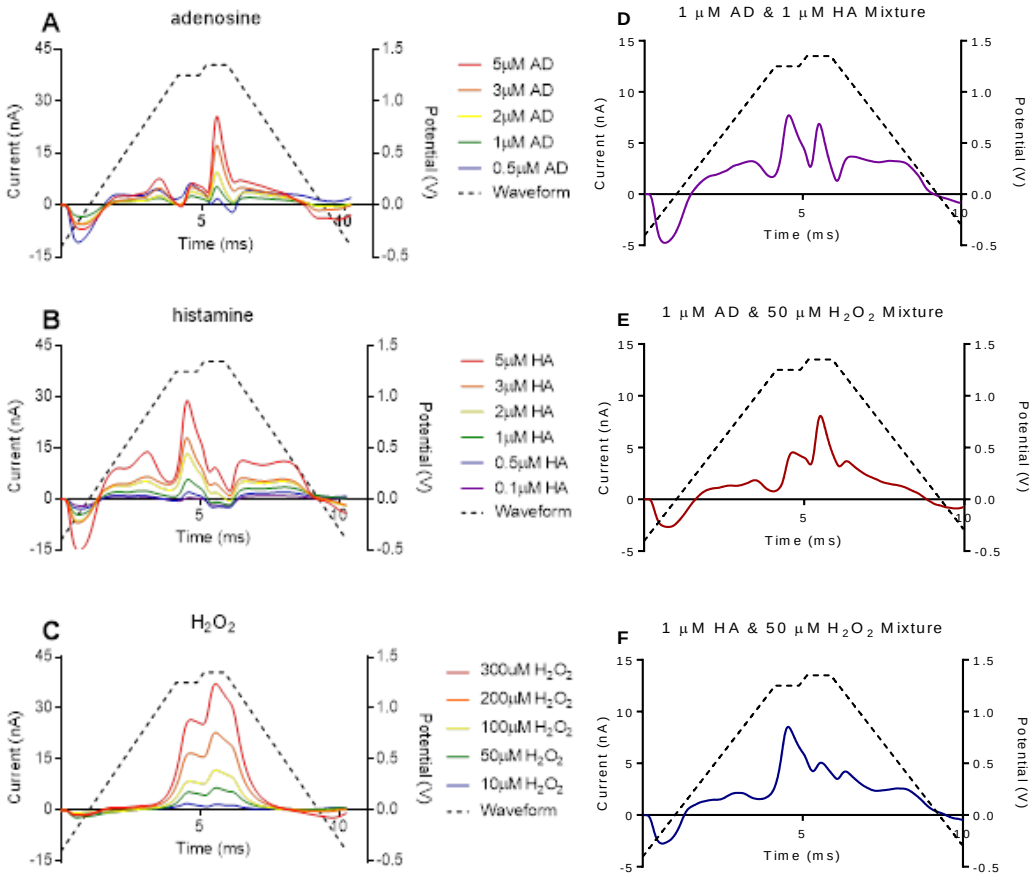

Figure 2.8: Training sets and mixtures of (**A**) adenosine, (**B**) histamine, and (**C**) H_2O_2 with the double-hold waveform. The adenosine oxidizes during the 1.35 V hold, histamine oxidizes during the 1.25 V hold, and H_2O_2 gives a large current during both holds, though the peak at each potential is broader. In the right column are the CVs of the mixtures tested with PCA. The three mixtures contain (**D**) 1 μM AD with 1 μM HA, (**E**) 1 μM AD with 50 μM H_2O_2, (**F**) 1 μM HA with 50 μM H_2O_2.

analyte from which PCA could extract the principal components that make each compound distinct (**Fig. 2.8**). The peak maximum of each analyte was selected as the point from which PCA could determine the concentration in an unknown mixture. Adenosine was quantified based on the peak during the second hold, whereas histamine oxidized almost entirely during the first hold and was therefore quantified from that peak. H_2O_2 has broader peaks during both holds but was quantified from the peak on the second hold because there is greater sensitivity for it at the higher potential. The lowest concentrations of adenosine and H_2O_2 were also removed from the training set as there was no discernible signal from 100 nM adenosine or 1 µM H_2O_2. The three unknown mixtures tested were (A) 1 µM adenosine with 1 µM histamine (B) 1 µM adenosine with 50 µM H_2O_2 and (C) 1 µM histamine with 50 µM H_2O_2. The average predicted concentrations (±SEM) are in **Table 2.1**.

In each mixture the double hold was able to correctly quantify the adenosine and histamine concentration with no significant difference from the actual concentration. As seen in **Fig. 2.8D**, the mixture of adenosine and histamine each give narrow peaks that don't overlap at all. Histamine has a clear peak during the first hold and adenosine has a clear sharp peak during the second hold. PCA was able to pick this out and correctly identify and quantitate the amount of each in the mixture (see **Table 2.1**). Similarly the mixtures containing H_2O_2 clearly show whether adenosine (**Fig. 2.8E**) or histamine (**Fig. 2.8F**) are the compound mixed with H_2O_2 and due to the broadness of

the H_2O_2 peaks, PCA was able to determine that it was present in the mixture. PCA was able to correctly predict when H_2O_2 was present. However, it predicted concentrations 40% lower than what was actually in solution. It is not entirely surprising that H_2O_2 would be the furthest off from the real value, as the means deviate much more for H_2O_2 than adenosine and histamine due to the lower sensitivity for H_2O_2 at CFMEs. This is evident by the higher standard errors. An error of 1 nA corresponds to an error of ± 0.2 µM adenosine but corresponds to an error of ± 7 µM H_2O_2. Additionally, H_2O_2 oxidizes during both holds, convoluting the signal with histamine during the first hold and adenosine during the second hold. This could lead to incorrect attribution of current.

Table 2.1: Principal components analysis of double-hold waveform on mixtures of adenosine, histamine and H_2O_2. All concentrations reported in µM.

	Mixture 1 (n=4)			Mixture 2 (n=4)			Mixture 3 (n=3)		
	Actual	*Observed*	*SEM*	***Actual***	*Observed*	*SEM*	***Actual***	*Observed*	*SEM*
adenosine	**1.0**	1.2	± 0.2	**1.0**	1.4	± 0.2	**-**	0.1	± 0.1
histamine	**1.0**	1.2	± 0.3	**-**	0.04	± 0.4	**1.0**	0.9	± 0.3
H_2O_2	**-**	-	-	**50**	****33	± 7	**50**	****28	± 4

**** represent significant difference from the actual concentration, $p < 0.0001$

2.3.4 Brain slice experiments

The sawtip waveform was tested in brain slices to compare how the sample matrix of a tissue sample would affect the separation. Electrodes were implanted in coronal slices of the caudate putamen. 50 µM histamine and 50 µM adenosine were

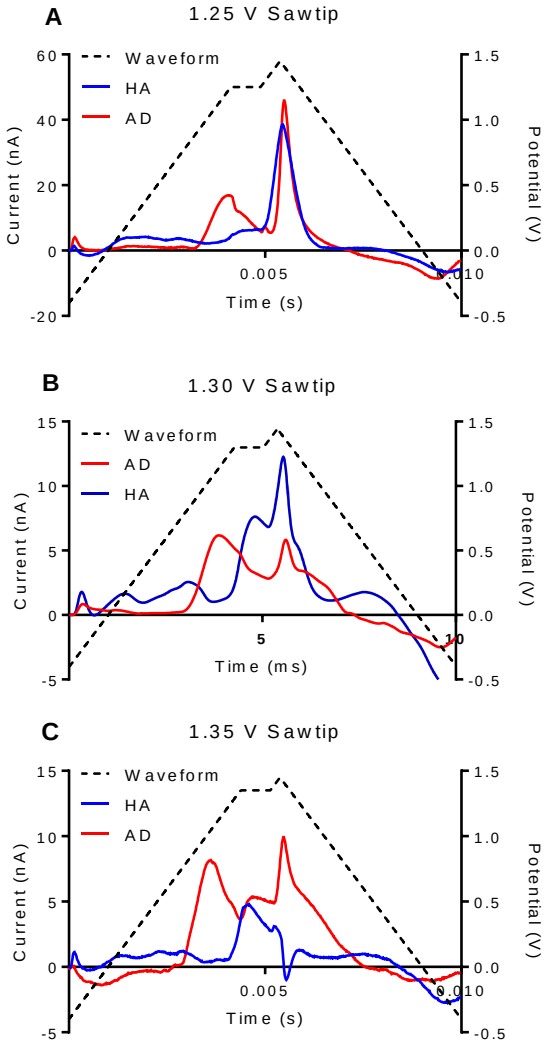

Figure 2.9: Sawtip waveform in brain tissue. Adenosine (red) and histamine (blue) were each picospritzed into the tissue near the CFME. (**A**) The optimized waveform fails to separate the primary oxidation peaks of adenosine and histamine. (**B**) Using a 1.30 V sawtip began to shift the histamine oxidation to the hold, but there is still quite a bit of current where adenosine oxidizes (**C**) Shifting the potential hold up to 1.35 V vs Ag/AgCl gets the oxidation peak of histamine to come through during the hold, but much of the adenosine signal shifts there as well. Currents do not reflect relative sensitivity as the proximity of the picospritzing pipette changes with every swap of solution

each picospritzed on to the electrode at 20psi for 300ms. This resulted in 14 nL of solution being puffed from the micropipette, equating to 0.71 pmols analyte. Using the sawtip waveform with a hold at 1.25 V, the signals of adenosine and histamine look very similar to each other, with the primary peak of each showing up after the switching potential (**Fig. 2.9A**). Shifting that hold up to a higher potential of 1.30 V causes some of the current from histamine to shift over to the hold, but most of the current still occurs on the cathodic scan where adenosine

oxidizes (**Fig. 2.9B**). Strangely, increasing the potential of this hold also increases the size of the secondary oxidation peak of adenosine relative to the primary peak. It is not until the plateau potential is increased to 1.35 V that the histamine peak shifts to occur primarily during the hold (**Fig. 2.9C**). However, some of the adenosine current shifted to the 1.35 V hold as well. Interestingly, the secondary peak of adenosine is higher using this waveform *in situ* compared to *in vitro*. The lower currents found with the higher potential (**Fig 2.8B-C**) are due to picospritzer pipette placement as opposed to actual sensitivity with the two different waveforms.

2.4 Discussion

2.4.1 Histamine oxidizes at a high potential

Histamine has typically been measured using very high oxidation potentials. Electropolymerization, cyclic voltammetry, and FSCV have all traditionally used potentials greater than 1.1 V to detect imidazoles.[11,13,14] In Hashemi's work, she proposes that the traditional peak near the switching potential is a non-faradaic process such as an adsorption peak and that the actual oxidation peak (with FSCV) is about 0.3 V vs Ag/AgCl. However, determining the characteristic oxidation potential of an analyte at a given electrode is fairly simple, and amperometry, which holds at a set potential, is the ideal technique to use. With amperometry, only compounds that oxidize below the chosen potential will generate a current and currents have minimal interference from non-faradaic processes such as capacitive current.[30] Our amperometry experiment

indicates no histamine oxidation using a potential of 0.4 V vs Ag/AgCl and even raising that potential up to 0.9 V generates no current in the presence of histamine. It is not until the potential reaches 1.0 V that the addition of histamine generates a spike in the current. That rise in current reaches a maximum when the applied potential is 1.2 V vs Ag/AgCl, so the formal oxidation potential for histamine at a glassy carbon electrode is around 1.2 V. Previous electrochemical literature on histamine and imidazole oxidation have suggested that the E^0 is 1.2 V, which agrees with our results here.[13,31–33]

Based on the complete lack of current using potentials lower than 1.0 V, it is very unlikely that the peak the Hashemi group sees at 0.3 V is a faradaic process. Their reasoning was based on that fact that non-faradaic adsorption peaks are common near the switching potential.[2] While this is true, it does not mean that all peaks near the switching potential are non-faradiac processes or that non-faradaic processes can't be observed at other potentials in the CV. Additionally, the peak they claim to be histamine oxidation is incredibly broad compared to most faradaic peaks in FSCV, including the peaks observed with the sawtip and double-hold waveforms for histamine. The other major difference is sensitivity. The histamine-selective waveform they propose has a limit of detection of 1 μM, whereas the limit of detection with the sawtip waveform is about 100 nM. An actual electron transfer of an oxidation should generate more current, and subsequently have higher sensitivity, than a background shift or other non-

faradaic process. This all supports the traditional theory that histamine requires a potential of 1.2 V vs Ag/AgCl to oxidize.

In contrast to dopamine, the amperometric signal for histamine decreases with time. On the first injection, the current drops back towards the baseline over time and a second injection of histamine produces less current than the first injection. The decrease in current over time and with a second injection indicates that the oxidation product is fouling the electrode. This is fairly typical of analytes that dimerize or polymerize on the surface of the electrode.[34–36] Wang, et. al. demonstrated that imidazoles can electrochemically polymerize via a one electron oxidation at one of the nitrogen atoms. The resulting radical can then dimerize with another oxidized imidazole radical.[13] Redistribution of the electrons in the conjugated system causes the un-dimerized nitrogen atoms to deprotonate, leaving them susceptible to a subsequent oxidation (see **Scheme 1**). This repeats following the same reaction pathway and results in an imidazole polymer. If this is what is happening with histamine, the product could be fouling in one or two ways. First, the polymer could adhere to surface of the electrode, preventing additional analyte from adsorbing to the carbon surface to undergo oxidation. This should decrease the current generated from any other analytes as the effective surface area of the electrode would decrease. However, from our data (**Fig. 2.2F**), injections of dopamine after injections of histamine still produce similar currents to when histamine was not detected. This implies the surface area of the

electrode and adsorption sites are not significantly changed. Second, the polymer could increase the electrical resistance of the electrode, decreasing the potential seen by the analyte. If the observed potential were to drop by a couple hundred mVs, the resulting histamine current should drop as well. However, dopamine has an oxidation potential of 0.2 V vs Ag/AgCl, so even if there is IR drop, it would still be detected.[37] Experimentally, we see that even after histamine fouls the electrode, dopamine current is still maintained, which suggests that the histamine oxidation product imposes some resistance to the system.

2.4.2 Structural insight with IR-SEC

The exact mechanism of histamine oxidation at a carbon electrode is unknown, as the only structural theories are based on the imidazole family of compounds with none addressing histamine specifically. The two reaction schemes proposed in this work are based on carbon electrode oxidations of imidazole (**Scheme 1**) and the secondary oxidation of adenosine which takes place on an imidazole ring (**Scheme 2**).[13,15] IR-SEC performs a thin-layer, bulk oxidation of histamine in solution and subsequently looks for changes in the molecular structure with IR spectroscopy. No changes were observed after applying potentials of 1.0 V vs Ag/AgCl to a buffered solution of histamine which is reasonable, given that only small amounts of oxidation were observed with 1.0 V in amperometry. However, at 1.3 V, the IR band at 3157 cm^{-1} increases. These data confirm

the amperometry data that show that histamine does not oxidize at low potentials but requires higher potentials in order to create a Faradaic reaction.

There are several possible explanations for the increase in the 3157 cm^{-1} band. The 3157 cm^{-1} band could be low enough to indicate a N-H stretch, implying both nitrogens of the imidazole ring become protonated after oxidation, which would fit the hypothesis that the C2 position is oxidized to a carbonyl in the same manner as the secondary oxidation of adenosine.[38] However, the band near 3150 cm^{-1} band has typically been attributed to sp^2 hybridized C-H stretches.[22,23] The 3157 cm^{-1} wavenumber is slightly higher than typical for sp^2 hybridized C-H stretches, but it is not an incredibly large shift considering the surrounding functional groups. The increase of a sp^2 C-H band would immediately suggest that another sp^2 hybridized C-H bond has been generated via the oxidation of histamine. The only place that an oxidation process could create new sp^2 C-H bonds is on the ethylamine tail but this would also cause a noticeable decrease of sp^3 hybridized C-H stretches in the 2900-3000 cm^{-1} region of the spectrum, and these bands were unaffected by the oxidation. Additionally, ^{13}C NMR of the oxidized solution fromm the CPE experiments show no shift in any of the 5 NMR peaks, suggesting there is no change to any of the carbon functionalization (**Fig. 2.4**). Another possible explanation for a peak for a sp^2 C-H bonds is that the structure of the carbon electrode surface is changing, since the IR could detect that as well. However, the control experiment shows that this structural change only occurs when histamine is

present, and is therefore not just due to applying higher voltages to etch the electrode.[39–41] Therefore, the best explanation for a more sp^2 C-H characters is the stabilization of an existing bond. Imidazolium ions have pK_a values of 16-20 for carbon deprotonation.[42] Therefore, the C2 carbon of histamine can be considered a weak Lewis acid. N-functionalization can increase the pK_a to even higher values suggesting that if histamine were undergoing dimerization and polymerization, the pK_a of that C-H bond should go up as well, resulting in a slight increase in the sp^2 hybridized C-H character of the bond. The IR indicates that changes are slight, so this seems like the best possible explanation, and it fits with the hypothesis that histamine is oxidized via 1-electron oxidation at an imidazole nitrogen group, followed by a subsequent 1-electron oxidation at the other nitrogen as the polymerization progresses.

Based on the amperometric results, the oxidation potential for histamine is 1.2 V vs Ag/AgCl and the rapid drop-off of current is indicative of electrode fouling, likely through histamine polymerization. Between this fouling effect seen during the amperometric readings and the increased sp^2 C-H character seen in the IR-SEC experiment, the one electron oxidation reaction scheme resulting in polymerized imidazole rings (**Scheme 1**) is the more likely candidate for histamine oxidation. The lack of changes in the N-H stretches in the IR spectra and the lack of changes to the ^{13}C NMR peaks disprove the generation of a carbonyl in the manner described in **Scheme 2**. However, this doesn't adamantly prove **Scheme 1** as the structural changes expected

with the electropolymerization would not be IR active. Additional spectroscopic techniques would help confirm the structure, such as mass spectrometry. In theory, the M^+ peak should increase by double, triple, or even further depending on how far the polymerization progresses.

2.4.3 Differentiating histamine and adenosine with FSCV

Due to the rapid time scale of FSCV, it is not uncommon to see oxidation peaks shift to higher potentials. The oxidation peak for dopamine with slow scan cyclic voltammetry is about 0.2 V vs Ag/AgCl, but the rapid scan rate of FSCV at 400 V/s results in a dopamine peak around 0.6 V, a difference of about 0.4 V which corresponds to a 1 ms delay in electron transfer. Histamine is no different. Based on research from the Lee lab[11] and our amperometric data, histamine should oxidize at around 1.2 V on the anodic scan. However, the fast scan rate and sluggish electron transfer kinetics moves the peak and it is more commonly observed on the cathodic scan around 1.3 V, similar to adenosine. Thus, they are difficult to differentiate with traditional waveforms.

The Venton lab is primarily interested in adenosine, but we would like to develop a waveform that gives us the adenosine information and either removes or separates the histamine signal. Using the knowledge gained from the Lee lab, we decided to take a similar approach with a sawhorse waveform.[11,12] The sawhorse waveform was chosen using the idea of chronoamperometry, or stepping to the oxidation potential, to build on a hypothesis that a lower potential can be used to completely oxidize histamine

without oxidizing adenosine. To get the adenosine oxidation, the scan is continued to a switching potential of 1.45 V vs Ag/AgCl or a second hold to oxidize adenosine. As seen in **Fig. 2.6**, there was almost no current for either histamine or adenosine with the 1.15 V sawhorse, but the current for histamine oxidation using a 1.20 V and 1.25 V sawhorse was fairly substantial relative to adenosine oxidation current. Higher potentials of a sawhorse waveform oxidized adenosine as well as histamine, as expected based on the research by Ross and Venton.[12] Using the 1.25 V sawhorse and reinitiating an anodic scan the rest of the way up to 1.45 V, this new 'sawtip' waveform results in a complete separation of the primary peaks of histamine and adenosine. Thus, the hypothesis is true and *in vitro*, there are waveforms that can effectively separate adenosine and histamine. With these waveforms, PCA is also useful to mathematically determine the concentration of each analyte.

The sawtip is not as good at discriminating other analytes, so a double hold waveform was developed to separate histamine, adenosine, and H_2O_2. The sawtip can quantitatively separate histamine from adenosine, and the sawhorse can quantitatively separate adenosine from H_2O_2. Therefore, the double-hold waveform was developed to determine if we could maintain histamine and adenosine separation, but also get H_2O_2 identification and possible ATP identification as well. As expected, the histamine current is most prominent during the first hold of this waveform. The signals of adenosine and ATP look different from what was observed with just the sawhorse waveform, where

the secondary peak, as well as a “shoulder” at the end of the voltammetric peak of adenosine, differentiated if from ATP. With the double-hold waveform, ATP and adenosine look nearly identical. Adenosine still had a stronger secondary peak, but it was not enough to differentiate the two. Fortunately, H_2O_2 still looks noticeably different from the other analytes due to the broader oxidation peaks during the holds in potential.

The training sets for adenosine, histamine, and H_2O_2 for PCA show clear differences in voltammetric profiles. Histamine oxidation occurs entirely during the 1.25 V hold, adenosine oxidation occurs during the 1.35 V hold and some current from the secondary oxidation during the initial anodic scan, and H_2O_2 gives broad peaks during both holds. This is a very clean separation of adenosine and histamine and there is nearly no extraneous current from adenosine on the first hold or from histamine on the second hold. This is clean enough that concentrations of histamine and adenosine can be accurately quantified in a mixture. Based on the predicted concentrations from PCA on the mixtures of these three compounds, H_2O_2 current being present during both holds convoluted the predictions a bit. With each mixture, PCA predicted the correct compounds present. However, whenever H_2O_2 was present, some of the signal was attributed to histamine and adenosine and, as a result, slightly over predicted those concentrations. This was not enough to significantly impact the predicted concentrations of adenosine or histamine, but it was enough to result in a significantly

different predicted H_2O_2 concentration relative to actual concentration. Therefore, while the double-hold waveform would be useful in analyte identification, it is not ideal in an environment where co-release of adenosine, histamine, and/or H_2O_2 is a possibility. It is however, good for discrimination of just adenosine and histamine *in vitro*.

2.4.4 Sawtip waveform in brain slices

There are many complications that can occur when FSCV is taken from the flow cell and transferred to tissue. The denser matrix can decrease diffusion of cations by a factor of 10 fold.[43] The tissue also has a higher resistance than PBS or aCSF which could cause greater impedance to the electrode. Additionally, biofouling is a very common problem with CFMEs.[44] Thus, the optimized sawtip waveform developed in the flow cell did not perform as well in tissue. While the signal of adenosine was largely unaffected, the histamine oxidation peak was shifted to higher values and did not occur during the initial lower hold. Increasing the hold potential to a higher potential then allowed adenosine to be detected as well. The tissue appears to affect histamine more than adenosine, and impedance is the likely culprit, as increased resistance would decrease the potential seen by the electrode. Problems with impedance and polymerization of histamine were observed during the amperometry, so it is apparent that histamine is very sensitive to small changes in impedance. An interesting effect of raising the hold potential up to 1.35 V is that the secondary peak of adenosine increased dramatically. This could indicate that adenosine is oxidizing during the 1.35 V hold and there is a

longer time for adenosine to more completely undergo the primary oxidation process. Alternatively, it could also suggest that this waveform affects the desorption kinetics of the primary oxidation product of adenosine, making it more likely to stick to the surface of the electrode for subsequent scans. This waveform does not look optimal for tissue, but it does show that they can be separated *in vitro*. Future experiments could use electrode treatments, such as Nafion that help prevent the electrode fouling, and would make the detection of adenosine with different waveforms easier.[45,46] Alternatively, carbon nanomaterials have been shown to exhibit electrocatalytic effects that could facilitate the oxidation of histamine at a lower potential which would help separate them better.[47,48] Once the complications that tissue imparts on the electrochemistry can be overcome, a clean separation of histamine and adenosine oxidation peaks should be possible through these waveform manipulations.

2.5 Conclusions:

Histamine oxidation at carbon electrodes is a complicated process. Two theories exist for the structure of the oxidation product of histamine, but the mechanism of oxidation at carbon electrodes had not been proven. The fouling nature of the product seen with amperometry, the subtle increase of sp^2 C-H character observed with IR-SEC, and the lack of change to the ^{13}C NMR of the oxidation product all suggest that the one-electron electropolymerization process is the oxidation scheme for histamine at carbon electrodes. A carbonyl formation should have greatly shifted the ^{13}C NMR peak and

should have decreased the sp^2 C-H character instead. This oxidation takes place at voltages over 1.0 V and is fastest around 1.2 to 1.3 V. Further work needs to be done to confirm the creation of the proposed polymer. The symmetric N-N bond created in this scheme would likely be Raman active. Alternatively, mass spectrometry may be the best option to tell us if histamine is dimerizing

The sawtip and double hold waveforms were developed to separate the signal of histamine from adenosine. Adenosine is still primarily oxidized over 1.35 V, whereas histamine is oxidized at a plateau at 1.25 V. The double-hold waveform allows a better differentiation of adenosine, histamine, and hydrogen peroxide. Depending on the application, either the double-hold waveform or sawhorse waveform could be implemented to get the differentiation of any two of the analytes addressed in this work. Whereas potentials for histamine oxidation shifted in brain slices and the method was less effective, future research on changing the electrode surface may correct for changes in impedance caused by brain tissue and help make this a feasible strategy for differentiating histamine and adenosine *in vivo* and *in situ*.

2.6 References

(1) Threlfell, S.; Cragg, S. J.; Kallo, I.; Turi, G. F.; Coen, C. W.; Greenfield, S. A. *J. Neurosci.* **2004**, *24* (40), 8704–8710.

(2) Samaranayake, S.; Abdalla, A.; Robke, R.; Wood, K. M.; Zeqja, A.; Hashemi, P. *Analyst* **2015**, *140* (11), 3759–3765.

(3) Haas, H. L.; Sergeeva, O. A.; Selbach, O. *Physiol. Rev.* **2008**, *88* (3), 1183–1241.

(4) Wada, H.; Inagaki, N.; Yamatodani, A.; Watanabe, T. *Trends Neurosci.* **1991**, *14* (9),

415–418.

(5) Brown, R. E.; Stevens, D. R.; Haas, H. L. *Prog. Neurobiol.* **2001**, *63* (6), 637–672.

(6) Flik, G.; Folgering, J. H. A.; Cremers, T. I. H. F.; Westerink, B. H. C.; Dremencov, E. *J. Mol. Neurosci.* **2015**, *56* (2), 320–328.

(7) Flik, G.; Dremencov, E.; Cremers, T. I. H. F.; Folgering, J. H. A.; Westerink, B. H. C. *Eur. J. Neurosci.* **2011**, *34* (11), 1747–1755.

(8) Hashemi, P.; Dankoski, E. C.; Wood, K. M.; Ambrose, R. E.; Wightman, R. M. *J. Neurochem.* **2011**, *118* (5), 749–759.

(9) Gemkow, M. J.; Davenport, A. J.; Harich, S.; Ellenbroek, B. A.; Cesura, A.; Hallett, D. *Drug Discovery Today*. 2009, pp 509–515.

(10) Denno, M. E.; Privman, E.; Borman, R. P.; Wolin, D. C.; Venton, B. J. *ACS Chem. Neurosci.* **2016**, *7* (3), 407–414.

(11) Chang, S.-Y.; Jay, T.; Muñoz, J.; Kim, I.; Lee, K. H. *Analyst* **2012**, *137* (9), 2158.

(12) Ross, A. E.; Venton, B. J. *Anal. Chem.* **2014**, *86* (15), 7486–7493.

(13) Wang, H. L.; O'Malley, R. M.; Fernandez, J. E. *Macromolecules* **1994**, *27* (4), 893–901.

(14) Dryhurst, G. *Electrochemistry of Biological Molecules*; 1977.

(15) Swamy, B. E. K.; Venton, B. J. *Anal. Chem.* **2007**, *79* (2), 744–750.

(16) Machan, C. W.; Sampson, M. D.; Chabolla, S. A.; Dang, T.; Kubiak, C. P. *Organometallics* **2014**, *Accepted A*, Ahead of Print.

(17) Zavarine, I. S.; Kubiak, C. P. *J. Electroanal. Chem.* **2001**, *495* (2), 106–109.

(18) Nichols, A. W.; Chatterjee, S.; Sabat, M.; Machan, C. W. *Inorg. Chem.* **2018**, *57* (4), 2111–2121.

(19) Swamy, B. E. K.; Venton, B. J. *Analyst* **2007**, *132* (9), 876–884.

(20) Ashley, K.; Pons, S. *Chem. Rev.* **1988**, *88* (4), 673–695.

(21) Kaim, W.; Fiedler, J. *Chem. Soc. Rev.* **2009**, *38* (12), 3373.

(22) Collado, J.; Ramirez, F. *J. Raman Spectrosc.* **1999**, *30* (November 1998), 391–397.

(23) Mukherjee, V.; Yadav, T. *Spectrochim. Acta - Part A Mol. Biomol. Spectrosc.* **2016**, *165*, 167–175.

(24) Nguyen, M. D.; Lee, S. T.; Ross, A. E.; Ryals, M.; Choudhry, V. I.; Venton, B. J. *PLoS One* **2014**, *9* (1), e87165.

(25) Keithley, R. B.; Mark Wightman, R.; Heien, M. L. *TrAC - Trends in Analytical Chemistry*. 2009, pp 1127–1136.

(26) Heien, M. L. A. V.; Johnson, M. A.; Wightman, R. M. *Anal. Chem.* **2004**, *76* (19), 5697–5704.

(27) Fortin, S. M.; Cone, J. J.; Ng-Evans, S.; McCutcheon, J. E.; Roitman, M. F. *Curr. Protoc. Neurosci.* **2015**, *2015*, 7.25.1-7.25.20.

(28) Johnson, J. A.; Rodeberg, N. T.; Wightman, R. M. *ACS Chem. Neurosci.* **2016**, *7* (3), 349–359.

(29) Sanford, A. L.; Morton, S. W.; Whitehouse, K. L.; Oara, H. M.; Lugo-Morales, L. Z.; Roberts, J. G.; Sombers, L. A. *Anal. Chem.* **2010**, *82* (12), 5205–5210.

(30) Michael, A. C.; Borland, L. M. *Front. Neuroeng.* **2010**, 544.

(31) Sarada, B. V.; Rao, T. N.; Tryk, D. A.; Fujishima, A. *Anal. Chem.* **2000**, *72* (7), 1632–1638.

(32) Zhang, L.; Huang, W.; Wang, Z.; Cheng, J. *Anal. Sci.* **2002**, *18* (10), 1117–1120.

(33) Bitziou, E.; O'Hare, D.; Patel, B. A. *Anal. Chem.* **2008**, *80* (22), 8733–8740.

(34) Griessenauer, C. J.; Chang, S.-Y.; Tye, S. J.; Kimble, C. J.; Bennet, K. E.; Garris, P. a; Lee, K. H. *J. Neurosurg.* **2010**, *113* (3), 656–665.

(35) Manica, D. P.; Mitsumori, Y.; Ewing, A. G. *Anal. Chem.* **2003**, *75* (17), 4572–4577.

(36) Abdalla, A.; Atcherley, C. W.; Pathirathna, P.; Samaranayake, S.; Qiang, B.; Peña, E.; Morgan, S. L.; Heien, M. L.; Hashemi, P. *Anal. Chem.* **2017**, *89* (18), 9703–9711.

(37) Gualandi, I.; Tonelli, D.; Mariani, F.; Scavetta, E.; Marzocchi, M.; Fraboni, B. *Sci. Rep.* **2016**, *6*.

(38) Swamy, B. E. K.; Venton, B. J. *Anal. Chem.* **2007**, *79* (2), 744–750.

(39) Hafizi, S.; Kruk, Z. L.; Stamford, J. A. *J. Neurosci. Methods* **1990**, *33* (1), 41–49.

(40) Heien, M. L. A. V; Phillips, P. E. M.; Stuber, G. D.; Seipel, A. T.; Wightman, R. M. *Analyst* **2003**, *128* (12), 1413–1419.

(41) Takmakov, P.; Zachek, M. K.; Keithley, R. B.; Walsh, P. L.; Donley, C.; McCarty, G. S.; Wightman, R. M. *Anal. Chem.* **2010**, *82* (5), 2020–2028.

(42) Alder, R. W.; Allen, P. R.; Williams, S. J. *J. Chem. Soc. Chem. Commun.* **1995**, No. 12, 1267.

(43) Rice, M. E.; Gerhardt, G. A.; Hierl, P. M.; Nagy, G.; Adams, R. N. *Neuroscience* **1985**, *15* (3), 891–902.

(44) Rodeberg, N. T.; Johnson, J. A.; Bucher, E. S.; Wightman, R. M. *ACS Chem. Neurosci.* **2016**, acschemneuro.6b00142.

(45) Ross, A. E.; Venton, B. J. *Analyst* **2012**, *137* (13), 3045–3051.

(46) Vreeland, R. F.; Atcherley, C. W.; Russell, W. S.; Xie, J. Y.; Lu, D.; Laude, N. D.; Porreca, F.; Heien, M. L. *Anal. Chem.* **2015**, *87* (5), 2600–2607.

(47) Yang, X.; Feng, B.; He, X.; Li, F.; Ding, Y.; Fei, J. *Microchim. Acta* **2013**, *180* (11–12), 935–956.

(48) Yang, C.; Denno, M. E.; Pyakurel, P.; Venton, B. J. *Anal. Chim. Acta* **2015**, *887*, 17–37.

Chapter 3

Regional variations of spontaneous, transient adenosine release in brain slices

Our doubts are traitors, and make us lose the good we oft might win, by fearing to attempt

-William Shakespeare

Abstract

Transient adenosine signaling has been recently discovered *in vivo*, where the concentration is on average 180 nM and the duration only 3-4 seconds. In order to rapidly screen different brain regions and mechanisms of formation and regulation, here we develop a rat brain slice model to study adenosine transients. The frequency, concentration, and duration of transient adenosine events were compared in the prefrontal cortex (PFC), hippocampus (CA1), and thalamus. Adenosine transients in the PFC were similar to those *in vivo*, with a concentration of 160 ± 10 nM, and occurred frequently, averaging one every 50 ± 5 s. In the thalamus, transients were infrequent, occurring every 280 ± 40 s, and lower concentration (110 ± 10 nM), but lasted twice as long as in the PFC. In the hippocampus, adenosine transients were less frequent than in the PFC, occurring every 79 ± 7 s, but the average concentration (240 ± 20 nM) was significantly higher. The response to adenosine A_1 antagonist 8-cyclopentyl-1,3-dipropylxanthine (DPCPX) differed by region; DPCPX had no significant effects in the PFC but increased the average transient concentration in the thalamus and both the transient frequency and concentration in the hippocampus. Thus, the amount of adenosine available to activate receptors, and the ability to upregulate adenosine signaling with DPCPX, varies by brain region. This is an important consideration for designing treatments that modulate adenosine in order to cause neuroprotective effects.

3.1 Introduction:

Adenosine is a neuromodulator that also protects the brain from adverse events such as hypoxia or traumatic brain injury.[1] Adenosine activates inhibitory A_1 receptors which, in turn, decrease cAMP concentrations resulting in a decrease in neuronal firing.[2] A_1 adenosine receptors play an inhibitory role, modulating neurotransmitter release and are found both presynaptically and postsynaptically.[3,4] The A_1 antagonist DPCPX increases cell excitability whereas the A_1 agonist N^6-cyclopentyladenosine decreases excitability.[5,6] Adenosine also activates excitatory A_{2A} receptors on blood vessels to cause vasodilation, increasing oxygen delivery to the brain.[7] Changes in extracellular adenosine concentrations have been observed on time scales ranging from minutes to hours.[8,9,10] However, a faster form of transient adenosine release has recently been characterized, which lasts only a few seconds.[11] While adenosine release can be electrically stimulated,[12] recent studies have found transient adenosine events that are not stimulated, but spontaneous, and occur randomly.[11,13,14] Rapid adenosine can modulate electrically-stimulated dopamine release.[15] There is also a correlation between transient adenosine and transient oxygen events, supporting the hypothesis that rapid adenosine serves a neuroprotective role.[16] However, there are many open questions about mechanisms of spontaneous adenosine release and the source of the adenosine that are not easy to decipher *in vivo* and different *in situ* or *in vitro* models are needed.

In anesthetized rats, the average concentration of a spontaneous adenosine transient is 170 nM in the caudate-putamen and 190 nM in the prefrontal cortex (PFC).[11] Each event lasts approximately 3 s and the average time between two consecutive events ranges from 1-3 min depending on the brain region. Adenosine transients are cleared in part by extracellular metabolic enzymes such as adenosine deaminase and adenosine kinase as well as equilibrative nucleoside transporters.[13] The previous work has elucidated some of the functions and mechanisms of transient adenosine, but it is unclear if transient adenosine behaves in a similar manner throughout the brain. So far, differences in concentration and frequency have been discovered in the caudate and PFC but other brain regions are largely unexplored. Adenosine is neuroprotective and adenosine transients may play a role in stressful circumstances such as hypoxia or ischemia.[17] As such, it is important to understand adenosine transients in regions typically studied in stroke, including the thalamus and the hippocampus.[18,19] Defining differences between regions could help determine the extent to which adenosine modulation varies throughout the brain.

To characterize neurochemical release, pharmacological experiments are often used and brain slice models are widely employed because they allow rapid screening while bypassing the blood brain barrier. Brain slices have been used to elucidate the basic mechanisms of long-term adenosine release, identifying intracellular and extracellular mechanisms of formation.[20,21,22,23] In particular, brain slices are convenient models for studying the effects of hypoxia and ischemia on adenosine pathways, by

restricting the flow of oxygenated buffer to the slice.[24,25,26,27] Using fast-scan cyclic voltammetry (FSCV), stimulated adenosine release has been measured in brain slices as well.[12,28] However, it is not as obvious whether spontaneous transients will occur in brain slices since only the terminals are present. In spinal cord slices of the dorsal horn, the Zylka group did report low frequency transient adenosine changes, occurring every few minutes, that were due to the breakdown of ATP in the extracellular space by prostatic acid phosphatase and ecto-5'-nucleotidase.[29,30] However, the extent to which transient adenosine is released in slices from central brain regions is unknown.

In this study, we used FSCV with carbon fiber microelectrodes (CFMEs) to characterize transient adenosine events in PFC, thalamus, and hippocampus brain slices and define differences in how they are regulated by A1 receptors. Adenosine frequency, as well as the concentration and duration of events, varied by brain region. The effect of the A_1 antagonist DPCPX also varied by brain region, showing there are regional differences in both the amount of adenosine neuromodulation and the regulation of adenosine transients by A_1 receptors. This work establishes brain slices as a platform for pharmacological experiments to understand the mechanism, formation, and regulation of transient adenosine release, facilitating experiments that are not feasible *in vivo* due to toxicity or blood-brain barrier permeability. Understanding these differences in how transient adenosine is regulated will lead to a better understanding of how much adenosine is available in different regions to act as a neuromodulator.

3.2 Methods:

3.2.1 Slice preparation

Protocols for animal experiments were approved by the Animal Care and Use Committee at the University of Virginia. Male Sprague-Dawley rats weighing between 250-350 grams were housed in a university vivarium and were provided food and water *ad libitum* prior to experimentation. Rats were anesthetized with isoflurane (approximately 1mL/100g) in a desiccator and promptly beheaded. The brain was quickly removed and placed in a beaker of cold (0-5°C) oxygenated aCSF to recover for 2 minutes. 400 µm thick coronal slices were collected from the PFC and thalamus. 400 µm thick sagittal slices were collected from the hippocampus. Slices were made with a Leica vibratome (LeicaVT1000S, Bannockburn, IL), and kept in a beaker of oxygenated aCSF at 37°C in a water bath for 1 hour of recovery. During experiments, 37°C oxygenated aCSF was perfused over the slices at a rate of 2 mL/min. Approximate coordinates are +4.6 mm anterior-posterior (AP), +2.0 mm mediolateral (ML), and −2.0 mm dorsoventral (DV) for the PFC; -3.1 mm AP, +3.0 mm ML, and −6.0 mm DV for the thalamus, and -4.5 mm AP, +3.8 mm ML, and −3.0 mm DV for the CA1 region of the hippocampus. After allowing the slice and the electrode to equilibrate in the slice chamber, electrodes were implanted 75 µm into the tissue. Once the electrode was implanted and the background stabilized (approximately 5 min), FSCV data was collected for 1 hour. After experimentation, each electrode was calibrated with 1 µM adenosine. Depending on the

length and taper of the electrode, the calibration factor varied between 6 and 37 nA/μM with most electrodes around 13 nA/μM.

3.2.2Chemicals

Slices were kept in oxygenated artificial cerebral spinal fluid (aCSF), as described previously.[51] aCSF was comprised of 126 mM NaCl, 2.5 mMKCl, 1.2 mM NaH_2PO_4 monohydrate, 2.4 mM $CaCl_2$ dihydrate, 1.2 mM $MgCl_2$ hexahydrate, 25 mM $NaHCO_3$, 11 mM glucose, and 15 mM tris(hydroxymethyl)aminomethane and was adjusted to pH 7.4 immediately prior to experimentation. A 10 mM stock solution of adenosine was prepared in 0.1 mM $HClO_4$ and this was diluted daily in aCSF to 1 μM for post-calibration of the CFMEs. One mM stock solutions of 8-cyclopentyl-1,3-dipropylxanthine (DPCPX, Sigma-Aldrich) were prepared in dimethyl sulfoxide (DMSO) and kept frozen until used. Stock DPCPX was added to perfusion aCSF to make a 100 nM solution and slices were perfused for 15 min before the electrode was implanted and adenosine measurements made while DPCPX was perfused.

3.2.3 Electrochemistry

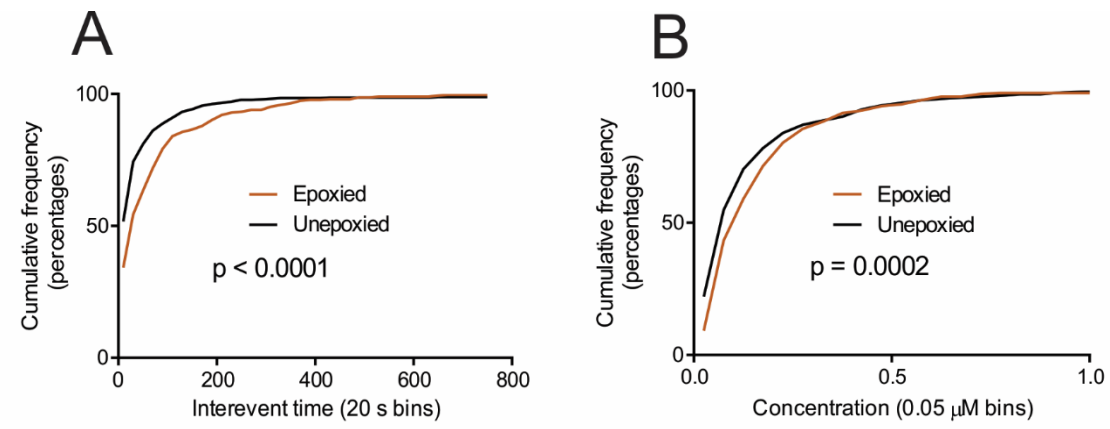

Figure 3.1: Epoxied electrodes are less sensitive to adenosine transients (**A**) Epoxied electrodes detect significantly fewer transients than those without epoxy. (**B**)This is due to an increase in sensitivity, exhibited by the 2-fold increase in the fraction of transients found in the smallest concentration bin (0 to 0.05 µM)

Adenosine transients were measured using FSCV with CFMEs as described previously.[31] Briefly, electrodes were fabricated by aspirating a 7 µm diameter T-650 carbon fiber (Cytec Engineering Materials, West Patterson, NJ, USA) into a glass capillary. The capillaries were pulled on a vertical puller and the exposed fiber subsequently cut to ~50 µm. Traditionally, the tips of electrodes are sealed with epoxy to prevent buffer from leaking into the capillary. However, we have found that this decreases our electrodes' sensitivity to adenosine transients (**Fig. 3.1**). If there is a long taper to the glass to ensure a watertight seal, the epoxy step is unnecessary to electrode fabrication. Waveform generation and cyclic voltammogram collection was performed through HDCV (from UNC Chemistry, Chapel Hill, NC) with a Dagan ChemClamp potentiostat (Dagan Corporation; Minneapolis, MN, USA). The waveform used for adenosine detection scans from a holding potential of -0.4V to a switching potential of +1.45V at a rate of 400V/s and a frequency of 10Hz.

3.2.4 Data Analysis and Statistics

Adenosine transients were analyzed using the principal components analysis (PCA) in the HDCV Analysis software as describe previously.[11] Briefly, the 5 largest transients from each slice were used to create a training set to which other transients would be compared. The principal components were extracted and the raw data was then transformed into a concentration vs time trace to identify and quantify transients while excluding any signal that generated excessive residual current. All statistics were performed using Graphpad Prism 6. Mean values are given ± standard error of the mean (SEM). The times between consecutive transients, or inter-event time, were pooled and binned in 20 second bins for cumulative frequency graphs. The inter-event times of the three brain regions were compared with each other using the Kruskal-Wallis test (non-parametric, unpaired, one-way ANOVA). Comparison of the impact of DPCPX on inter-event time was analyzed with the Kolmogorov-Smirnov test (non-parametric, unpaired t-test). 8 brain slices were used for each brain region with no more than 3 slices coming from the same animal (each group of 8 slices was from at least 4 different animals). 8 additional slices were also used for each brain region for DPCPX experiments. There was no noticeable effect of different coordinates within each region.

3.3 Results and Discussion

3.3.1 Adenosine detection in slices with FSCV

The main goal of this study was to compare spontaneous, transient adenosine efflux in multiple brain regions. Adenosine was measured in real-time with FSCV, where

it undergoes two oxidation processes that are visualized as two oxidation peaks.[31] Using a voltage waveform from -0.4 V to 1.45 V and back at 400 V/s, the primary oxidation process yields a peak at 1.4 V on the cathodic scan. On subsequent scans, a secondary oxidation process occurs, giving a peak at 1.2 V on the anodic scan which has less current than the primary peak. These peaks are seen in **Fig. 3.2**, a 3D color plot of an adenosine transient in the PFC. The applied voltage is displayed on the y-axis, time on the x-axis, and the current in false color. There are two green/purple peaks in the center of the plot that are due to adenosine oxidation, and the secondary peak at 1.2 V always comes after the primary peak at 1.4 V. The inset is the cyclic voltammogram, which plots the current at each voltage and is a fingerprint for adenosine detection. There is also an artifact at the onset of the adenosine transients *in situ,* seen as a vertical colored line in the color plot (**Fig. 3.2**). This artifact is largest around 0.5 V, but the duration is much shorter than adenosine release and we hypothesize it is due to ionic changes. Additionally, there is a small peak at -0.2 V. However, this negative peak is at the start of the anodic scan so it's more likely to be a background shift due to adsorption than a reduction process. To examine how adenosine changes over time, the current at the peak potential of the primary oxidation peak (i *vs* t) is shown above the color plot. The duration of a transient is calculated as the time it takes to rise from and decline to 10% of the maximum current; this transient lasts about 2.8 s. The peak concentration of this transient is 500 nM, converted from the current using a post-calibration factor, and this is an example of one of the larger transients that are observed.

3.3.2 Regional variation of spontaneous adenosine

From previous work studying stimulated adenosine release and long-term adenosine changes, we hypothesized that there would be regional differences in spontaneous adenosine transients in brain slices. Three brain regions were chosen: the PFC, where frequent transients had been reported *in vivo*,[11] and two new regions where spontaneous adenosine had not been explored *in vivo*: the hippocampus CA1 and the thalamus. All of these regions express intermediate to high levels of adenosine A_1 receptors and are important in memory formation and recollection.[32] The PFC is, in part, responsible for cognitive control, connecting working memory and personality.[33,34] The hippocampus is associated with declarative and spatial memory in both humans and rats,[35] and the CA1 plays an important role

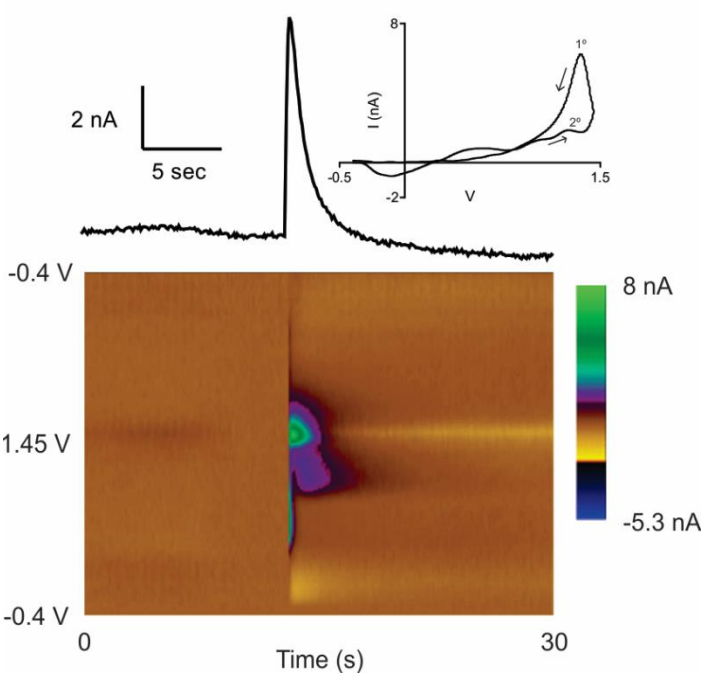

Figure 3.2: Adenosine transient in the hippocampus. The color plot shows all data, with scanned voltage on the y-axis, time on the x-axis, and current depicted in color. A horizontal slice in the 3D color plot results in the i vs t plot (above) and a vertical slice gives the cyclic voltammogram at a given time (inset).

in maintaining an individual's autobiographical memory and ability to mentally place themselves in time frames other than the present.[36] The thalamus is involved with memory, learning, speech, personality and relaying sensory information, all of which can be compromised due to a stroke.[37]

Fig. 3.3 shows example color plots and data traces in each region. In the PFC, transients occur frequently, with 9 transients happening within this 2 min window (**Fig. 3.3A**). In the thalamus, transient adenosine events are less frequent with only 3 events in 2 min (**Fig. 3.3B**). Although the events in the thalamus were relatively infrequent, some do still occur in rapid succession which results in a broad range of inter-event times for this region. In the hippocampus CA1, transient adenosine events are less frequent than in the PFC but more frequent than in the thalamus. Seven transient adenosine events are identified in this 2-minute sample (**Fig. 3.3C**). Other regions of the hippocampus, including the CA2, CA3, and dentate gyrus were also tried, but robust transients were rarely seen in those locations.

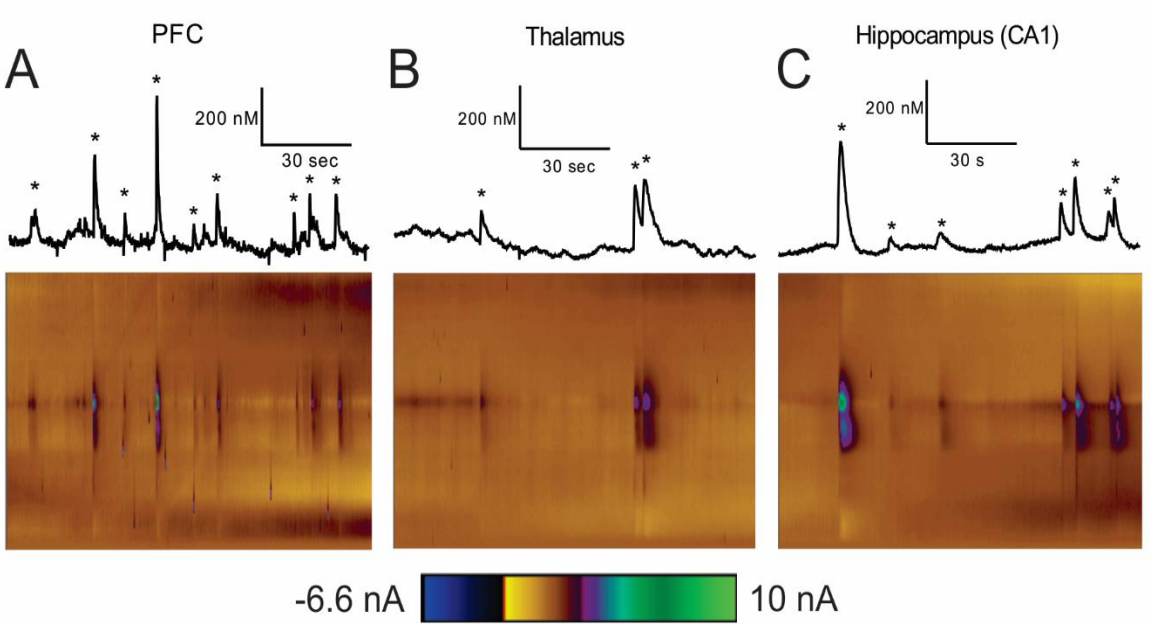

Figure 3.3: Concentration traces (top) and 3D color plots (bottom) for the (**A**) PFC, (**B**) thalamus, and (**C**) CA1. Adenosine transients are marked with stars in the concentration traces, which are all scaled the same to highlight the variety of concentrations in each region. (*) denotes an adenosine transient.

In order to evaluate differences in regions statistically, one hour of data was collected from 8 slices per region. The number of transients varied by region, with 65 ± 17 transients per hour in the PFC, 10 ± 2 transients in the thalamus, and 42 ± 7 transients in the CA1. There is an overall significant effect of brain region on number of transients (one-way ANOVA, $p = 0.005$) and a significant difference between the PFC and

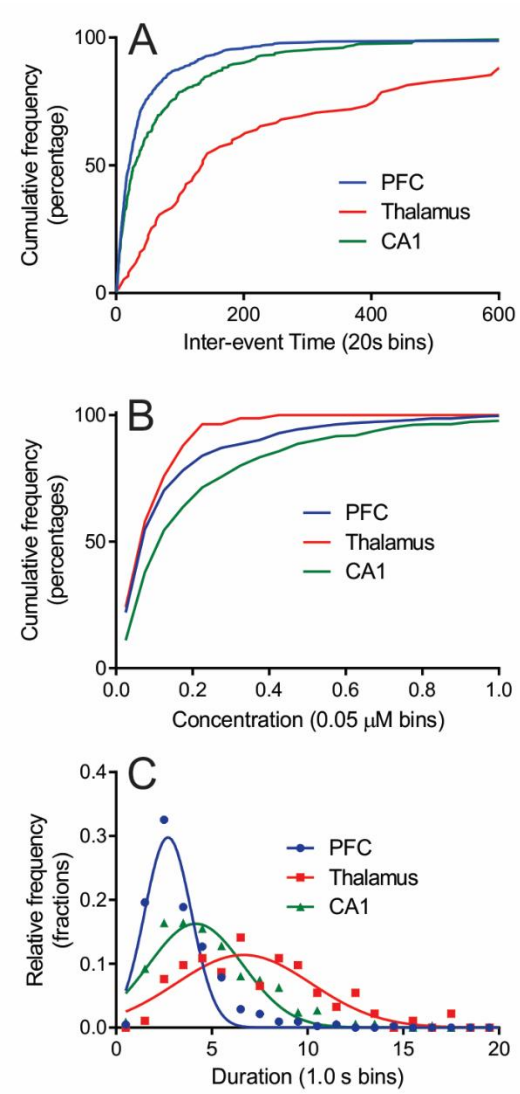

Figure 3.4: Differences in (**A**) interevent time (K–W test, $p < 0.0001$), (**B**) concentration (K–W test, $p < 0.0001$), and (**C**) duration (ANOVA, $p < 0.0001$) between the prefrontal cortex, thalamus, and CA1 region of the hippocampus. All are n = 8 slices.

the thalamus (Bonferroni post-test, p = 0.004), but there is no significant difference between the CA1 and the PFC (p = 0.20) or the thalamus (p = 0.28). In all brain regions, the frequency of adenosine events is higher in the initial part of the hour (**Fig. 3.5A**). However, this drop in frequency was consistent between slices and the time measured was the same for all slices. The drop in frequency may be due to the tissue being unable to synthesize adenosine, and a previous study found improvement by adding ribose and adenine in the perfusion buffer.[26] However, adenine is electroactive and adding large amounts of it to the slice interferes with adenosine detection by FSCV. Alternatively, the increased frequency at the beginning could be due to electrode implantation disturbing tissue and causing more release.[38] Sample colors plots in **Fig. 3.3** were taken from the first 10 minutes in their respective experiments when the transient frequencies were

highest, and trends in concentration, duration, and relative frequency were also compared for both 1 hour and the first 10 min, and no differences were observed.

To examine frequency, we compared the distribution of inter-event times, which is the time between two consecutive transients. The inter-event times for each region were binned into 20 second bins and plotted as a cumulative distribution due to the Poisson nature of the relative frequency distribution (**Fig. 3.4A**). The distribution of inter-event times in the PFC (blue) rises rapidly, indicating a high frequency of events, whereas the rise for the CA1 (green) is slower. In the thalamus (red), the distribution rises very slowly, not even reaching 50% until the 120-140 s bin, indicating that half of all transients were more than 2 min apart. A Kruskal-Wallis (K-W) test indicates a significant difference in the cumulative inter-event frequency distributions ($p < 0.0001$, n = 510 transients in the PFC, 75 in the thalamus, and 328 in the CA1). Dunn's post-tests indicate a significant difference between inter-event time distributions for the CA1 and the PFC ($p = 0.0007$), the CA1 and the thalamus ($p < 0.0001$), and the PFC and the thalamus ($p < 0.0001$). **Table 3.1** lists the median and mean inter-event times for each region.

Fig. 3.3 also demonstrates that there is a large range of concentrations of adenosine transients. Many transients are small, less than 50 nM, and the majority of transients have concentrations around or below 100 nM. Larger transients are also observed; for example, the large event in the CA1 trace is 350 nM and the largest shown in the PFC is 470 nM. In general, larger transients were more likely to be observed in the hippocampus. Concentrations ranged from 10 nM up to 2.7 µM and **Fig. 3.4B** shows the

cumulative distribution of transients (50 nM bins). The relative frequency distribution of concentration is not Gaussian, so we assume a Poisson distribution, as we did with inter-event time. The thalamus has a larger percentage of transients in the small concentration bins causing it to reach 100% quickly whereas the PFC has several transients higher than 200 nM so it takes longer to reach 100%. The CA1 has the most large concentration transients, so it takes longer for its cumulative frequency curve to rise. A K-W test reveals a main effect of brain region for the concentration distribution ($p < 0.0001$). Dunn's post-test indicates the distribution in the CA1 is significantly different from that in the PFC ($p < 0.0001$, n = 336 and 518, respectively) as well as the thalamus ($p < 0.0001$, n = 336 and 83, respectively). However, there was no significant difference between the PFC and thalamus ($p > 0.99$, n = 518 and 83, respectively). **Table 3.1** gives mean and median event concentrations in each region. The mean concentration of each adenosine transient was 160 ± 10 nM in the PFC, 110 ± 10 nM in the thalamus, and 240 ± 20 nM in the CA1.

Another parameter to compare between brain regions is the event duration, defined here as the time it takes for a transient to rise and decline to 10% of its maximum concentration. **Table 3.1** compares the mean duration of transients which were 3.4 ± 0.1 s in the PFC, 7.4 ± 0.4 s in the thalamus, and 4.9 ±0.1 s in the CA1. The frequency distribution in **Fig. 3.4C** shows that the distribution of durations is Gaussian in each brain region, allowing for a one-way ANOVA for comparison. Overall, there was a main effect of brain region on event duration (ANOVA, $p < 0.0001$). Bonferroni

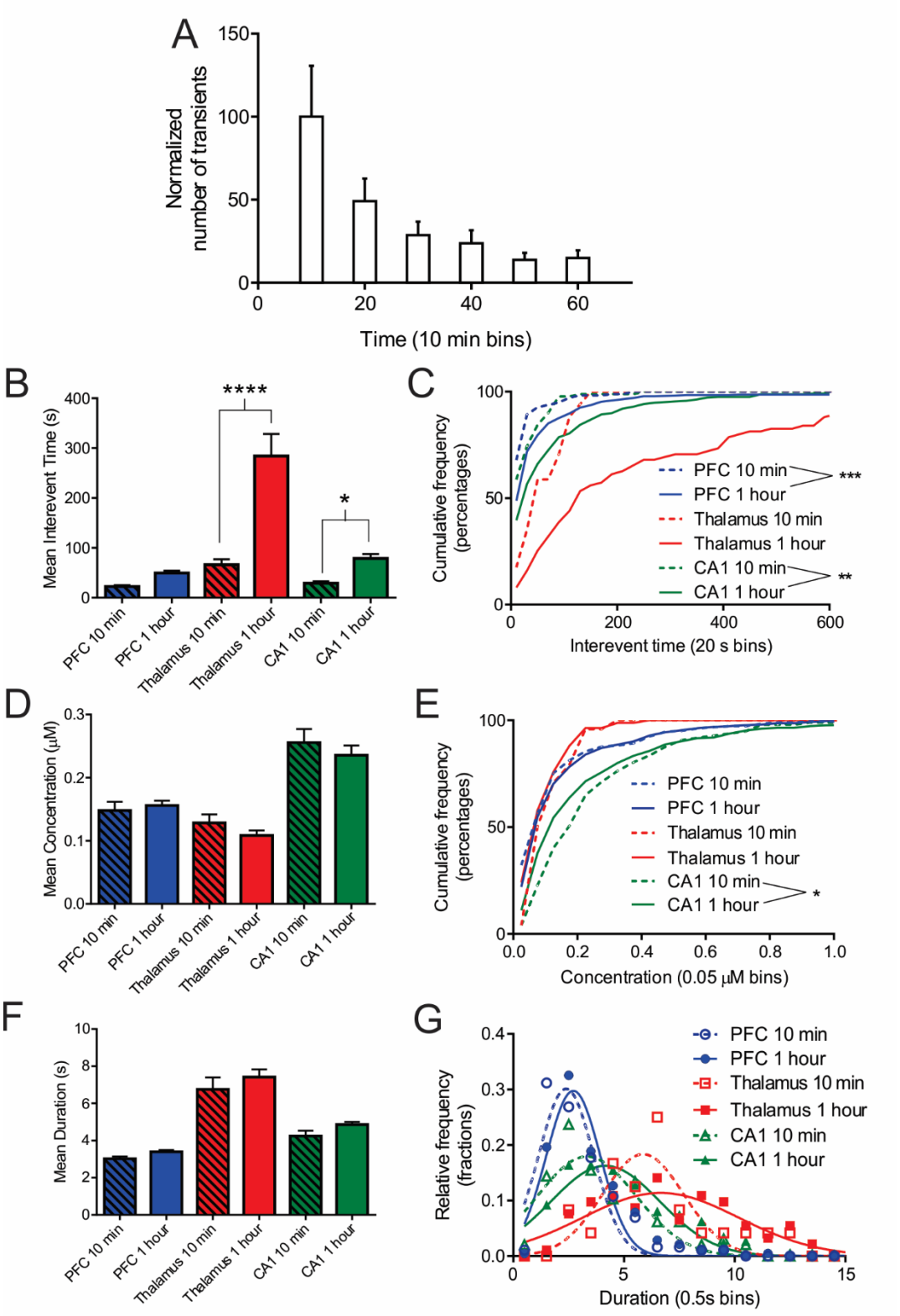
A
Normalized number of transients
150
100
50
0
0
20
40
60
Time (10 min bins)
B
Mean Interevent Time (s)
400
300
200
100
0
****
*
PFC 10 min
PFC 1 hour
Thalamus 10 min
Thalamus 1 hour
CA1 10 min
CA1 1 hour
C
Cumulative frequency (percentages)
100
50
0
PFC 10 min
PFC 1 hour
Thalamus 10 min
Thalamus 1 hour
CA1 10 min
CA1 1 hour
***
**
0
200
400
600
Interevent time (20 s bins)
D
Mean Concentration (μM)
0.3
0.2
0.1
0.0
PFC 10 min
PFC 1 hour
Thalamus 10 min
Thalamus 1 hour
CA1 10 min
CA1 1 hour
E
Cumulative frequency (percentages)
100
50
0
PFC 10 min
PFC 1 hour
Thalamus 10 min
Thalamus 1 hour
CA1 10 min
CA1 1 hour
*
0.0
0.2
0.4
0.6
0.8
1.0
Concentration (0.05 μM bins)
F
Mean Duration (s)
10
8
6
4
2
0
PFC 10 min
PFC 1 hour
Thalamus 10 min
Thalamus 1 hour
CA1 10 min
CA1 1 hour
G
Relative frequency (fractions)
0.4
0.3
0.2
0.1
0.0
PFC 10 min
PFC 1 hour
Thalamus 10 min
Thalamus 1 hour
CA1 10 min
CA1 1 hour
0
5
10
15
Duration (0.5s bins)

Figure 3.5: 10-minute analysis of adenosine transients (**A**) Transients are most frequent during the first 10 minutes of a 1 hour experiment (n=8 slices). As such, if only the first 10 minutes of data is analyzed from each slice, the mean inter-event times (**B**) and inter-event time distributions (**C**) are significantly affected. However, this makes no impact on the mean concentration of transients (**D**) and only slightly affects the concentration distribution of transients in the CA1 (**E**). The 10 minute analysis made no impact on the average duration of transients (**F-G**). Due to the marginal differences between the two methods of analysis, the full hour of data from each slice was used for subsequent experiments to ensure a large enough sample size for confident analysis, particularly in the thalamus.

post-tests indicate a significant difference between the PFC and thalamus ($p < 0.0001$), and a significant difference for the CA1 with both the PFC ($p = 0.01$) and the thalamus ($p = 0.002$). All three regions have transients that last less than 2 s. However, the distribution is very narrow, in the PFC, whereas the distribution is broader in the CA1 and even more so in the thalamus.

Because of the drop off of adenosine transients with time, we also repeated this analysis with only the first 10 minutes of data (**Figs. 3.5**). Frequency of release was higher in the first 10 min, as expected, (**Figs. 3.5B-C**) but the trends were the same, with the PFC producing the most frequent events and the thalamus the least frequent events.[11] The 10 min. data have similar trends to the 1 hour data, with no changes in the mean concentration or durations of transients compared to the 1 hour analysis (**Fig. 3.5D-G**). Because the number of transients is low in only 10 min, particularly in the thalamus, it would take many more slices to have enough transients to fully define the distribution, so the full hour of data from each slice was analyzed for the subsequent drug experiments.

3.3.3 Biological Implications of Regional Variations in Adenosine

One of the main findings of this work is that the frequency of adenosine transients varies dramatically between regions. Past pharmacological experiments *in vivo* have pointed to the frequency of transients as the primary way that transient adenosine is regulated, and this work extends that to show frequency has major differences between brain regions.[11,39] The median inter-event time in the thalamus (132 s) is 6 times larger than the PFC (20 s) and 4 times larger than the hippocampus (30 s). In the thalamus, the median inter-event time is similar to the frequency observed by Zylka's group in spinal cord slices, where transients were not as frequent.[29] These differences in frequency show that the number of transient adenosine release events that could modulate neurotransmission or blood flow is substantially higher in the PFC. In particular, more frequent transients would increase the chance that receptors were activated, and the highest frequency transients occur in the PFC which has a lower expression of A_1 receptors than the thalamus or CA1, so more transients might be needed to activate receptors that are more diffuse.[32]

The concentration of adenosine transients also varied by brain region. The hippocampus CA1 had more large events than the other two regions, the largest of which was 2.7 µM. In contrast, the highest concentration in the PFC was just over 1 µM and only 400 nM in the thalamus. Most events in both the thalamus and the PFC were less than 90 nM, which is about the affinity of adenosine for A_1 receptors.[40] However, these transients are occurring on top of the basal concentration of adenosine, which is

about 33 nM in the thalamus and cortex, and 200 nM in the hippocampus.[41,42] Thus, most transients would be large enough to active A_1 receptors.[41] Since excitatory A_{2A} receptors require a higher concentration of adenosine to become activated (K_d~150 nM), the wide distribution of transient concentrations in the CA1 and PFC may be to differentiate the need for A_1 activation versus A_{2A} activation.[40] In addition, the concentrations are highest in the hippocampus, which has lower vascular density, and where adenosine might have to diffuse further to provide blood flow modulation.[16,43]

Duration is important because it, along with concentration, would control how long adenosine receptors could be activated. Transient adenosine is cleared fastest in the PFC and much slower in the thalamus. Equilibrative nucleoside transporter 1 (ENT1), adenosine kinase, and adenosine deaminase are all clearance mechanisms for transient adenosine.[13] Interestingly, ENT1 is expressed at higher levels in the thalamus and cortex, where clearance is slower, than in the hippocampus.[44] Likewise, the thalamus also exhibits higher activity of adenosine deaminase than either of the other two regions.[45] Thus, the slow clearance of adenosine in the thalamus suggests that ENT1 and adenosine deaminase are not the primary mechanisms of transient adenosine clearance. Previously, even when ENT1, adenosine kinase, and adenosine deaminase were blocked simultaneously, there was still fast clearance, so other mechanisms of clearance may be responsible for the rapid clearance rates in the PFC.[13] There is an inverse relationship between frequency/concentration and duration, with the thalamus having lower frequencies and concentrations, but longer durations. The longer duration

may therefore compensate for the lower frequency and allow more receptor activation. Alternatively, the need for adenosine may vary among regions, particularly since the differences between transients in each region would likely result in different downstream effects such as glutamate modulation.

3.3.4 Adenosine transients are similar in vivo and in situ

In the first report of transient adenosine measurements *in vivo,* the mean inter-event time in the PFC was 108 s, whereas it is 48 s in brain slices.[11] The established detection limit *in vivo* was 40 nM, but lower background noise in slices allows a lower limit of detection, 10 nM. This increased sensitivity means more small events are detected and counted, driving both the average concentration and the average inter-event time down. Excluding all events in PFC slices below 40 nM increases the mean inter-event time from 48 s to 63 s, which is still more frequent than *in vivo*. Excluding these low concentration events also increases the mean concentration to 190 nM, the same as the 190 nM average found *in vivo*. Transient adenosine release lasts longer in brain slices than *in vivo*. The mean duration *in vivo* in the PFC was 2.8 (± 0.1) s whereas *in situ*, it was 3.6 (± 0.1) s. This may indicate that transporters or metabolic processes are impaired in slices compared to *in vivo* measurements. However, the concentrations, frequencies, and durations are still very similar between the two models which indicates that slices are a viable method to study transient adenosine release and will be useful for understanding mechanisms of release or pharmacological studies in the future.

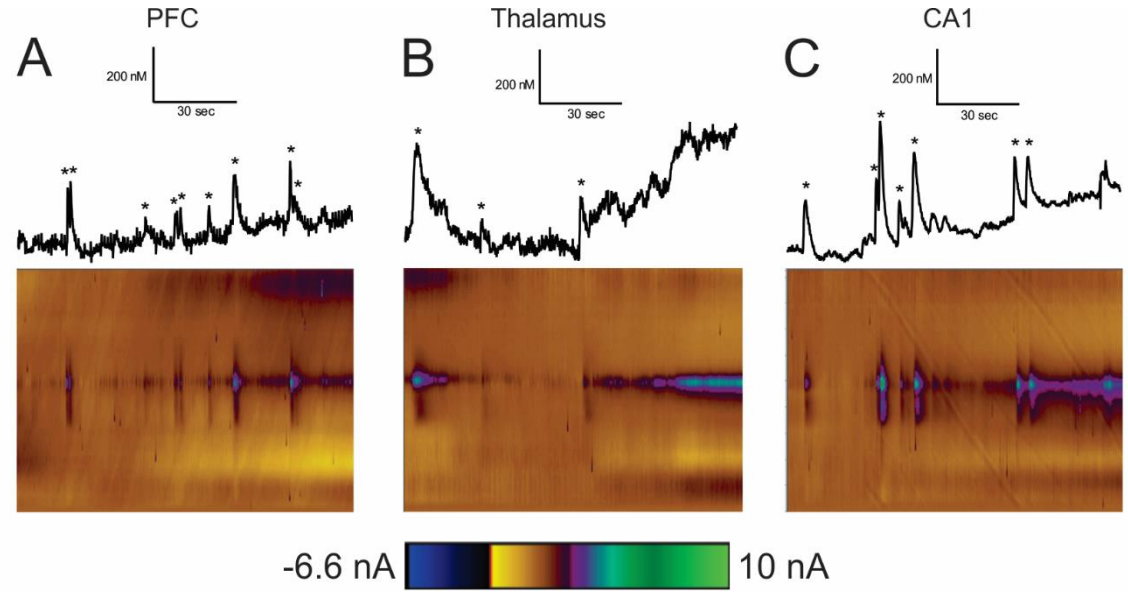

Figure 3.6: Concentration changes (top) and 3D color plots (bottom) for the (**A**) PFC, (**B**) thalamus, and (**C**) CA1 when treated with 100 nM DPCPX. Verified adenosine transients are marked with a star in the concentration traces.

3.3.5 Effect of A_1 antagonism on transients in each of the brain regions

Spontaneous adenosine release is mediated by A_1 receptors but the extent to which this occurs in different brain regions is not known.[11] A_1 receptors are inhibitory G protein coupled receptors, lowering cAMP levels and subsequently decreasing cell excitability.[2] Adenosine modulates glutamate and GABA release through activation of presynaptic A_1 autoreceptors.[49] DPCPX is a high affinity inhibitor of adenosine A_1 receptors (K_i = 0.5 nM).[50] Brain slices were bathed in aCSF containing 100 nM DPCPX[50] before and during measurements of adenosine. **Fig. 3.6** shows sample color plots and concentration traces**.** The number of transients in each region is about the same as control (**Fig. 3.3)**, but the concentrations do change, particularly in the thalamus and

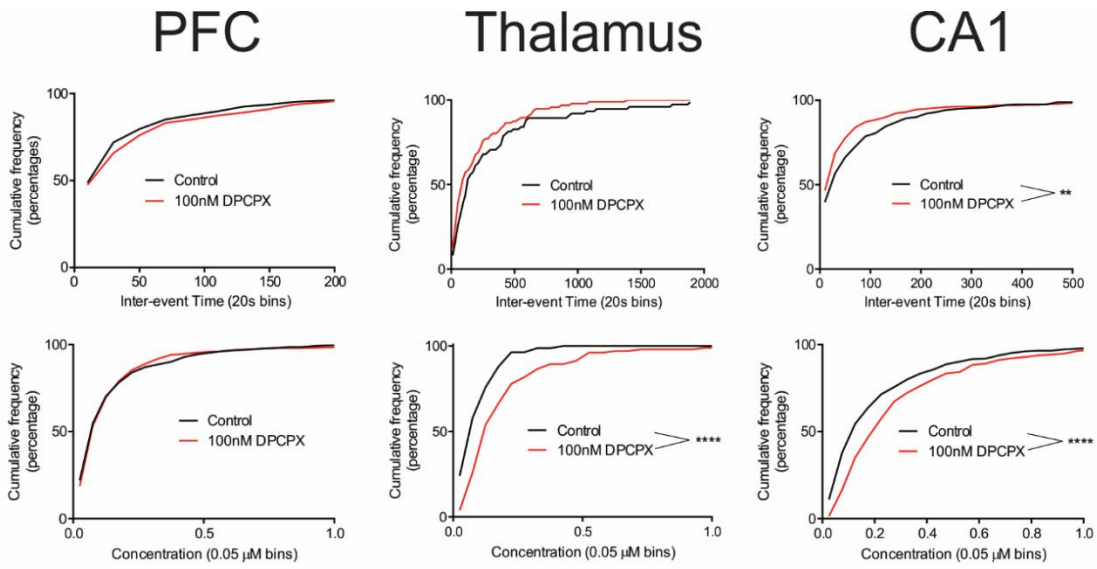

Figure 3.7. Cumulative distributions of the inter-event times (top) and concentrations (bottom) of adenosine transients in the PFC (left), thalamus (middle), and CA1 (right) with DPCPX. Control is black, and treated with 100 nM DPCPX is red. A K–S test was performed for all graphs, and significant differences are marked by asterisks, **p < 0.01, ****p < 0.0001.

hippocampus where larger transients are more commonly observed after DPCPX. The average number of transients per hour in the PFC (65 ± 8) after DPCPX was exactly the same as in control slices (65 ± 17). The average number of transients were also not significantly different in other regions, going up only slightly after DPCPX in the thalamus from 10 ± 2 to 13 ± 3, (*t*-test, $p = 0.49$, n = 8) and in the CA1 from 42 ± 7 to 51 ± 12 (*t*-test, $p = 0.31$, n = 8). **Fig. 3.7** shows cumulative frequency distributions for each brain region with and without DPCPX. There is no change in cumulative distribution of inter-event times in PFC slices treated with DPCPX (KS-test, $p = 0.15$) or in the thalamus (KS-test, $p = 0.14$). However, there was a significant increase in the inter-event time distribution in the CA1 (KS-test, $p = 0.003$), as the transients became more frequent

(**Table 3.1**). This significant change in frequency is interpreted with some caution because the number of transients did not also significantly change.

The average concentration of all transient adenosine events in the PFC remained unchanged with DPCPX, but the distribution of concentrations increased significantly in the CA1 (KS, $p < 0.0001$) and the thalamus (KS, $p < 0.0001$). This means that there were more large transients after A_1 inhibition. The change was particularly large in the thalamus, where the event concentration doubled with DPCPX. Thus, DPCPX had more of an effect on concentration than frequency, with large changes in both the CA1 and thalamus. However, DPCPX had little effect in the PFC on either frequency or concentration. No significant difference was anticipated of DPCPX on duration since A1 receptors are not responsible for clearance. The only significant effect was in the thalamus, where duration decreased with DPCPX, but the sample size was small.

Table 3.1: Inter-event time, concentration, and duration of spontaneous adenosine transients in the pre-frontal cortex, thalamus, and CA1 region of the hippocampus under control conditions and with A_1 antagonist, DPCPX (100 nM)

Brain Region	**Inter-event Time (s)**			**Concentration (nM)**			**Duration (s)**	
	Median	*Mean*	*100nM DPCPX*	*Median*	*Mean*	*100nM DPCPX*	*Mean*	*100nM DPCPX*
Prefrontal cortex	20	50 (±5)	53 (±4)	90	160 (±10)	160 (±10)	3.4 (±0.1)	3.6 (±0.1)
Thalamus	133	280 (±40)	210 (±30)	90	110 (±10)	210 (±20)****	7.4 (±0.4)	6.2 (±0.4)*
Hippocampus (CA1)	30	79 (±7)	58 (±7)**	140	240 (±20)	310 (±10)****	4.9 (±0.2)	5.4 (±0.2)

Errors are SEM *Significantly different distributions than control for that region (Kolmogorov-Smirnov tests for inter-event times and concentrations; unpaired t-test for duration)

3.3.6 Biological implications of regional differences in response to A_1 antagonist

DPCPX blocks the inhibitory effects of adenosine A_1 receptors and previous work *in vivo* shows that adenosine transients increased in frequency in both the PFC and caudate-putamen after DPCPX.[11] In contrast, in PFC slices, there were no significant differences in the inter-event time, concentration, or duration of adenosine transients when perfused with 100 nM DPCPX. As described above, adenosine transients *in situ* occur at a higher frequency than *in vivo* and the PFC has the highest rate of adenosine transients, so it is possible that A_1 receptors may not be able to increase the rate in this region. DPCPX did have effects in both the CA1 and thalamus. It is especially interesting that the concentration shifts in the hippocampus, where it was already large without drug. The average concentration in the CA1 after DPCPX indicates that a higher proportion of transients here are large enough to activate A_{2a} receptors, and thus may better link adenosine signaling to blood flow.[40] There was also a significant increase in the concentration of transients in the thalamus with DPCPX which would also shift more transients to values that are able to activate A_{2a} receptors.

These results are interesting because they show that A_1 receptors may not regulate adenosine transients to the same magnitude in all brain regions. A_1 receptors are highly expressed in both the thalamus and the hippocampus and only moderately expressed in the cortex.[32] Thus, the effects may be correlated to A_1 expression levels. A_1 receptors may have less effect in the PFC, leading to the higher frequency without drug and no change in frequency when they are blocked with A_1 antagonist DPCPX. A_1

receptors self-regulate adenosine release and these results are important because A_1 receptor antagonists might be used to increase the amount of adenosine available to act as a neuroprotective agent, particularly during events that stress the tissues such as ischemia or physical damage.[5,11] However, the regional differences suggest that the drug might not be equally effective in all regions, showing that regulation of adenosine neuromodulation via A_1 activation states may differ regionally.

3.4 Conclusions

Here, we demonstrate regional differences in spontaneous, transient adenosine release in brain slices. The release frequency is highest in the PFC, whereas the hippocampus has the largest concentration, and the thalamus has the longest duration. Because frequency, concentration, and duration control the amount of adenosine available to act at receptors, the profile of rapid adenosine release varies between regions. A_1 inhibition with DPCPX increased the concentration of adenosine transients in the hippocampus and the thalamus but not in the PFC. The differences in regulation by A_1 inhibition show that drugs that regulate adenosine release also have different effects in different regions. Overall, this study is important because if shows the amount of adenosine available to provide neuromodulatory and neuroprotective effects varies by brain region, and that regional difference may be an important consideration when designing experiments to promote the neuroprotective effects of adenosine.

3.5 References

(1) Tominaga, K.; Shibata, S.; Watanabe, S. *Neurosci. Lett.* **1992**, *145* (1), 67–70.

(2) Cunha, R. a. *Purinergic Signal.* **2005**, *1* (2), 111–134.

(3) Rebola, N.; Coelho, J. E.; Costenla, A. R.; Lopes, L. V.; Parada, A.; Oliveira, C. R.; Soares-da-Silva, P.; de Mendonca, A.; Cunha, R. A. *Eur. J. Neurosci.* **2003**, *18* (4), 820–828.

(4) Stockwell, J.; Jakova, E.; Cayabyab, F. S. *Molecules* **2017**, *22* (4), 676.

(5) Cechova, S.; Elsobky, A. M.; Venton, B. J. *Neuroscience* **2010**, *171* (4), 1006–1015.

(6) Miranda, M. F.; Hamani, C.; de Almeida, A.-C. G.; Amorim, B. O.; Macedo, C. E.; Fernandes, M. J. S.; Nobrega, J. N.; Aarão, M. C.; Madureira, A. P.; Rodrigues, A. M.; Andersen, M. L.; Tufik, S.; Mello, L. E.; Covolan, L. *Front. Cell. Neurosci.* **2014**, *8* (October), 312.

(7) Belardinelli, L.; Shryock, J. C.; Snowdy, S.; Zhang, Y.; Monopoli, A.; Lozza, G.; Ongini, E.; Olsson, R. A.; Dennis, D. M. *J. Pharmacol. Exp. Ther.* **1998**, *284* (3), 1066–1073.

(8) Lloyd, H. G.; Fredholm, B. B. *Neurochem. Int.* **1995**, *26* (4), 387–395.

(9) Pazzagli, M.; Pedata, F.; Pepeu, G. *Eur. J. Pharmacol.* **1993**, *234* (1), 61–65.

(10) Cui, M.; Bai, X.; Li, T.; Chen, F.; Dong, Q.; Zhao, Y.; Liu, X. *PLoS One* **2013**, *8* (2), e57065.

(11) Nguyen, M. D.; Lee, S. T.; Ross, A. E.; Ryals, M.; Choudhry, V. I.; Venton, B. J. *PLoS One* **2014**, *9* (1), e87165.

(12) Pajski, M. L.; Venton, B. J. *ACS Chem. Neurosci.* **2010**, *1* (12), 775–787.

(13) Nguyen, M. D.; Ross, A. E.; Ryals, M.; Lee, S. T.; Venton, B. J. *Pharmacol. Res. Perspect.* **2015**, *3* (6), e00189.

(14) Adamah-Biassi, E. B.; Almonte, A. G.; Blagovechtchenski, E.; Grinevich, V. P.; Weiner, J. L.; Bonin, K. D.; Budygin, E. A. *J. Neurosci. Methods* **2015**, *256*, 56–62.

(15) Ross, A. E.; Venton, B. J. *J. Neurochem.* **2015**, *132* (1), 51–60.

(16) Wang, Y.; Venton, B. J. *J. Neurochem.* **2017**, *140* (1), 13–23.

(17) Dale, N.; Pearson, T.; Frenguelli, B. G. *J. Physiol.* **2000**, *526 Pt 1*, 143–155.

(18) Seo, H. G.; Kim, D.-Y.; Park, H. W.; Lee, S.-U.; Park, S.-H. *J. Korean Med. Sci.* **2010**, *25* (11), 1638–1645.

(19) Popp, A.; Jaenisch, N.; Witte, O. W.; Frahm, C. *PLoS One* **2009**, *4* (3), e4764.

(20) Cunha, R. A.; Vizi, E. S.; Ribeiro, J. A.; Sebastião, A. M. *J. Neurochem.* **1996**, *67* (5), 2180–2187.

(21) Mitchell, J. B.; Lupica, C. R.; Dunwiddie, T. V. *J. Neurosci.* **1993**, *13* (8), 3439–3447.

(22) Wall, M.; Dale, N. *Curr. Neuropharmacol.* **2008**, *6* (4), 329–337.

(23) Diógenes, M. J.; Neves-Tomé, R.; Fucile, S.; Martinello, K.; Scianni, M.; Theofilas, P.; Lopatář, J.; Ribeiro, J. A.; Maggi, L.; Frenguelli, B. G.; Limatola, C.; Boison, D.; Sebastião, A. M. *Cereb. Cortex* **2014**, *24* (1), 67–80.

(24) Chauhan, N. K.; Young, A. M. J.; Gibson, C. L.; Davidson, C. *Eur. J. Pharmacol.* **2013**, *698* (1–3), 322–329.

(25) Frenguelli, B. G.; Llaudet, E.; Dale, N. *J. Neurochem.* **2003**, *86* (6), 1506–1515.

(26) Nedden, S. Zur; Doney, A. S.; Frenguelli, B. G. *J. Neurochem.* **2014**, *128* (1), 111–124.

(27) Duarte, J. M.; Cunha, R. A.; Carvalho, R. A. *J Neurochem* **2016**, *136* (5), 947–957.

(28) Pajski, M. L.; Venton, B. J. *Purinergic Signal.* **2013**, *9* (2), 167–174.

(29) Street, S. E.; Walsh, P. L.; Sowa, N. A.; Taylor-Blake, B.; Guillot, T. S.; Vihko, P.; Wightman, R. M.; Zylka, M. J. *Mol. Pain* **2011**, *7* (27), 80.

(30) Street, S. E.; Kramer, N. J.; Walsh, P. L.; Taylor-Blake, B.; Yadav, M. C.; King, I. F.; Vihko, P.; Wightman, R. M.; Millan, J. L.; Zylka, M. J. *J. Neurosci.* **2013**, *33* (27), 11314–11322.

(31) Ross, A. E.; Nguyen, M. D.; Privman, E.; Venton, B. J. *J. Neurochem.* **2014**, *130* (1), 50–60.

(32) Swamy, B. E. K.; Venton, B. J. *Anal. Chem.* **2007**, *79* (2), 744–750.

(33) Goodman, R. R.; Snyder, S. H. *J. Neurosci.* **1982**, *2* (9), 1230–1241.

(34) Koechlin, E.; Ody, C.; Kouneiher, F. *Science (80-.).* **2003**, *302* (5648), 1181–1185.

(35) Raine, A.; Lencz, T.; Bihrle, S.; LaCasse, L.; Colletti, P. *Arch. Gen. Psychiatry* **2000**, *57* (2), 119.

(36) Bunsey, M.; Eichenbaum, H. *Nature* **1996**, *379* (6562), 255–257.

(37) Bartsch, T.; Dohring, J.; Rohr, a.; Jansen, O.; Deuschl, G. *Proc. Natl. Acad. Sci.* **2011**, *108* (42), 17562–17567.

(38) Van Der Werf, Y. D.; Scheltens, P.; Lindeboom, J.; Witter, M. P.; Uylings, H. B. M.; Jolles, J. *Neuropsychologia* **2003**, *41* (10), 1330–1344.

(39) Ross, A. E.; Nguyen, M. D.; Privman, E.; Venton, B. J. *J. Neurochem.* **2014**, *130* (1), 50–60.

(40) Nguyen, M. D.; Wang, Y.; Ganesana, M.; Venton, B. J. *ACS Chem. Neurosci.* **2017**, *8* (2), 376–385.

(41) Fredholm, B. B.; IJzerman, A. P.; Jacobson, K. A.; Linden, J.; Müller, C. E. *Pharmacol. Rev.* **2011**, *63* (1), 1–34.

(42) Porkka-Heiskanen, T.; Strecker, R. E.; McCarley, R. W. *Neuroscience* **2000**, *99* (3), 507–517.

(43) Pedata, F.; Corsi, C.; Melani, A.; Bordoni, F.; Latini, S. *Ann. N. Y. Acad. Sci.* **2001**, *939*, 74–84.

(44) Coney, A. M.; Marshall, J. M. *J. Physiol.* **1998**, *509 (Pt 2* (2), 507–518.

(45) Jennings, L. L.; Hao, C.; Cabrita, M. A.; Vickers, M. F.; Baldwin, S. A.; Young, J. D.; Cass, C. E. *Neuropharmacology* **2001**, *40* (5), 722–731.

(46) Geiger, J. D.; Nagy, J. I. *J. Neurosci.* **1986**, *6* (9), 2707–2714.

(47) Li, Y.; Fan, S.; Yan, J.; Li, B.; Chen, F.; Xia, J.; Yu, Z.; Hu, Z. *Hippocampus* **2011**, *21* (3), 265–280.

(48) Sebastião, A. M.; Stone, T. W.; Ribeiro, J. A. *Br. J. Pharmacol.* **1990**, *101* (2), 453–459.

Chapter 4

Probing the release mechanisms of spontaneous, transient adenosine release

It's not overkill if we used what it took.

- Percival Fredrickstein Von Musel Klossowski de Rolo III

Abstract:

Spontaneous, transient adenosine release events have recently been characterized in the rat central nervous system that last only about three seconds. This rapid form of adenosine signaling plays a role in acute neuromodulation as well as acute neuroprotection. However, there is still little knowledge of the mechanism of spontaneous, transient adenosine release. In this study, we investigate two of the possible mechanisms of release: action potential dependent exocytosis and pannexin channels. We tested activity dependence with tetrodotoxin, which blocks sodium channels that lead to action potentials; 200 nM TTX has no significant effect on the concentration of adenosine transients and while the frequency slightly decreased, release is largely maintained. Pannexin channels are known to release ATP and their effects were studied in a variety of models. In rats, Pannexin 1 (PANX1) inhibition with 20 μM spironolactone significantly decreased frequency and concentration but in mice, spironolactone caused no significant changes. In mice, the non-specific gap junction protein inhibitor carbenoxolone, which inhibits pannexin and connexin channels, significantly decreased the concentration of adenosine release, but only at low doses. In PANX1 KO mice, there were no significant differences from control of frequency or concentration of adenosine transients. Ultimately, these results suggest that neither PANX1 nor action-potential dependent exocytosis is the main mechanism of adenosine release. More studies are needed to determine the mechanism, including studies of spontaneous exocytosis, or other channels, such as in PANX2 knock-out mice.

4.1 Introduction:

Adenosine is formed through a variety of mechanisms and can act at receptors in the extracellular space to cause neuromodulation and neuroprotection.[1–3] Teasing out the mechanism of adenosine release is very difficult. Early literature using electrically stimulated release of radio-labeled adenosine identified that adenosine could be formed intracellularly, and then released, or extracellularly after breakdown of released ATP.[4,5] For the intracellular mechanism, the breakdown of nucleic acid and nucleotides leads to a high concentration of adenosine which can then be released through nucleoside transporters.[3,6] Extracellularly, ATP is released through a variety of mechanisms, including exocytosis,[5,7] connexin channels,[8–10] pannexin channels,[11–13] or transporters[3,6] and then broken down rapidly to adenosine via extracellular ectonucleotides.[14,15] Complicating the story is the fact that adenosine is released by different mechanisms, depending on whether it is released in response to an electrical stimulation, mechanical stimulation, or ischemia.[16–20] Therefore, the mechanism of adenosine release must be carefully studied for every form of adenosine release.

There are many different stimuli that can cause adenosine release. However, a rapid, spontaneous mode of adenosine release has been recently discovered. This rapid, unstimulated mode of adenosine was first observed in mouse spinal column slices and occurred every few minutes.[15] In some regions of brain however, transient adenosine occurs at a much faster rate, particularly the hippocampus, caudate putamen, and the

prefrontal cortex.[21–23] Our lab has been focused on determining the regulation and release mechanisms of rapid adenosine signaling. Transient adenosine is self-regulating through A_1 autoreceptors, which decrease the frequency of adenosine release.[21] Spontaneous adenosine release is cleared by a combination of mechanisms, primarily metabolism and reuptake by equilibritive nucleoside transporters although there is likely another mode of clearance that has yet to be determined.[24] However, we still do not know the mechanism of spontaneous adenosine release or the cell type from which it is released. Possible mechanisms for generating transient adenosine include exocytotic release, pannexin channel release, or nucleoside transporters.[25] Previous work on equilibrative nucleoside transporters (ENTs) demonstrated that blocking them increased clearance times, but did not decrease release, so the primary mechanism of release is not through ENTs.[24]

Exocytosis is the process of cellular secretion by which molecules packaged in vesicles are released into the extracellular space when the vesicle fuses with the cell membrane. ATP is well known to be packaged and released from vescicles.[26–28] However, evidence of direct release of vesicular adenosine has been elusive;[1] there is one paper that shows activity dependent adenosine release in an ecto-5'-nucleotidase knock-out (KO) mouse, where ATP cannot be broken down to adenosine extracellularly.[29] The time course of rapid adenosine transients, which are several hundred nM adenosine released and cleared in about 3 seconds, is of similar order of

magnitude, both in concentration and duration, as vesicular dopamine or serotonin release.[21,30] Much of exocytotic release is action potential, or activity, dependent so the vesicles are released after membrane depolarization due to neuronal firing; this mechanism is typically blocked by tetrodotoxin (TTX) which blocks voltage activated sodium channels. Our lab has shown that electrically stimulated adenosine release is partially TTX sensitive so spontaneous adenosine release may also be due to activity dependent exocytosis.[16]

Another possible mechanism for transient adenosine release is pannexin channels. Pannexins are channel forming proteins that allow the passage of ions and small molecules through the cell membrane, the most heavily studied of which is ATP.[13,31,32] Pannexins are hemichannels related to the gap junction proteins, connexins, but only connect the intracellular space with the extracellular space, whereas connexins also connect the intracellular spaces of two cells.[33] Pannexin 1 (PANX1) is the most heavily studied of the pannexin channels and is ubiquitous throughout the body. Another pannexin, pannexin 2 (PANX2) is only expressed in the central nervous system.[34,35] There are several methods by which pannexins may be modulated. One theory is that NMDA activation can increase NO production which opens pannexin channels.[36] α 1-adrenergic receptor activation with phenylephrine can cause a 'flickering' behavior of pannexin channels, which causes them to rapidly open and close more frequently.[37,38] This sort of 'flickering' process could be a cause of the rapid

spontaneous adenosine transients. However, no studies have examined the effects of pannexin channels as the mechanism for rapid, spontaneous adenosine release.

In this work, we investigated the mechanism of spontaneous transient adenosine release in brain slices, specifically testing the mechanisms of activity-dependent exocytosis and pannexin channels. These mechanisms would be difficult to study *in vivo* as there can be complications with blood-brain barrier permeability and use of toxins that would kill a live test subject. Brain slices allow us to keep the tissue viable while perfusing drug straight to the brain, without any concerns about drug clearance or toxicity.[16,22,39,40] We investigated the role of action potential dependent exocytotic release by inhibiting sodium channels with tetrodotoxin (TTX). For pannexin channels, we treated slices with PANX1 specific inhibitor, spironolactone, as well as the non-specific gap junction inhibitor, carbenoxolone,[13,41,42] and used a PANX1 KO mouse. The rate of adenosine transients was unchanged with TTX and in PANX1 KO mice. Spironolactone had a small effect on adenosine concentration in rats but not in mice, whereas carbenoxolone had some small effects at a low dose, but not a high dose. Taken together, these data demonstrate that neither PANX1 nor activity dependent exocytosis are the main mechanisms of spontaneous adenosine release. Future work could delve more into the role of PANX2 or connexins as possible mechanisms, as these were only partially tested with one non-selective drug. Another possible mechanism is spontaneous exocytosis, where vesicles are released in a spontaneous, activity-

independent manner. Both glutamate and GABA cells produce spontaneous exocytosis and ATP is known to be released from these types of cells, either as co-transmitter or from its own vesicles.[27,43] Understanding the mechanism of spontaneous, transient adenosine release is important to understanding how adenosine is regulated and how this form of adenosine signaling might be harnessed to provide protective effects during pathologies such as stroke, ischemia, or traumatic brain injury.

4.2 Methods:

4.2.1 Brain slice preparation and experimental setup

Protocols used for all animal experiments were approved by the Animal Care and Use Committee at the University of Virginia. Male Sprague-Dawley rats weighing 250-350 g were anesthetized with isoflurane (1 mL/100 g rat weight) in a desiccator. Once the rat is unresponsive to a toe-pinch, it is promptly beheaded, and the brain is extracted in less than two minutes and added to chilled, (0-5 °C) oxygenated aCSF and allowed to recover for 2-4 minutes. 400 µm thick sagittal slices are then collected from one hemisphere using a Leica VT1000S vibratome and added to room temperature, oxygenated aCSF. Once slice collection is complete, the beaker of aCSF with the brain slices is set in a water bath to heat up to 37 °C to simulate body temperature. Slices then recover in this environment for 30 minutes prior to experimentation. Mice underwent the same dissection procedure. The wild type strain for mice are C57Bl6 and the PANX1

KO mice (gifted by Kodi Ravichandran) were Lox-Cre mice developed from the same wild-type strain.[46]

During the experiment, a slice is placed in a slice chamber that is constantly being perfused with 37° oxygenated aCSF and allowed to equilibrate for 15 minutes while the CFME also equilibrates in the surrounding aCSF. The Ag/AgCl reference electrode is placed in the perfusion aCSF away from the slice. After 15 minutes, the CFME is implanted in the CA1 region of the hippocampus, about 100 µm deep. Once the background stabilizes and adenosine transients are observed, 1 hour of data is collected. If no transients are observed, the electrode is repositioned elsewhere in the CA1.

4.2.2 Chemicals

All experiments were performed in artificial cerebral spinal fluid (aCSF). aCSF was comprised of 126 mM NaCl, 2.5 mM KCl, 1.2 mM NaH_2PO_4 monohydrate, 1.2 mM $MgCl_2$ hexahydrate, 25 mM $NaHCO_3$ (all from Fisher), 2.4 mM $CaCl_2$ dihydrate, 11 mM glucose, and 15 mM tris(hydroxymethyl)aminomethane (all from Sigma). One solution of aCSF was allowed to chill overnight prior to each experiment and was used for tissue recovery and slicing. A room temperature solution of aCSF was made the day of each experiment and was used as the working solution during experimentation. Both the chilled and room temperature aCSF solutions were adjusted to a pH of 7.4 daily. Drugs used for this project include the PANX1 antagonist, spironolactone (SPIR, Sigma)[37], the non-specific gap junction antagonist carbenoxolone (CBX, Sigma)[31,44], the α 1-adrenergic receptor

agonist, phenylephrine (Sigma) and the sodium channel blocker tetrodotoxin (TTX, Tocris).

Stock solutions of 10 mM SPIR and 10 mM PE were prepared in DMSO, aliquoted and kept in the freezer until use. Stock solutions of 50 mM CBX were prepared in MilliQ water and stored in the same manner. Aliquots were added to room temperature aCSF for perfusion over brain slices. Working concentrations of these drugs in aCSF were 5 µM or 20 µM SPIR, 10 µM or 100 µM CBX, and 2 µM phenylephrine. TTX was reconstituted to 3 mM in 0.2 M citrate buffer, diluted to 50 µM aliquots, and kept frozen until use. 50 µM aliquots were added to perfusion aCSF to make a 200 nM working solution which was perfused over slices. Safety note: Because TTX is a biotoxin, all solutions and surfaces that came into contact with TTX were treated with 10% bleach after each experiment to deactivate any residual TTX.

4.2.3 Electrochemistry

The working electrodes were made from T-650 carbon fibers (gift from Cytec Engineering Materials) as described previously.[45] Fibers 7 µm in diameter were aspirated through a glass capillary. Capillaries were heated and pulled to create two carbon fiber microelectrodes (CFMEs) each. The exposed fibers were cut to 50-100 µm in length. We have traditionally epoxied the tips of electrodes to ensure a tight seal around the fiber. However, recent findings have shown that epoxied electrodes are less

sensitive to adenosine transients, decreasing the apparent concentration observed.[22] Thus, electrodes were not epoxied. The reference electrode is a Ag/AgCl wire.

FSCV was performed using a ChemClamp potentiostat (Dagan) with a Pine 5 MΩ headstage. Data was collected using HDCV software (courtesy of Mark Wightman, UNC). The waveform used for FSCV of transient adenosine uses a holding potential of -0.4 V vs Ag/AgCl, scans up to 1.45 V at 400 V/s., and back down to -0.4 V at the same rate. This scan was repeated at a rate of 10 Hz, giving us 0.1 second temporal resolution of adenosine concentration changes.

4.2.4 Data analysis

Whereas previous work has utilized the principal components analysis (PCA) feature of the HDCV Analysis software to analyze adenosine transients[21–23], this form of analysis is time consuming, tedious, and susceptible to biased interpretation. Therefore, an automated algorithm was created that identifies and quantifies adenosine transients, providing information such as event concentration, event duration, and inter-event time.[47] Durations are the peak width at half height. All bar graphs and tables report values as the mean ± standard error of the mean. Unpaired t-tests and ANOVA determined significant differences between the concentrations or durations of adenosine transients in control slices vs treated slices (or PANX1 KO slices). Cumulative frequency distributions were made to demonstrate the differences in inter-event time distributions between sets of slices and the Kolmogorov-Smirnoff (K-S) test was used to

determine whether those differences were statistically significant. All statistics were performed using Graphpad Prism 6.

4.3 Results:

4.3.1 Effect of TTX on adenosine transients in rats

In the first set of experiments, the activity dependence of adenosine transients was tested by applying TTX to brain slices. Separate groups of control and TTX slices were collected, with one hour of data collected in each slice. Dale's group has shown that rapid, stimulated adenosine in the cerebellum is mainly activity dependent.[29] Two hundred nM tetrodotoxin (TTX) was used to block Na^+ channels, inhibiting activity dependent exocytotic release. TTX activity was confirmed in the slice by first measuring stimulated dopamine release in the caudate putamen, then perfusing with 200 nM TTX in aCSF for 20 minutes. This concentration of TTX eliminated the stimulated dopamine signal (**Fig. 4.1**), which is known to be due to exocytosis.

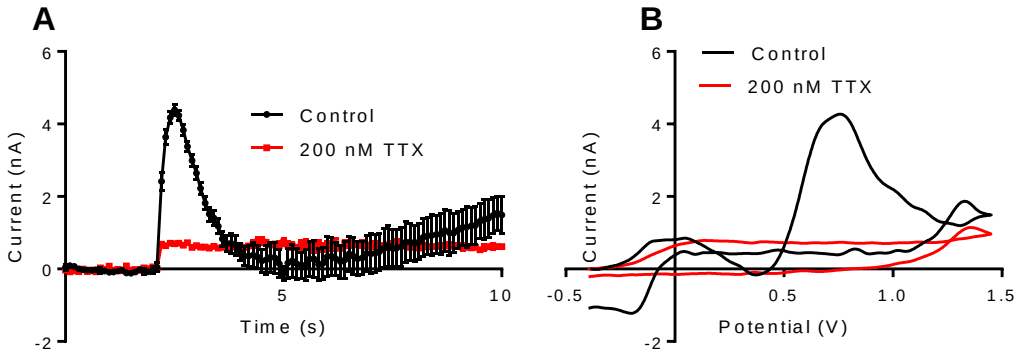

Figure 4.1: 200 nM TTX eliminates stimulated dopamine signal. (**A**) Current vs time of electrically stimulated dopamine (220 nM) before (black) and after (red) TTX perfusion. (**B**) CV of dopamine before (black) and after (red) TTX perfusion.

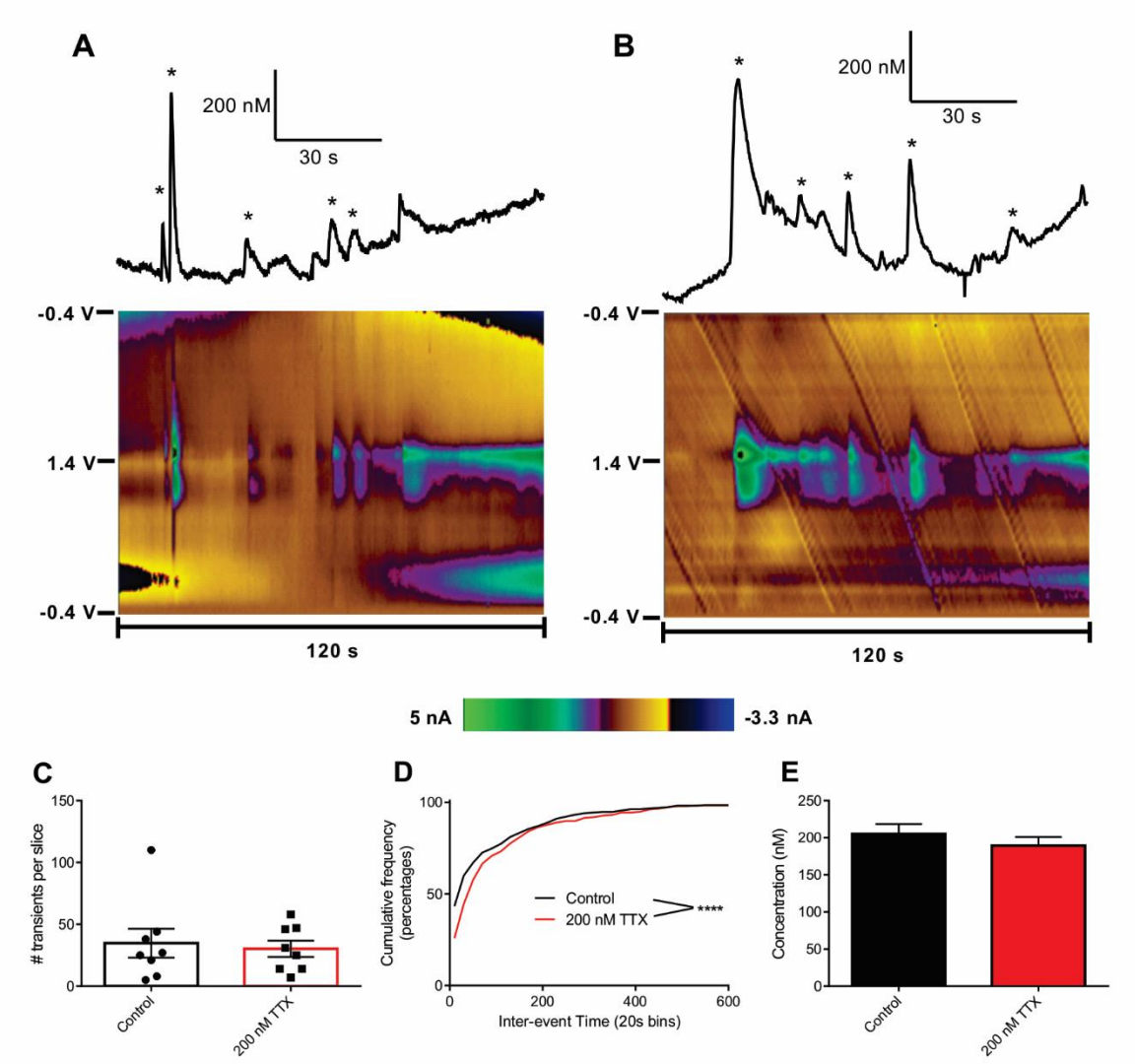

Figure 4.2: 200 nM TTX does not eliminate adenosine transients. n = 8 slices each. Sample color plot and concentration trace of adenosine transients in (**A**) a control slices and (**B**) a slice perfused with 200 nM TTX. (*) indicates transients detected by automated peak detection. (**C**) No significant difference in the average number of transients per hour with TTX (t-test, $p = 0.74$). (**D**) The distributions of inter-event times with TTX were significantly different (K-S test, $p < 0.0001$). (**E**) No significant difference in the average adenosine transient concentration (t-test, $p=0.38$).

The electrode was then moved to the CA1 in the same slice and transient adenosine detected. As seen in **Fig. 4.2A-B**, adenosine transients were still observed in

the CA1 with 200 nM TTX. The sample color plots both show five peaks identified as adenosine by the computer algorithm in these 2-minute windows. Control slices had an average of 34 ± 12 transients per hour and slices with TTX had 30 ± 7 transients per hour. There was no significant difference in the mean inter-event time (t-test, 101 ± 9 s TTX vs 79 ± 7 s control p = 0.11, n = 8 slices each) or concentration (t-test,190 ± 10 nM TTX vs 240 ± 20 nM control, p =0.38, n = 8 slices each, **Fig. 4.2E**) between control slices and slices perfused with TTX. When plotting distributions, there is a significant difference in the cumulative distribution of inter-event times with TTX (KS test, p < 0.0001) (**Fig 1D**).

4.3.2 PANX1 inhibition with spironolactone in rats

Two doses of the PANX1 specific inhibitor spironolactone (5 and 20 µM) were tested in rat hippocampus slices, specifically in the CA1. The sample color plots show a decrease in both frequency and concentration of transients with five transients in the two-minute window of the control slices and only one in window from the 20 µM spironolactone perfused slices (**Fig. 4.3A-C**). The concentration profile also shifts with spironolactone, as there are no large transients observed with the drug. There was no significant difference in the average number of events (ANOVA, p = 0.91, n = 8 slices each) between the control and two concentrations of spironolactone (**Fig. 4.3D)**, but there was an effect on the inter-event time distribution. The difference in the

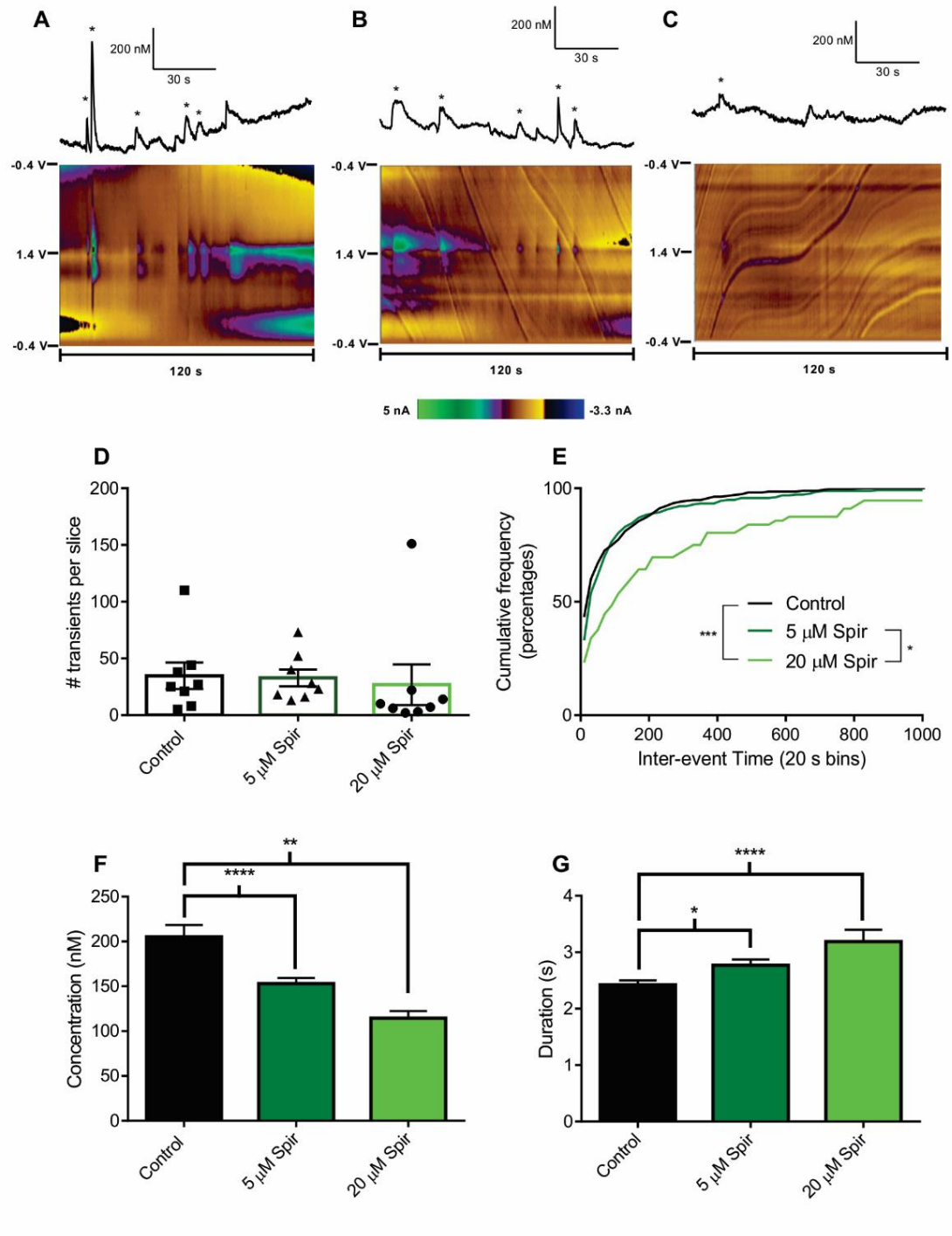
A
B
C
200 nM
30 s
-0.4 V
1.4 V
120 s
5 nA
-3.3 nA
D
transients per slice
Control
5 μM Spir
20 μM Spir
E
Cumulative frequency (percentages)
Inter-event Time (20 s bins)
***
*
F
Concentration (nM)
**
****
G
Duration (s)
*
****

Figure 4.3: Effect of PANX1 inhibitor, spironolactone in rat brain slices. n = 8 slices each. Sample color plot and concentration trace of (**A**) a control slice, (**B**) a slice perfused with 5 µM spironolactone, and (**C**) a slice perfused with 20 µM spironolactone. (*) represents an adenosine transient. (**D**) There was no significant difference in the number of transients per slice with spironolactone (**E**) Twenty µM spironolactone significantly affects the inter-event time distribution of adenosine transients. (**F**) Transient adenosine concentration significantly decreases with both a 5 µM and 20 µM dose of spironolactone. (**G**) The duration of transients also significantly increased with increased concentration of spironolactone.

cumulative distribution of inter-event times (**Fig. 4.3E**) was significant (KW test, p = 0.0002, n = 8 slices each) as the 20 µM spironolactone treatment was lower than both the control (Dunn's post-test, p = 0.0002, n = 8 slices each) and the 5 µM spironolactone treatment (Dunn's post-test, p = 0.02, n = 8 slices each). There was also an overall effect of spironolactone on mean event concentration (ANOVA, p < 0.0001, n = 8 slices each) as the concentration per transient dropped with 5 µM spironolactone from 205 ± 15 nM to 153 ± 6 nM (Tukey post-test, p < 0.001, n = 8 slices each) and even further with 20 µM spironolactone at 122 ± 9 nM (Tukey post-test, p < 0.01, n = 8 slices each) (**Fig. 4.3F**). There was also a significant difference in the duration of spontaneous adenosine transients with spironolactone (ANOVA, p = 0.0004, n = 8 slices each). The mean duration of adenosine transients in control slices was 2.4 ± 0.1 s whereas the mean duration with 5 µM spironolactone was 2.8 ± 0.1 s (Tukey's post-test, p = 0.02, n = 8 slices each) and 20 µM spironolactone was 3.2 ± 0.2 s (Tukey's post-test, p = 0.0009, n = 8 slices each).

4.3.3 Adenosine transients in mice are smaller than in rats

Our lab has traditionally used rats. However, knockouts and other genetically-altered mutants are available for mice, so the rest of the experiments were performed in mouse brain slices. First, we compared the number and frequency of transients observed in mouse hippocampal slices to those found in rat hippocampal slices. As seen in the sample color plots (**Fig. 4.4A-B**), spontaneous adenosine release occurred at about the same frequency with 5 and 6 transients in the sample two-minute windows for rats and mice, respectively. In rats, there are some large adenosine transients, with one almost 500 nM, whereas in mice all of the transients are below 200 nM. The average number of transients per slice was not significantly different between the two species (t-test, $p = 0.80$, $n = 8$ slices each). Rats had an average of 35 ± 12 transients per hour whereas mice averaged 39 ± 12 transients per hour (**Fig. 4.4C**) and the inter-event time distribution of adenosine transients was also not significantly different (**Fig. 4.4D**, K-S test, $p = 0.15$, $n = 8$ slices each). The average concentration of adenosine transients in rat slices (205 ± 15 nM), was significantly higher (**Fig. 4.4E,** t-test, $p < 0.0001$, $n = 8$ slices each) than the concentration of transients in mouse slices (117 ± 6 nM). There was also a small, but significant difference between the duration of transients in mouse slices vs rat slices (t-test, $p = 0.005$, $n = 8$ slices each). Transients in rats last longer, 2.4 ± 0.1 s compared to 2.1 ± 0.1 s in mice, which is likely because larger transients last longer (**Fig. 4.4F**).

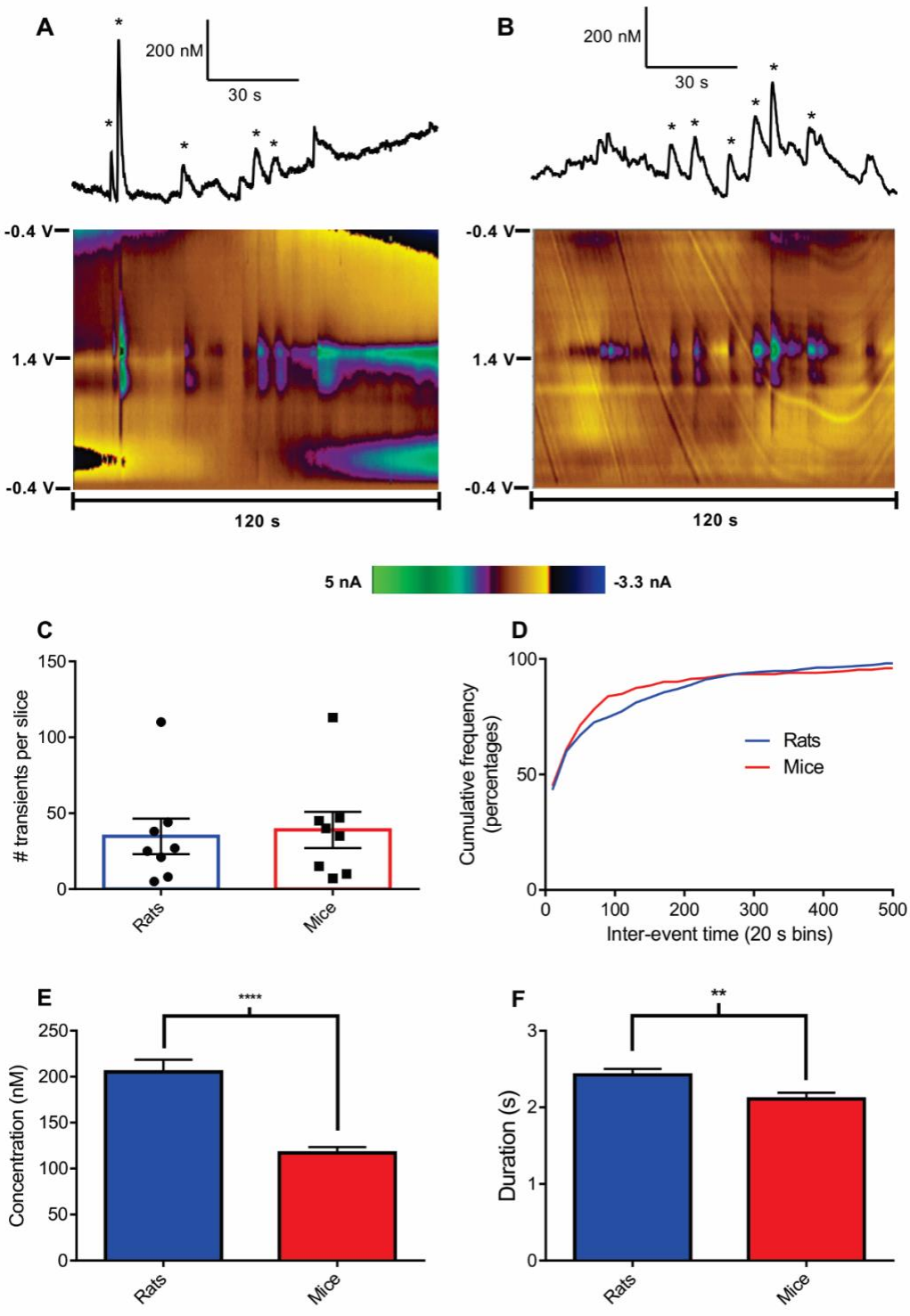
A
200 nM
30 s
B
200 nM
30 s
-0.4 V
1.4 V
-0.4 V
120 s
-0.4 V
1.4 V
-0.4 V
120 s
5 nA
-3.3 nA
C
transients per slice
150
100
50
0
Rats
Mice
D
Cumulative frequency (percentages)
100
50
0
0
100
200
300
400
500
Inter-event time (20 s bins)
Rats
Mice
E
****
Concentration (nM)
250
200
150
100
50
0
Rats
Mice
F
**
Duration (s)
3
2
1
0
Rats
Mice

Figure 4.4: Variations in transient adenosine events between rat and mouse brains slices. n = 8 slices each Sample color plot and concentration trace of (**A**) a rat slice and (**B**) a mouse slice (*) represents an adenosine transient. (**C**) The average number of transients per hour was not different between rats and mice (**D**) There was no significant difference in the inter-event time distribution between rats and mice, but there was (**E**) a significantly lower mean concentration of adenosine transients in mice compared to rats. (**F**) There was also a small, but significant difference between the mean duration of transients between rats and mice.

4.3.4 Spironolactone has no effect on adenosine transients in mice

In mice, we tested the high dose of PANX1 inhibitor, spironolactone (20 µM). The sample color plots (**Fig. 4.5A-B**) show a similar frequency with 6 and 5 transients in the two-minute windows of control and 20 µM spironolactone slices respectively. Additionally, there are transients both small (30 nM) and large (500 nM) after spironolactone (**Fig. 4.5B)** and so the average concentration is similar to that observed in control slices. There was no significant difference (t-test, p = 0.91, n = 8 slices each) in the average number of transients per hour between control slices (39 ± 12) and 20 µM spironolactone slices (37 ± 13) (**Fig. 4.5C**). The distribution of inter-event times of adenosine transients was also not significantly different between control slices and spironolactone treated slices (KS test, p = 0.26). There was no difference between the mean concentration of adenosine transients (t-test, p = 0.08), but the number trended toward a decrease in concentration, similar to rats. The duration of transients was also not different after spironolactone (t-test p = 0.23). Thus, the effects of spironolactone seen in rats were not observed in mice. However, even in rats the effects were small and spironolactone did not fully eliminate adenosine transients.

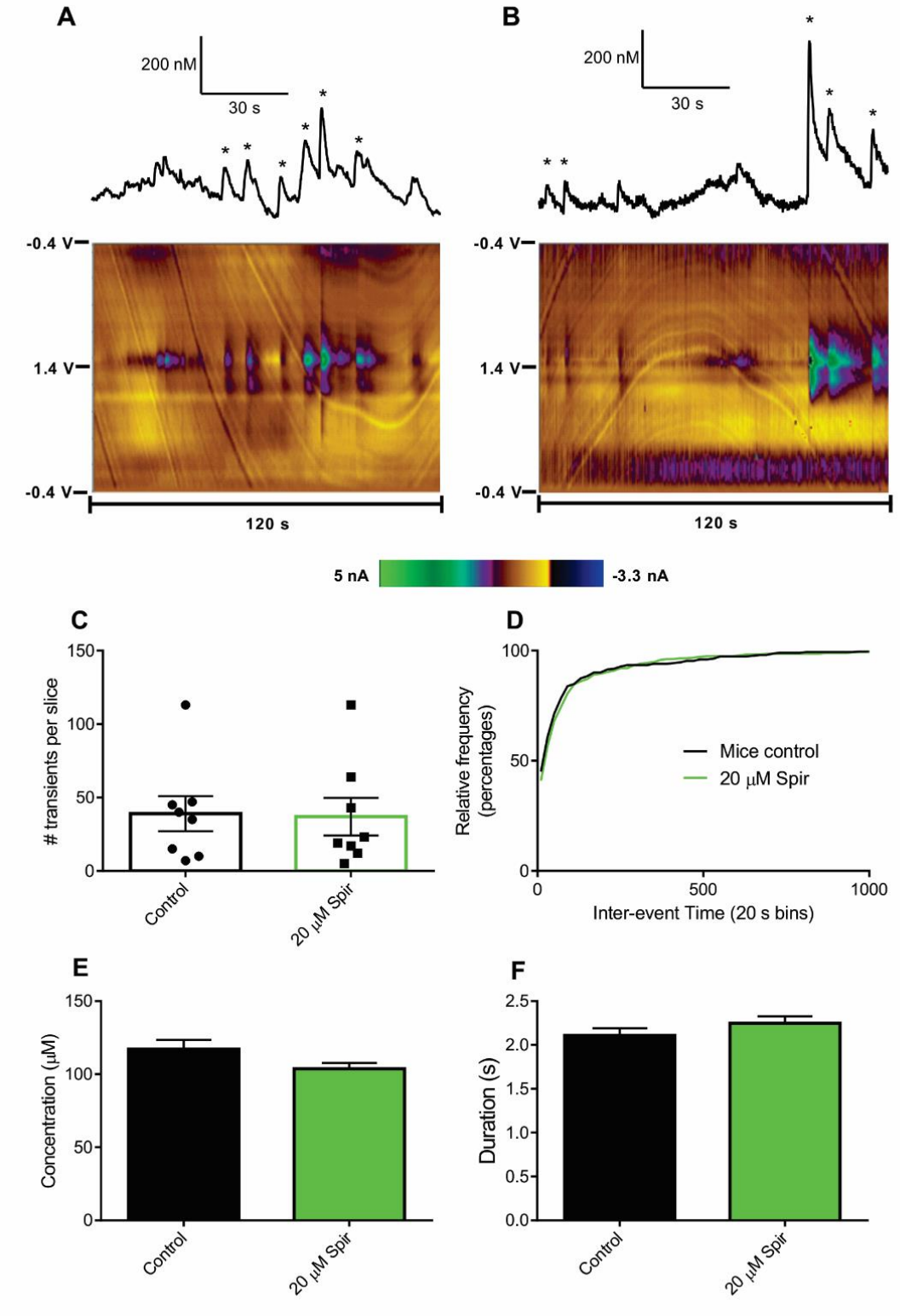
A
200 nM
30 s
-0.4 V
1.4 V
-0.4 V
120 s
B
200 nM
30 s
-0.4 V
1.4 V
-0.4 V
120 s
5 nA
-3.3 nA
C
transients per slice
150
100
50
0
Control
20 μM Spir
D
Relative frequency (percentages)
100
50
0
0
500
1000
Inter-event Time (20 s bins)
Mice control
20 μM Spir
E
Concentration (μM)
150
100
50
0
Control
20 μM Spir
F
Duration (s)
2.5
2.0
1.5
1.0
0.5
0.0
Control
20 μM Spir

Figure 4.5: No effects with PANX1 inhibitor spironolactone in mice. n = 8 slices each. Sample color plot and concentration trace of (**A**) a control slice and (**B**) a slice perfused with 20 µM spironolactone (*) represents an adenosine transient. (**C**) The average number of transients per hour was not different with spironolactone treatment in mice. Additionally, with 20 µM spironolactone, transient adenosine events occured with the same (**D**) frequency, (**E**) concentration, (**F**) and duration as those seen in control slices.

4.3.5 PANX1 KO mice still exhibit spontaneous adenosine transients

Drugs such as spironolactone are rarely specific for their target and there may be other off target effects. In order to determine the extent to which PANX1 is a mechanism of release for spontaneous, transient adenosine, a PANX1 KO strain of mice was tested. The sample color plots (**Fig. 4.6A-B**) show slightly fewer transients in PANX1 KO mice, but the average number of transients per hour was not significantly different between wild type (C57Bl6) slices, which had 39 ± 12 transients per hour, and PANX1 KO slices, which had 29 ± 10 transients per hour (**Fig. 4.6C,** t-test, p = 0.56, n = 8 slices each). Transients still occur frequently in the PANX1 KO slices, with no significant change in inter-event time (**Fig. 4.6D**, KS test, p = 0.10, n = 8 slices each) or concentration (**Fig. 4.6E**, t-test, p = 0.40, n = 8 slices each) compared to wild type mice. There was a significant decrease in the average duration of transients in PANX1 KO mice (**Fig. 4.6F**), but only by less than 0.3 seconds (t-test, p = 0.02, n = 8 slices each). The results of the PANX1 KO aligns with the results of 20 µM spironolactone in mice, showing very little effect on spontaneous, transient adenosine release. Thus, in mice, PANX1 does not seem to be a primary mechanism of spontaneous adenosine release.

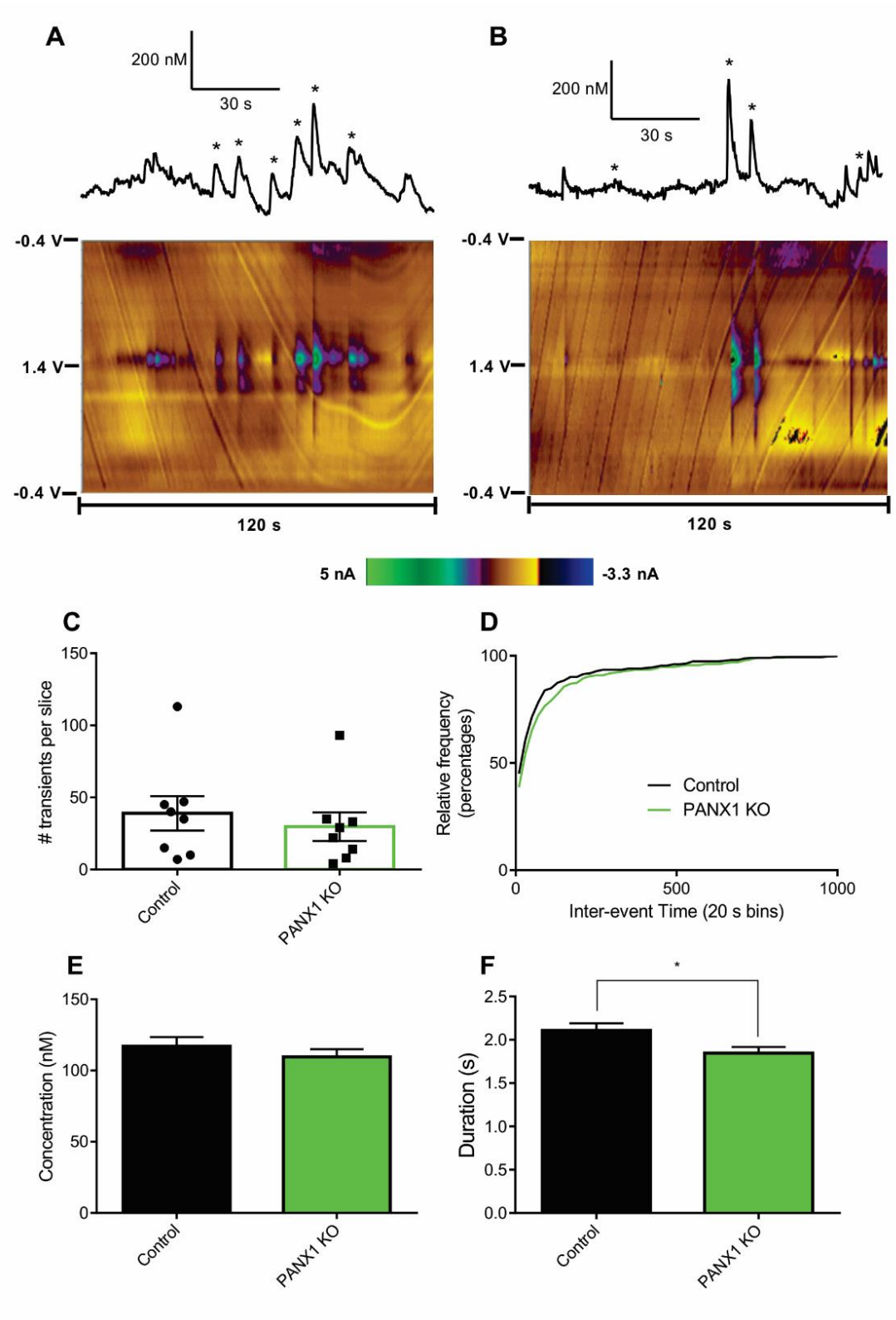
A
200 nM
30 s
-0.4 V
1.4 V
-0.4 V
120 s
B
200 nM
30 s
-0.4 V
1.4 V
-0.4 V
120 s
5 nA
-3.3 nA
C
transients per slice
Control
PANX1 KO
D
Relative frequency (percentages)
Control
PANX1 KO
Inter-event Time (20 s bins)
E
Concentration (nM)
Control
PANX1 KO
F
Duration (s)
Control
PANX1 KO

Figure 4.6: PANX1 KO mice show little change in spontaneous, transient adenosine compared to controls. n = 8 slices each. Sample color plot and concentration trace of (**A**) a wild-type slice and (**B**) a PANX1 KO slice. (*) represents an adenosine transient. There was no significant decrease in (**C**) number of transients per hour, (**D**) the inter-event time distributions, or (**E**) transient concentration. (**F**) There was a small be significant decrease in duration with PANX1 KO compared to control.

α 1-adrenergic receptor activation with phenylephrine decreases the frequency and concentration of adenosine transients

Chiu, et al. showed that PANX1 channels undergo a 'flickering' process where the channel opens very briefly and that this process is activated by α 1-adrenergic receptor activation.[37] Phenylephrine is an α-1 adrenergic receptor agonist that is commonly used as a decongestant. The hypothesis is that adding phenylephrine will increase the amount of flickering and thus transient adenosine release. With 2 μM phenylephrine, slices show an effect opposite of what was expected for PANX1 activation. The sample color plots show fewer transients and the concentration trace shows similar concentrations between the two sets of data (**Fig. 4.7A-B**). There was no significant difference in the average number of transients per hour (**Fig. 4.7C**) between control (39 ± 12) and phenylephrine (28 ± 5) slices (t-test, p = 0.55, n = 8 slices for control, n = 4 slices for phenylephrine). However, there was a difference in the inter-event time distributions (**Fig. 4.7D**) with 2 μM phenylephrine (KS test, p = 0.0003, n = 8 slices for control, n = 4 slices for phenylephrine). The average transient concentration (**Fig. 4.7E**)

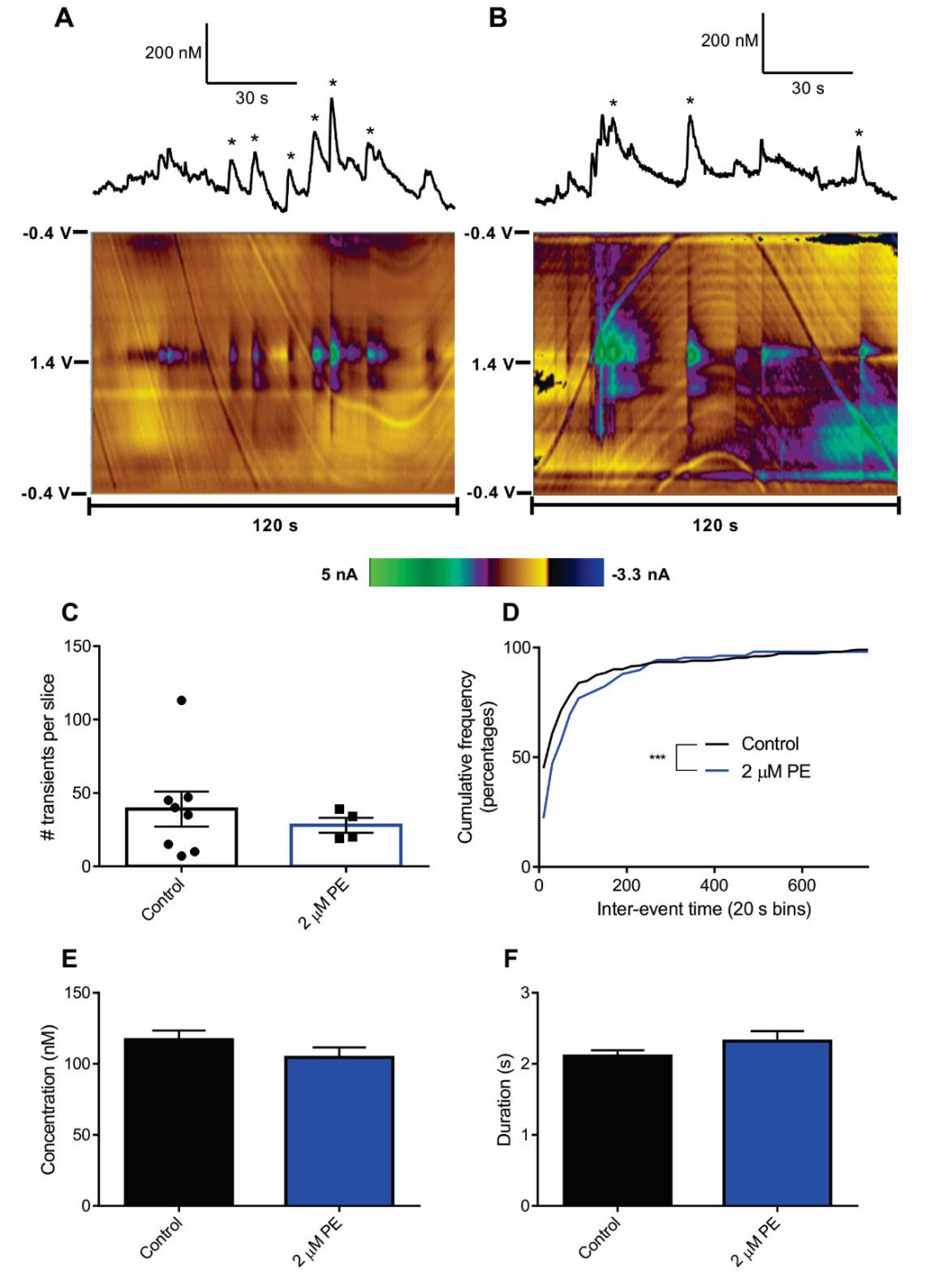
A
200 nM
30 s
-0.4 V
1.4 V
-0.4 V
120 s
B
200 nM
30 s
-0.4 V
1.4 V
-0.4 V
120 s
5 nA
-3.3 nA
C
transients per slice
150
100
50
0
Control
2 μM PE
D
Cumulative frequency (percentages)
100
50
0
***
Control
2 μM PE
0
200
400
600
Inter-event time (20 s bins)
E
Concentration (nM)
150
100
50
0
Control
2 μM PE
F
Duration (s)
3
2
1
0
Control
2 μM PE

Figure 4.7: α 1-adrenergic receptor agonist, phenylephrine in mouse slices. n = 8 slices for control. n = 4 slices for phenylephrine. Sample color plot and concentration trace of (**A**) a control slice and (**B**) a slice perfused with 2 μM phenylephrine. (*) represents an adenosine transient. (**C**) Although there was no effect of phenylephrine on the average number of transients per hour, (**D**) 2 μM phenylephrine significantly affected the inter-event time distribution. (**E**) There was no significant effect of 2 μM phenylephrine on the concentration or (**F**) duration of transients.

did not significantly differ what was observed in control slices (t-test, p = 0.28, n = 8 slices for control, n = 4 slices for phenylephrine). There was also no significant difference in the duration of adenosine transients with phenylephrine (t-test, p = 0.18, n = 8 slices for control, n = 4 slices for phenylephrine).

4.3.7 Low dosage of CBX shows a decrease in frequency and concentration of adenosine transients

Carbenoxolone (CBX) is a non-specific inhibitor of pannexin channels, gap junction proteins, postsynaptic NMDA receptors, and calcium channels.[48–50] At lower concentrations (~10 μM) CBX is considered to be PANX1 specific, whereas at higher concentrations it would also inhibit PANX2 and connexin channels.[51,52] We tested two doses of carbenoxolone in slices, 10 μM CBX or 100 μM CBX, to test the more PANX1 specific dose and the dose that blocked more channels and receptors. The sample color plots (**Fig. 4.8A-C**) show that different frequencies of adenosine transients with CBX. The sample concentration traces show 6 transients in the control slice, 4 transients in the 10 μM CBX trace, and 2 transients in the 100 μM CBX trace. Additionally, the transients in the 10 μM CBX trace are noticeably smaller than the transients in the control trace and

the 100 µM CBX trace. There was no significant difference in the average number of transients per hour (**Fig. 4.8D**) between the control slices (39 ± 12), slices perfused with

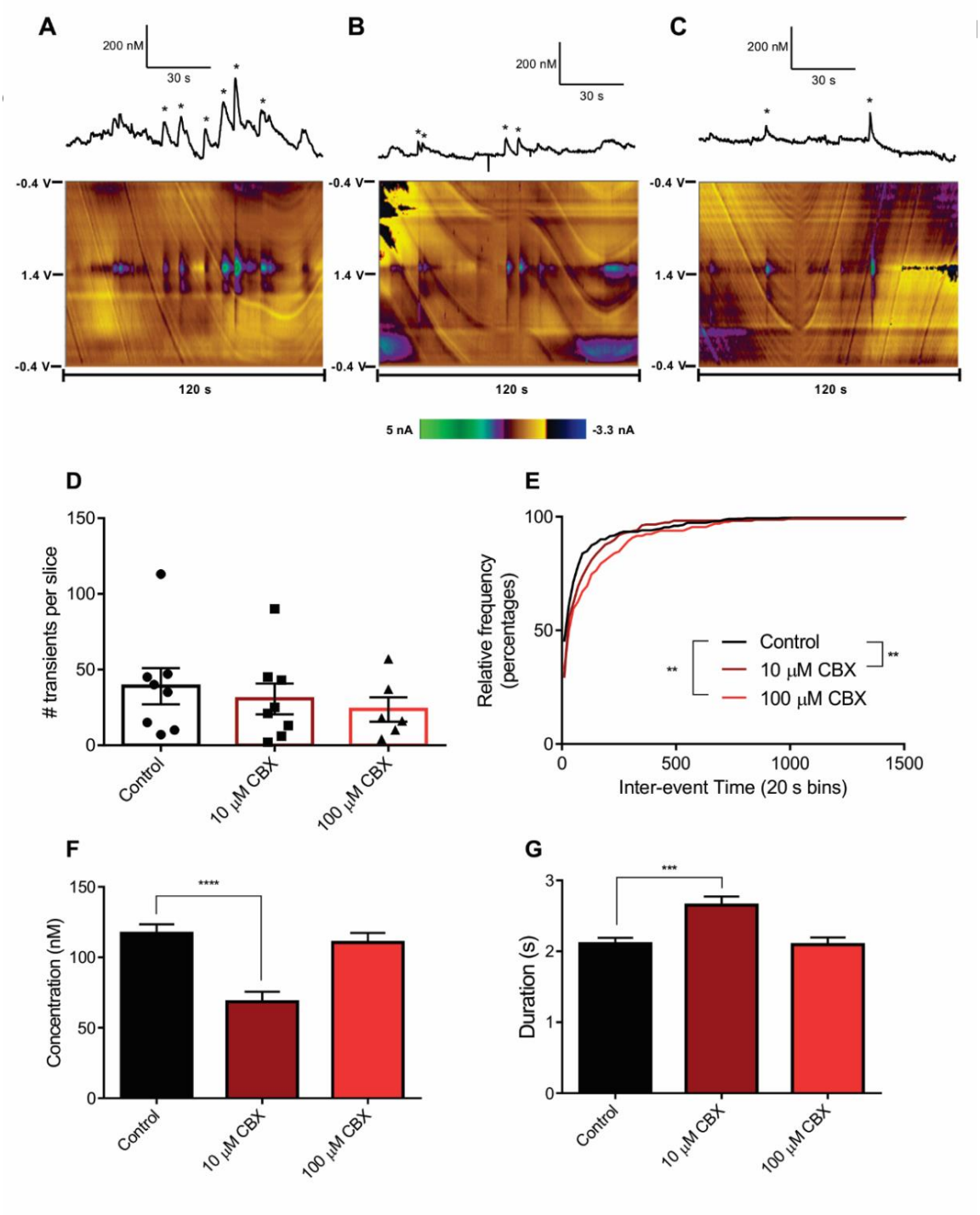

Figure 4.8: Pannexin channel inhibition with carbenoxolone (CBX), the non-specific antagonist of pannexin channels and gap junction proteins. Sample color plot and concentration trace of (**A**) a control slice, (**B**) a slice perfused with 10 µM CBX, and (**C**) a slice perfused with 100 µM CBX. (*) represents an adenosine transient. (**D)** No significant difference in average number of transients. (**E**) There was a significant difference in the inter-event time distribution of adenosine transients with both a low (10 µM) and high (100 µM) concentration. (**F**) CBX also caused a decrease in average concentration of adenosine transients when used at a low concentration, but not with a high concentration. (**G**) Duration significantly increased with 10 µM CBX, but not with the high dose of 100 µM.

treated with CBX (KW test, p = 0.0003 n = 8 slices for control and 10 µM CBX, n = 6 slices for 100 µM CBX). Transients occurred less frequently when treated with either 10 µM CBX (Dunn's post-test, p = 0.003, n = 8 slices each) or 100 µM CBX (Dunn's post-test, p = 0.002, n = 8 slices for control, n = 6 slices for 100 µM CBX), although there was no significant difference between the two concentrations of CBX (Dunn's post-test p > 0.9999, n = 8 slices for 10 µM CBX, n = 6 slices for 100 µM CBX). There was also an overall effect of CBX on the concentration of adenosine transients (one-way ANOVA, p < 0.0001, n = 8 slices for control and 10 µM CBX, n = 6 for 100 µM CBX). When treated with a low dose of CBX (10 µM) the average concentration of adenosine transients dropped significantly (**Fig. 4.8F**) from 117 ± 6 nM to 68 ± 7 nM (Tukey's post-test, p < 0.0001, n = 8 slices each). However, there was no significant difference from control for the average transient concentration with 100 µM (110 ± 7 Tukey's post-test, p = 0.52, n = 8 slices for control, n = 6 for 100 µM CBX). Similarly, the duration of adenosine transients significantly increased (**Fig. 4.8G**) when slices were perfused with CBX (ANOVA, p = 0.0002, n = 8 slices for control and 10 µM CBX, n = 6 for 100 µM CBX). The duration increased from 2.1 ± 0.1 s to 2.7 ± 0.1 s (Tukey's post-test, p = 0.0002, n = 8

slices each) when treated with 10 µM CBX but the higher concentration of 100 µM did not significantly change the average duration of adenosine transients (Tukey's post-test, p = 0.996 n = 8 for control, 6 for 100 µM).

Table 4.1: Characterization of adenosine transients in mice hippocampal slices with various pannexin treatments. Mean values of the inter-event time (IET), concentration, and duration of spontaneous adenosine transients are given. Significant differences are bolded and based on the KS test for IET and t-test for concentration and duration. (Means ± SEM, **p < 0.01, *** p < 0.001, **** p < 0.0001, different than control)

Treatment	*Drug Concentration*	*Mean IET ± SEM (s)*	*Mean [ADO] ± SEM (nM)*	*Mean Duration ± SEM (s)*
control	-	79 ± 9	117 ± 6	2.1 ± 0.1
carbenoxolone	10 µM	**100 ± 9	****68 ± 7	***2.7 ± 0.1
	100 µM	**113 ± 14	110 ± 7	2.0 ± 0.1
spironolactone	20 µM	87 ± 12	104 ± 4	2.2 ± 0.1
phenylephrine	2 µM	100 ± 17	78 ± 6	2.3 ± 0.1
PANX1 KO	-	95 ± 11	110 ± 5	1.8 ± 0.1

4.4 Discussion:

In this work, we investigated the two possible mechanisms for the release of spontaneous, transient adenosine events: activity dependent vesicular release and pannexin channels. We used pharmacology and genetic mutants to shut down these two pathways and found that transients still persisted. Inhibiting sodium channels with TTX to shut down action potentials had little effect on the frequency of transients and no effect on event concentration. Additionally, in mice, adenosine transients were completely unaffected by PANX1 specific inhibitor spironolactone or PANX1 genetic knockout. CBX, the general hemichannel inhibitor, did decrease the frequency and

concentration of transients but only slightly and did not eliminate them. Therefore, we establish that action-potential dependent exocytosis and pannexin channels, particularly PANX1, are not the main mechanism of transient adenosine release, but future work will be needed to examine other mechanisms.

4.4.1 Spontaneous, transient adenosine is not activity dependent

TTX is commonly used in neuroscience research to inhibit Na^+ channels and thereby prevent action potentials from firing in neurons. This is commonly used to determine if a release mechanism is due to activity dependent exocytosis and has been used on several neurotransmitters including dopamine, glutamate and adenosine.[17,31,53] Previous work has found electrically stimulated adenosine release in the caudate putamen and motor cortex with FSCV.[54] While in some cases the adenosine has been released as ATP that has been rapidly broken down, other studies have found direct release of adenosine that is activity dependent.[4,55] If transient adenosine were activity dependent, TTX should have eliminated the transients entirely.

In this work, 200 nM TTX completely eliminated stimulated dopamine signal, but transient adenosine events continued to occur. Whereas the mean inter-event time and concentration of transients were unchanged compared to control, there was a slight difference in the inter-event time distribution with TTX, suggesting adenosine transients occurred less frequently. However, the change was very slight, not the dramatic effects we expected if this was the main mechanism of release. The difference in the

distribution of inter-event times may be due to downstream effects of other neurotransmitters, such as glutamate, that can modulate transient adenosine. If those neurotransmitters were inhibited, downstream release of adenosine may also be inhibited. Thus, adenosine release events are not primarily due to activity dependent exocytosis as the frequency and concentration of release is largely maintained with doses of TTX that eliminate exocytotic release of dopamine. This does contradict our hypothesis as the concentration and duration of spontaneous adenosine transients are both on the same scale of observed dopamine events that are known to be exocytotic.[30] Thus, we explored an alternative, novel hypothesis that pannexin channels are responsible for release.

4.4.2 PANX1 is not the main mechanism of spontaneous adenosine release.

Pannexins are membrane channels that can release ATP into the extracellular space and can be activated by a variety of mechanisms including mechanical perturbation, or high levels of intracellular calcium or extracellular potassium.[12,56,57] PANX1 can be permanently opened via caspase cleavage of the C-terminal tail on the intracellular side of the channel.[58] Alternatively, it can be activated to undergo a "flickering" behavior by activating α 1-adrenergic receptors with phenylephrine.[37] These brief openings of the channel could reflect the brief adenosine transients we have been observing. To investigate the role of pannexins, we used the PANX1 specific drug spironolactone, the general hemichannel inhibitor CBX, the α 1-adrenergic receptor agonist phenylephrine, and a PANX1 KO mutant mouse. In all cases, we saw little to no

effect with any of these treatments in mice, implying that PANX1 is not the predominant mechanism for the release of spontaneous, transient adenosine.

Spironolactone is an antihypertensive drug that has traditionally been used to reduce blood pressure. Recently, Good et al demonstrated that it is also a specific PANX1 inhibitor with an IC_{50} of 8 μM.[42] In rats, we used 2 different concentrations of spironolactone, and found some small effects. There is also a noticeable dose dependency on both concentration and duration of adenosine transients. The frequency of transients drops significantly, with the average inter-event time increasing by more than 3-fold that observed in control slices. There was also a significant decrease in transient concentration, almost 50% and an increase the average transient duration. This suggests that PANX1 may contribute to adenosine release in rats, but is not the main mechanism, as much of the release is maintained, even at higher doses of spironolactone.

In mice, the effects of spironolactone are much less noticeable. At the high dose of 20 μM, there are no effects of spironolactone on concentration or frequency of adenosine transients. This data is a bit surprising, given the significant effects seen in rats, but it could be caused by the smaller transients observed in mice. For example, the average concentration of transients is about one half that in mice than rats, mainly due to the absence of very large transients that are observed in rats. About 10% of adenosine transients in rats exceeded 400 nM whereas the largest transients both with spironolactone and in mice were around 350 nM. Spironolactone did reduce some of

the large transients in rats, but it may be that the smaller transients were less affected, and these are what are observed in mice. Based on work by Cone et al, the expression levels of PANX1 in mouse brain regions are very similar to what they observed in rats so the pharmacology experiments should behave similarly between mice and rats if PANX1 were responsible.[59] The pharmacological data in mice confirm that PANX1 is not the main mechanism of release.

PANX1 KO mice have been developed by the Ravichandran lab at University of Virginia. These transgenic mice were floxed for PANX1 and bred to an E2A-Cre mouse for global knockout of the PANX1 gene in all tissues. Those offspring were then bred back to the control C57Bl6 line to remove the Cre gene from the background.[46] This PANX1 knockout would confirm whether or not PANX1 plays the primary role in the mechanism of spontaneous adenosine.[23]

Similar to the pharmacology results, PANX1 KO mice showed no significant change the transient adenosine frequency, concentration, or duration. If PANX1 was the main mechanism of release, the hypothesis was that the frequency and/or concentration of release would have decreased dramatically, but no decreases were observed. Thus, PANX1 deletion does not at all inhibit spontaneous adenosine release. These mice have a global deletion of PANX1, so if release was from neurons or astrocytes, it would have been affected. Thus, the conclusion is the same from pharmacology and genetic KO mice: PANX1 is not a main mechanism by which spontaneous transient adenosine is released.

PANX1 can be activated by α 1-adrenergic receptors through a $G_{\alpha q}$ pathway that is still not fully understood.[60] Phenylephrine is a common agonist of α 1-adrenergic receptors and was the drug used to discover that PANX1 is modulated by α 1-adrenergic receptors.[38] They demonstrated that inhibiting pannexin channels resulted in a significantly decreased level of phenylephrine-induced vasoconstriction. Application of phenylephrine has a downstream effect of initiating the "flickering" process of PANX1 channels opening.[37] The spironolactone and PANX1 KO data suggested that PANX1 was not a main mechanism of release, but activating PANX1 would be interesting to determine if it could contribute to release. The hypothesis was that if PANX1 could be recruited for rapid adenosine release, activating PANX1 via an α 1-adrenergic agonist should increase release. However, when slices were treated with 2 μM phenylephrine, there was a small but significant decrease in the transient adenosine event frequency but no change to the average adenosine event concentration. These data demonstrate the PANX1 is not activated to cause adenosine release by phenylephrine. The small decrease could be due to other downstream effects of phenylephrine that might activate other cells that decrease adenosine release. Another possible function of α 1-adrenergic receptor activation is vasoconstriction, but how that would affect brain slices and adenosine release is unclear. These data show that activation of PANX1 by phenylephrine does not activate spontaneous adenosine release.

All of these experiments lead us to conclude that PANX1 is not the main mechanism of spontaneous transient adenosine release. Many researchers are now studying PANX1 and its role in ATP release; for example, Chiu et al. found a role for rapid release of ATP in ischemia.[21,32,37,61] Our studies are the first to study pannexin release for spontaneous adenosine signaling and we demonstrate it not involved in this signaling in mice. However, pannexins could be a factor in other forms of adenosine release, such as mechanosensitive release.[17] Pannexin channels have been shown to play a role in calcium wave propagation, initiated by mechanical perturbation, resulting in the release of ATP and the activation of purinergic receptors.[12] However, with regard to spontaneous adenosine, the evidence here is that it is not a contributing factor.

4.4.3 Carbenoxolone has small effects on adenosine frequency

While the focus of this research was on PANX1, due to the existence of KO mice and specific pharmacological inhibitors and activators, there are other possible gap-junction channels that could be responsible for spontaneous adenosine release. PANX2 is also heavily expressed in the brain and serves a similar function to PANX1.[62] PANX1 and PANX2 have also been observed to co-localize in a few regions of the brain, including the hippocampus.[63] The brain localization of PANX2 means it could be involved in spontaneous adenosine release as well.[24] Alternatively, connexin channels, in addition to forming gap junctions with neighboring cells, can release ATP directly into the extracellular space, making it a plausible target as well.[8,33]

Carbenoxolone is a non-specific inhibitor of pannexin channels, connexin channels, and postsynaptic NMDA receptors, in additional to suppressing action potentials.[48–50] Therefore, it is a more general inhibitor of all gap junction proteins when used at high concentrations (100 µM). At a low concentration (10 µM), CBX is considered fairly PANX1 specific.[51] Neither dose of carbenoxolone dramatically decreased adenosine release in mice, although the low dose did significantly decrease transient frequency and transient concentration whereas the high dose of CBX decreased transient frequency while having no effect on the concentration. If adenosine release was primarily controlled by other gap junction proteins, more dramatic effects would have been expected for higher doses, but more effects were not observed with the high dose. Carbenoxolone is widely considered to be a "dirty" drug because it acts at many different receptors and proteins.[64] For instance, CBX inhibits NMDA receptors and NMDA receptor antagonism has been shown to increase the frequency and concentration of spontaneous adenosine transients.[65] This NMDA effect could explain the decreases in frequency and concentration with 10 µM CBX, but why with the higher concentration 100 µM CBX appeared to recover the concentration. Thus, these data do not suggest that other gap junction proteins are having dramatic effects on adenosine transients, but more specific tests of other hemichannel proteins are likely still warranted.

4.4.4 Other possible mechanisms of adenosine release.

Our work has ruled out activity-dependent exocytosis and PANX1 channels as the main mechanisms of release for spontaneous adenosine transients but there are other possible mechanisms remaining: concentrative nucleoside transporters, other hemichannels including PANX2 and connexins, and spontaneous, action potential-independent exocytosis. Previous work has already demonstrated that equilibrative nucleoside transporters (ENTs) are not responsible for the release of adenosine, but do play a role in reuptake of adenosine.[24] There has been no work on the role of concentrative nucleoside transporters (CNTs) on spontaneous, transient adenosine release. This is largely because there are no potent specific inhibitors of the purine specific transporters CNT2 or CNT3, although phloridzin is a moderate non-specific CNT inhibitor.[66] However, active transport is a slower process than exocytosis or diffusion through hemichannels, so CNTs are a less likely candidate to fit the time frame of adenosine transients as well as the either two methods. It is still a viable route of transient release, but the lack of pharmacological agents to study CNTs well also make spontaneous exocytosis or other hemichannels more approachable hypotheses to investigate.

PANX1 is the most heavily studied pannexin channel, but PANX2 is specific to the central nervous system and could therefore be specially designed to release adenosine for the purposes of neuromodulation or neuroprotection.[23,34,35,67] Additionally, ischemia research has demonstrated that a double knockout of PANX1 and PANX2 is necessary to

observe any significant impact on the infarct volume of an ischemic insult.[68] Thus, the channels may be working together. Measuring spontaneous adenosine in the PANX1/2 double KO would effectively show if knocking out both channels has any effect on spontaneous adenosine. Alternatively, when they are not involved in the creation of a gap junction, connexin channels can also release ATP directly into the extracellular space.[8–10] Whereas carbenoxolone can inhibit each of these channels, the promiscuity of the drug would make it prudent to investigate more specific pharmacological experiments or genetic knockouts of the specific channels. The Dale group found that connexins can be activated by decreasing extracellular Ca^{2+} or increasing arterial CO_2 levels and this process can be reversed with the inhibitors 5-nitro-2-(3-phenylpropylamino)benzoic acid (NPPB) or proadifen.[69] Employing either of these inhibitors could help elucidate the role of connexins in transient adenosine release.

Another possible mechanism of transient adenosine release is exocytotic release that is not activity dependent. Glutamate can be spontaneously released on a very short time scale in events known as mini excitatory postsynaptic potentials (mEPSPs).[70] These events are spontaneous and occur with a frequency of one or two events per minute per release site, which is similar to the frequency of adenosine transients.[21,22,71] Because they are not activity dependent, the technique used to study mEPSPs includes the application of TTX so as to exclude any interference from processes that are activity dependent.[72] Additionally, glutamate and ATP are known to be co-released via vesicles

in this manner.[27,73] mEPSPs are commonly attenuated by Ca^{2+} chelation with BAPTA or EGTA and they are mediated by both AMPA receptors and NMDA receptors.[74,75] Since ATP can be co-packaged in vesicles with GABA, we could also test the role of miniature inhibitory postsynaptic potentials (mIPSPs) which are similar to mEPSPs except GABA is released to cause inhibition of neurotransmission.[43] mIPSPs can be inhibited with methionine-enkephalin.[76] The frequency of spontaneous adenosine release matches well with the known frequency of these spontaneous mEPSPs measured with electrophysiology, so it should be the next mechanism tested. Future electrophysiology experiments that accompany adenosine measurements might truly pinpoint the cells that are releasing adenosine.

4.5 Conclusions:

This study examined 2 possible mechanisms of adenosine release: activity dependent exocytosis and PANX1 channels. The results indicate that spontaneous, transient adenosine is not activity dependent, as release was largely maintained during application of TTX. There was a slight decrease in the frequency of adenosine events with TTX, but it is likely due to a downstream effect of another neurotransmitter that is TTX sensitive, like glutamate. The evidence also demonstrates that PANX1 is not the main mechanism of transient adenosine release either as there was little to no decrease in the frequency or concentration of adenosine transients with PANX1 inhibition, especially in mice, or with PANX1 KO mice. Other processes still need to be investigated

including spontaneous glutamate and GABA release, which could co-release ATP, as well as PANX2 and connexin channels due to a small effect from the nonspecific hemichannel inhibitor, CBX.

4.6 References:

(1) Wall, M.; Dale, N. *Curr. Neuropharmacol.* **2008**, *6* (4), 329–337.

(2) Nedden, S. Zur; Doney, A. S.; Frenguelli, B. G. *J. Neurochem.* **2014**, *128* (1), 111–124.

(3) Wall, M. J.; Dale, N. *J. Physiol.* **2013**, *591* (Pt 16), 3853–3871.

(4) Mitchell, J. B.; Lupica, C. R.; Dunwiddie, T. V. *J. Neurosci.* **1993**, *13* (8), 3439–3447.

(5) Schubert, P.; Lee, K.; West, M.; Deadwyler, S.; Lynch, G. *Nature* **1976**, *260* (5551), 541–542.

(6) White, T. D.; MacDonald, W. F. *Ann. N. Y. Acad. Sci.* **1990**, *603* (1), 287-98-9.

(7) Dale, N. *Islets* **2012**, *4* (1), 64–70.

(8) Nualart-Marti, A.; Del Molino, E. M.; Grandes, X.; Bahima, L.; Martin-Satué, M.; Puchal, R.; Fasciani, I.; González-Nieto, D.; Ziganshin, B.; Llobet, A.; Barrio, L. C.; Solsona, C. *Glia* **2013**, *61* (12), 1976–1989.

(9) Kang, J.; Kang, N.; Lovatt, D.; Torres, A.; Zhao, Z.; Lin, J.; Nedergaard, M. *J. Neurosci.* **2008**, *28* (18), 4702–4711.

(10) Schock, S. C.; LeBlanc, D.; Hakim, A. M.; Thompson, C. S. *Biochem. Biophys. Res. Commun.* **2008**, *368* (1), 138–144.

(11) Ransford, G. A.; Fregien, N.; Qiu, F.; Dahl, G.; Conner, G. E.; Salathe, M. *Am. J. Respir. Cell Mol. Biol.* **2009**, *41* (5), 525–534.

(12) Bao, L.; Locovei, S.; Dahl, G. *FEBS Lett.* **2004**, *572* (1–3), 65–68.

(13) Lopatář, J.; Dale, N.; Frenguelli, B. G. *Neuropharmacology* **2015**, *93*, 219–228.

(14) Augusto, E.; Matos, M.; Sévigny, J.; El-Tayeb, A.; Bynoe, M. S.; Müller, C. E.; Cunha, R. a; Chen, J.-F. *J. Neurosci.* **2013**, *33* (28), 11390–11399.

(15) Street, S. E.; Walsh, P. L.; Sowa, N. A.; Taylor-Blake, B.; Guillot, T. S.; Vihko, P.; Wightman, R. M.; Zylka, M. J. *Mol. Pain* **2011**, *7* (27), 80.

(16) Pajski, M. L.; Venton, B. J. *ACS Chem. Neurosci.* **2010**, *1* (12), 775–787.

(17) Ross, A. E.; Nguyen, M. D.; Privman, E.; Venton, B. J. *J. Neurochem.* **2014**, *130* (1), 50–60.

(18) Pedata, F.; Latini, S.; Pugliese, A. M.; Pepeu, G. *J. Neurochem.* **1993**, *61* (1), 284–289.

(19) Chu, S.; Xiong, W.; Zhang, D. L.; Soylu, H.; Sun, C.; Albensi, B. C.; Parkinson, F. E. *Acta Pharmacol. Sin.* **2013**, *34* (1), 60–66.

(20) Martín, E. D.; Fernández, M.; Perea, G.; Pascual, O.; Haydon, P. G.; Araque, A.; Ceña, V. *Glia* **2007**, *55* (1), 36–45.

(21) Nguyen, M. D.; Lee, S. T.; Ross, A. E.; Ryals, M.; Choudhry, V. I.; Venton, B. J. *PLoS One* **2014**, *9* (1), e87165.

(22) Lee, S. T.; Venton, B. J. *ACS Chem. Neurosci.* **2017**, acschemneuro.7b00280.

(23) Wang, Y.; Venton, B. J. *J. Neurochem.* **2017**, *140* (1), 13–23.

(24) Nguyen, M. D.; Ross, A. E.; Ryals, M.; Lee, S. T.; Venton, B. J. *Pharmacol. Res. Perspect.* **2015**, *3* (6), e00189.

(25) Dunwiddie, T. V; Masino, S. A. *Annu. Rev. Neurosci.* **2001**, *24* (1), 31–55.

(26) Fader, C. M.; Aguilera, M. O.; Colombo, M. I. *Autophagy* **2012**, *8* (12), 1741–1756.

(27) Pankratov, Y.; Lalo, U.; Verkhratsky, A.; North, R. A. *Pflugers Archiv European Journal of Physiology*. 2006, pp 589–597.

(28) Falchi, A. M.; Sogos, V.; Saba, F.; Piras, M.; Congiu, T.; Piludu, M. *Histochem. Cell Biol.* **2013**, *139* (2), 221–231.

(29) Klyuch, B. P.; Dale, N.; Wall, M. J. *J. Neurosci.* **2012**, *32* (11), 3842–3847.

(30) John, C.; Jones, S. In *Electrochemical Methods for Neuroscience*; 2007; pp 1–13.

(31) Heinrich, A.; Andõ, R. D.; Túri, G.; Rõzsa, B.; Sperlágh, B. *British Journal of Pharmacology*. 2012, pp 1003–1020.

(32) Kim, Y.; Davidson, J. O.; Green, C. R.; Nicholson, L. F. B.; O'Carroll, S. J.; Zhang, J. *Biochimica et Biophysica Acta - Biomembranes*. 2018, pp 224–236.

(33) Lohman, A. W.; Isakson, B. E. *FEBS Lett.* **2014**, *588* (8), 1379–1388.

(34) Bruzzone, R.; Hormuzdi, S. G.; Barbe, M. T.; Herb, A.; Monyer, H. *Proc. Natl. Acad.*

Sci. **2003**, *100* (23), 13644–13649.

(35) Wicki-Stordeur, L. E.; Boyce, A. K. J.; Swayne, L. A. *Cell Commun. Adhes.* **2013**, *20* (3–4), 73–79.

(36) Nakamura, T.; Tu, S.; Akhtar, M. W.; Sunico, C. R.; Okamoto, S. ichi; Lipton, S. A. *Neuron*. 2013, pp 596–614.

(37) Chiu, Y.-H.; Jin, X.; Medina, C. B.; Leonhardt, S. A.; Kiessling, V.; Bennett, B. C.; Shu, S.; Tamm, L. K.; Yeager, M.; Ravichandran, K. S.; Bayliss, D. A. *Nat. Commun.* **2017**, *8*, 14324.

(38) Billaud, M.; Lohman, A. W.; Straub, A. C.; Looft-Wilson, R.; Johnstone, S. R.; Araj, C. A.; Best, A. K.; Chekeni, F. B.; Ravichandran, K. S.; Penuela, S.; Laird, D. W.; Isakson, B. E. *Circ. Res.* **2011**, *109* (1), 80–85.

(39) Lloyd, H. G. E.; Lindström, K.; Fredholm, B. B. *Neurochem. Int.* **1993**, *23* (2), 173–185.

(40) Pérez-Pinźon, M. A.; Mumford, P. L.; Rosenthal, M.; Sick, T. J. *Neuroscience* **1996**, *75* (3), 687–694.

(41) Frenguelli, B. G.; Wigmore, G.; Llaudet, E.; Dale, N. *J. Neurochem.* **2007**, *101* (5), 1400–1413.

(42) Good, M. E.; Chiu, Y.-H.; Poon, I. K.; Medina, C. B.; Butcher, J. T.; Mendu, S. K.; DeLalio, L. J.; Lohman, A. W.; Leitinger, N.; Barrett, E. J.; Lorenz, U. M.; Desai, B. N.; Jaffe, I. Z.; Bayliss, D.; Isakson, B. E.; Ravichandran, K. S. *Circ. Res.* **2017**, CIRCRESAHA.117.312380.

(43) Jo, Y. H.; Schlichter, R. *Nat. Neurosci.* **1999**, *2* (3), 241–245.

(44) Poon, I. K. H.; Chiu, Y. H.; Armstrong, A. J.; Kinchen, J. M.; Juncadella, I. J.; Bayliss, D. A.; Ravichandran, K. S. *Nature* **2014**, *507* (7492), 329–334.

(45) Pelegrin, P.; Surprenant, A. *EMBO J.* **2006**, *25* (21), 5071–5082.

(46) Swamy, B. E. K.; Venton, B. J. *Analyst* **2007**, *132* (9), 876–884.

(47) Borman, R. P.; Wang, Y.; Nguyen, M. D.; Ganesana, M.; Lee, S. T.; Venton, B. J. *ACS Chem. Neurosci.* **2016**, acschemneuro.6b00262.

(48) Rouach, N.; Segal, M.; Koulakoff, A.; Giaume, C.; Avignone, E. *J. Physiol.* **2003**, *553* (3), 729–745.

(49) Vessey, J. P.; Lalonde, M. R.; Mizan, H. A.; Welch, N. C.; Kelly, M. E. M.; Barnes, S. *J.*

Neurophysiol. **2004**, *92* (2), 1252–1256.

(50) Tovar, K. R.; Maher, B. J.; Westbrook, G. L. *J. Neurophysiol.* **2009**, *102* (2), 974–978.

(51) Bruzzone, R.; Barbe, M. T.; Jakob, N. J.; Monyer, H. *J. Neurochem.* **2005**, *92* (5), 1033–1043.

(52) Silverman, W.; Locovei, S.; Dahl, G. *AJP Cell Physiol.* **2008**, *295* (3), C761–C767.

(53) Jin, S.; Johansson, B.; Fredholm, B. B. *J. Pharmacol. Exp. Ther.* **1993**, *267* (2), 801–808.

(54) Pajski, M. L.; Venton, B. J. *Purinergic Signal.* **2013**, *9* (2), 167–174.

(55) Sims, R. E.; Dale, N. *PLoS One* **2014**, *9* (1).

(56) Locovei, S.; Wang, J.; Dahl, G. *FEBS Lett.* **2006**, *580* (1), 239–244.

(57) Silverman, W. R.; de Rivero Vaccari, J. P.; Locovei, S.; Qiu, F.; Carlsson, S. K.; Scemes, E.; Keane, R. W.; Dahl, G. *J. Biol. Chem.* **2009**, *284* (27), 18143–18151.

(58) Chekeni, F. B.; Elliott, M. R.; Sandilos, J. K.; Walk, S. F.; Kinchen, J. M.; Lazarowski, E. R.; Armstrong, A. J.; Penuela, S.; Laird, D. W.; Salvesen, G. S.; Isakson, B. E.; Bayliss, D. A.; Ravichandran, K. S. *Nature* **2010**, *467* (7317), 863–867.

(59) Cone, A. C.; Ambrosi, C.; Scemes, E.; Martone, M. E.; Sosinsky, G. E. *Front. Pharmacol.* **2013**, *4 FEB*.

(60) Billaud, M.; Chiu, Y. H.; Lohman, A. W.; Parpaite, T.; Butcher, J. T.; Mutchler, S. M.; DeLalio, L. J.; Artamonov, M. V.; Sandilos, J. K.; Best, A. K.; Somlyo, A. V.; Thompson, R. J.; Le, T. H.; Ravichandran, K. S.; Bayliss, D. A.; Isakson, B. E. *Sci. Signal.* **2015**, *8* (364).

(61) Bargiotas, P.; Krenz, A.; Monyer, H.; Schwaninger, M. *Channels* **2012**, *6* (6), 453–456.

(62) Baranova, A.; Ivanov, D.; Petrash, N.; Pestova, A.; Skoblov, M.; Kelmanson, I.; Shagin, D.; Nazarenko, S.; Geraymovych, E.; Litvin, O.; Tiunova, A.; Born, T. L.; Usman, N.; Staroverov, D.; Lukyanov, S.; Panchin, Y. *Genomics* **2004**, *83* (4), 706–716.

(63) Vogt, A.; Hormuzdi, S. G.; Monyer, H. *Mol. Brain Res.* **2005**, *141* (1), 113–120.

(64) Juszczak, G. R.; Swiergiel, A. H. *Progress in Neuro-Psychopharmacology and Biological Psychiatry*. 2009, pp 181–198.

(65) Nguyen, M. D.; Wang, Y.; Ganesana, M.; Venton, B. J. *ACS Chem. Neurosci.* **2017**, *8* (2), 376–385.

(66) Gupte, A.; Buolamwini, J. K. *Bioorganic Med. Chem. Lett.* **2009**, *19* (3), 917–921.

(67) Ross, A. E.; Venton, B. J. *J. Neurochem.* **2015**, *132* (1), 51–60.

(68) Bargiotas, P.; Krenz, A.; Hormuzdi, S. G.; Ridder, D. A.; Herb, A.; Barakat, W.; Penuela, S.; von Engelhardt, J.; Monyer, H.; Schwaninger, M. *Proc. Natl. Acad. Sci.* **2011**, *108* (51), 20772–20777.

(69) Huckstepp, R. T. R.; IdBihi, R.; Eason, R.; Spyer, K. M.; Dicke, N.; Willecke, K.; Marina, N.; Gourine, A. V.; Dale, N. *J. Physiol.* **2010**, *588* (20), 3901–3920.

(70) Paré, D.; Lebel, E.; Lang, E. J. *J. Neurophysiol.* **1997**, *78* (3), 1735–1739.

(71) Sara, Y.; Virmani, T.; Deák, F.; Liu, X.; Kavalali, E. T. *Neuron* **2005**, *45* (4), 563–573.

(72) Atasoy, D.; Ertunc, M.; Moulder, K. L.; Blackwell, J.; Chung, C.; Su, J.; Kavalali, E. T. *J. Neurosci.* **2008**, *28* (40), 10151–10166.

(73) Lalo, U.; Verkhratsky, A.; Burnstock, G.; Pankratov, Y. *Wiley Interdisciplinary Reviews: Membrane Transport and Signaling*. 2012, pp 297–309.

(74) Renger, J. J.; Egles, C.; Liu, G. *Neuron* **2001**, *29* (2), 469–484.

(75) Cummings, D. D.; Wilcox, K. S.; Dichter, M. A. *J. Neurosci.* **1996**, *16* (17), 5312–5323.

(76) Vaughan, C. W.; Ingram, S. L.; Connor, M. A.; Christie, M. J. *Nature* **1997**, *390* (6660), 611–614.

Chapter 5

Conclusions and Future Directions

The great tragedy of Science: the slaying of a beautiful hypothesis by an ugly fact

- Thomas H. Huxley

Fast-scan cyclic voltammetry (FSCV) is a powerful analytical tool that has allowed us to discover and characterize a rapid form of adenosine signaling in the central nervous system. In this thesis, I have investigated the electrochemical behavior of histamine, an interfering analyte in adenosine detection. I have also used FSCV to observe differences in frequency, concentration, and duration of spontaneous, transient adenosine events in several brain regions and have found that neither activity dependent channels nor pannexin 1 channels are the primary mechanism of transient adenosine release. In this chapter, I will summarize my findings, discuss aspects of histamine oxidation and transient adenosine release that are still unknown, and describe how the field is progressing.

5.1 Histamine electrochemistry and waveform development

In Chapter 2, the oxidation mechanism for histamine at carbon electrodes was characterized using spectroscopic and amperometric techniques. Previous research had proposed two possible mechanisms for the oxidation of histamine. The first was an electropolymerization reaction via a one electron oxidation, creating a nitrogen radical on the imidazole, followed by dimerization and a subsequent one electron oxidation of the second imidazole nitrogen for elongation of the polymer.[1] The second scheme was a two electron oxidation forming a carbonyl between the imidazole nitrogens, similar to the secondary oxidation of adenosine.[2] Both of these schemes are based on literature that states that a high potential is required to oxidize imidazoles, greater than 1.0 V vs

Ag/AgCl but typically closer to 1.2 V.[3–6] However, recent research proposed that the oxidation could happen around 0.3 V vs Ag/AgCl.[7] Amperometry demonstrated that the histamine requires a potential of at least 1.0 V to oxidize as there was no current generated by histamine with 0.4 V or even 0.9 V. Whereas there was very faint current generated with 1.0 V and 1.1 V, the current reached a maximum with 1.2 V. However, unlike dopamine, the current did not plateau, but it fell off gradually toward baseline, suggesting a fouling of the electrode. This indicated a polymerization was likely occurring.

Spectroscopic determination of histamine and oxidized histamine with IR show no change to the structure of histamine at all with a bulk oxidation potential of 1.0 V or below. Using 1.3 V, there was a noticeable increase in the sp^2 hybridized C-H band. Since carbonyl formation should have made this peak diminish instead of increase, this provided more evidence for the electropolymerization mechanism as there should be no new IR active bonds formed by it. Additionally, ^{13}C NMR was performed on histamine and bulk oxidized histamine. The NMR showed no changes in the carbon shifts which again shows that carbonyl formation is not occurring.

The spectroscopic results indicated that histamine oxidation does not occur via carbonyl formation. However, they do not definitively confirm the structure of the electropolymerization product. However, there are other spectroscopic techniques that could detect the predicted structural changes. The best option for studying

polymerization would be mass spectrometry. If the polymerization is occurring, the M^+ peak should double, triple, or so forth based on how far the polymerization goes. Fragments from the mass spectrum should also give further support as to where the polymerization occurs. Additionally, if the oxidation of histamine is a completely separate mechanism from those described above, mass spectrometry will still give useful insight into the structural differences between histamine and the oxidation product.

The development of the sawtip waveform provided further evidence of the narrow gap between the oxidation potentials of adenosine and histamine. The sawhorse waveform optimization proved that the oxidation of histamine could happen at 1.25 V vs Ag/AgCl without adenosine generating much current. Therefore, using the sawtip waveform, histamine could oxidize at 1.25 V during a 0.75 ms hold at that potential. Completing the scan up to 1.45 V and back down would result in adenosine oxidizing at the usual potential of 1.35 V on the cathodic scan. Using the knowledge that this could separate the peaks of adenosine and histamine with the previous work that a 1.35 V sawhorse waveform could separate adenosine from H_2O_2, a hybrid of the two waveforms, the double-hold waveform, was created. This waveform could separate the signals of adenosine, histamine, and H_2O_2 and correctly identify which compounds were present in a mixture. It did consistently underestimate H_2O_2, attributing the corresponding current to slightly higher concentrations of adenosine and histamine.

Although, the predicted values for adenosine and histamine were not significantly different from what was actually in the samples.

Using an altered waveform in tissue proved difficult. The separation of the peaks by incorporating a hold at a very specific potential is useful but in tissue there are complications in the sample matrix including electrode fouling by proteins and an impedance problem. As such, neither the optimized sawtip waveform nor the double-hold waveform worked in tissue to differentiate adenosine and histamine. The histamine oxidation peak was shifted to higher potentials with a hold of 1.35 V, but at that potential, you could also oxidize adenosine, as it had not shifted as much. It is also possible that biological material fouling the electrode interferes with the ability of histamine to adsorb to the surface of the electrode. Further work needs to be done to cleanly separate the signals of adenosine and histamine in tissue, either by combatting the impedance problem or incorporating electrode modifications such as polymer coatings (e.g. Nafion) or carbon nanomaterials to counteract histamine fouling or facilitate the electron transfer rate of histamine oxidation.

Having a tool that can simultaneously measure adenosine and histamine in real-time would be a very powerful strategy for neurochemistry research. Adenosine and histamine are both neuromodulators and both play an immunological role in the brain and regulate sleep.[8–10] Additionally, ATP is known to be co-released with other neurotransmitters like glutamate, GABA, and norepinephrine, so it is possible that it is

co-released with adenosine as well.[11–13] Co-detection of adenosine and histamine with FSCV would allow researchers to investigate the rapid signaling of both analytes in tandem and their ability to modulate not only other neurotransmitters, but each other as well.[14,15]

5.2 Spontaneous transient adenosine in brain slices

In Chapter 3, I demonstrated that spontaneous, transient adenosine can be detected in rodent brain slices and compared differences in frequency, concentration, and duration of adenosine transients in 3 separate brain regions. *In vivo*, adenosine transients were characterized with regard to the frequency with which they occurred, their concentrations, and the duration of the transients. On average, adenosine transients occurred once every 2 minutes, had an average concentration of 180 nM, and lasted 2.6 seconds. That work also found that A_1 and A_{2A} receptors are responsible for the regulation of adenosine transients.[16] Additionally, *in vivo* experiments determined some of the clearance mechanisms of transient adenosine, the role of transient adenosine in neuroprotection, and factors regulating the release of transient adenosine.[17–19] Brain slice experiments can complement the *in vivo* work performed, because drugs that cannot pass the blood-brain barrier can be used on the tissue, as well as pharmacological agents that would normally be toxic to a living test subject.

Adenosine transients in brain slices occurred with similar frequency, concentration, and duration to transients found *in vivo*.[16] Transients occurred about

once a minute in prefrontal cortex (PFC) slices, had an average concentration of 160 nM, and lasted 3.5 seconds. In the thalamus, transients occurred much less frequently, only about once every 5 minutes and lasted twice as long as those found in the PFC. In the CA1 region of the hippocampus, adenosine transients had similar frequency to those found in the PFC but had an average concentration of 240 nM and a duration of 4.9 seconds. The differences in frequency, duration, and concentration show the modulation of adenosine differs between each region. Additionally, the higher average concentration of transients in the hippocampus could be related to the lower vascular density of that brain region. If adenosine transients play a role in modulating blood flow, adenosine transients in the hippocampus may have to be larger as they would have to diffuse further on average to bind with vesicular A_{2A} receptors.[18,20]

A_1 regulation of transient adenosine release, as probed with DPCPX, also differed by brain region. DPCPX increased the concentration of transients in the hippocampus and thalamus, but had no effect in the PFC. This is likely due to the fact that the cortex expresses lower levels of A_1 receptors than either the thalamus or the hippocampus.[21] These differences show that the selection of brain region is critical in investigating pharmacological impacts on spontaneous, transient adenosine. Drug effects vary in magnitude by brain region, which makes characterizing the pathways responsible for transient adenosine difficult.

In Chapter 4, I addressed the source of spontaneous, transient adenosine release in the hippocampus by investigating two likely release mechanisms, exocytosis and pannexin channels. Previous work has shown that rapid adenosine release via electrical and mechanical stimulation was in part due to activity dependent release due to a decrease in signal with TTX.[22,23] Additionally, ATP is widely known to co-release with other neurotransmitters, including GABA, norepinephrine, and acetylcholine and that process should have a time-course comparable to spontaneous, transient adenosine.[12,24,25] Perfusing 200 nM tetrodotoxin (TTX) over brain slices did not affect the mean concentration or duration of adenosine transients in the hippocampus, despite completely shutting down stimulated dopamine release in the caudate putamen. Although the difference was slight, the inter-event time distribution did significantly change, indicating that there is likely some downstream effect of a neurotransmitter that is activity dependent on transient adenosine. This could possibly be GABA as the effect appeared inhibitory and GABA has been shown to modulate transient adenosine release.[19] ATP could be co-released via vesicles with either GABA or glutamate during miniature inhibitory postsynaptic potentials (mIPSPs) or miniature excitatory postsynaptic potentials (mEPSPs) respectively. These are vesicular release events that are not activity dependent. mIPSPs can be blocked by perfusing 100 µM picrotoxin over the slices.[26] Both mEPSPs and mIPSPs can be blocked by perfusing a Ca^{2+} chelator such as BAPTA-AM (20 µM).[27] Either could co-release ATP as activation of glutamate receptors (specifically NMDA receptors) and $GABA_B$ receptors both increased the

amount of transient adenosine released.[19] Both pathways should be tested to investigate their involvement in spontaneous, transient adenosine release.

Pannexin channels are not the main mechanism of transient adenosine release. Inhibition of pannexin 1 (PANX1) channels in rat brain slices with 20 μM spironolactone showed a marked decrease in adenosine release. The average inter-event time tripled and the average concentration was almost cut in half. However, mouse slices showed no impact on adenosine transients with spironolactone nor did a PANX1 KO strain. A low concentration (10 μM) of a non-specific inhibitor of gap junction proteins, carbenoxolone (CBX), showed inhibition of adenosine transients. At the low concentration, CBX is fairly PANX1 specific.[28,29] At the higher concentration of 100 μM, CBX didn't significantly change the frequency, concentration, or duration of adenosine transients. This discrepancy suggests that some off-target of CBX could be affecting adenosine transients. But based on this evidence, PANX1 is not the primary mechanism of transient adenosine release. The carbenoxolone data suggest that blocking all gap junction channels does not cause an effect. However, other experiments should be performed with KO mice to confirm these findings. PANX2 could be compensating for PANX1, so a PANX2 KO and a PANX1/PANX2 double-KO would be necessary to confirm the role of pannexin channels in spontaneous, transient adenosine release. Previous work has shown that the double-KO of PANX1 and PANX2 resulted in smaller infarct volumes from ischemic insult than control mice or either individual pannexin KO.[30]

Alternatively, concentrative nucleoside transporters (CNTs) could be playing a role. However, there are no known knockout mice for any of the CNTs, nor are there any specific, high affinity inhibitors, making CNTs difficult to study. [31]

5.3 Future of the field

Spontaneous, transient adenosine has been characterized over the past 7 years and most of the research has been based on 4 questions: how is it formed, how is it regulated, what receptors is it acting on, and what are its functions? In this work, we've begun to address the formation of transient adenosine. However, the primary mechanism of release has not been determined and there are still several other mechanisms of release to test, including non-activity dependent exocytosis (mEPSPs and mIPSPs), PANX2 and connexin channels, and CNTs. Additionally, we still don't know what cell type adenosine transients are coming from. This will be easier to determine once the mechanism is determined because we could then design lox-cre mouse lines to knockout the genes responsible for transient adenosine function in specific cell types. Nguyen, et al, addressed the receptor activation by looking at several different clearance mechanisms and found that transient adenosine is cleared in part by metabolic pathways and reuptake equilibrative nucleoside transporters.[17] Outside of those mechanisms, the clearance is still too rapid to be dependent only on diffusion so there has to be another mode of clearance for transient adenosine. Nguyen also looked at receptor activation and found adenosine transients are self-regulating via A_1

receptors and are also regulated by NMDA receptors.[16,19] It is known that adenosine acts at A_1, A_{2A}, A_{2B}, and A_3 receptors to modulated neurotransmitters such as transient modulation of dopamine,[32] but it is still not clear to what degree transient adenosine is able to act at each of these receptors or if there are differences in susceptibility to transient adenosine neuromodulation between different neurotransmitters (e.g. dopaminergic vs serotonergic neurons). Ross and Wang each addressed the function of transient adenosine by demonstrating neuromodulatory and neuroprotective roles for transient adenosine, respectively.[18,32] However, the neuroprotective role only states a correlation between adenosine transients and oxygen transients.[18] A global A_{2A} knockout mouse would remove A_{2A} receptors, activation of which causes blood vessels to dilate. If adenosine transients persisted without the correlated oxygen events, that would confirm that transient adenosine events cause transient oxygen events.

Aside from determining the primary mechanisms of release and clearance, most of the spontaneous, transient adenosine research will be focused on understanding how transients behave under different neurological conditions, primarily ischemia. *In vivo*, there is ongoing research in our lab developing stroke models via bilateral common carotid artery occlusion and vertebral artery occlusion. Incorporating oxygen detection with FSCV can provide information on blood flow to different brain regions during ischemia and reperfusion.[18] Brain slice experiments can help complement the ischemia work performed *in vivo* by depriving the perfusion buffer of oxygen and/or glucose to

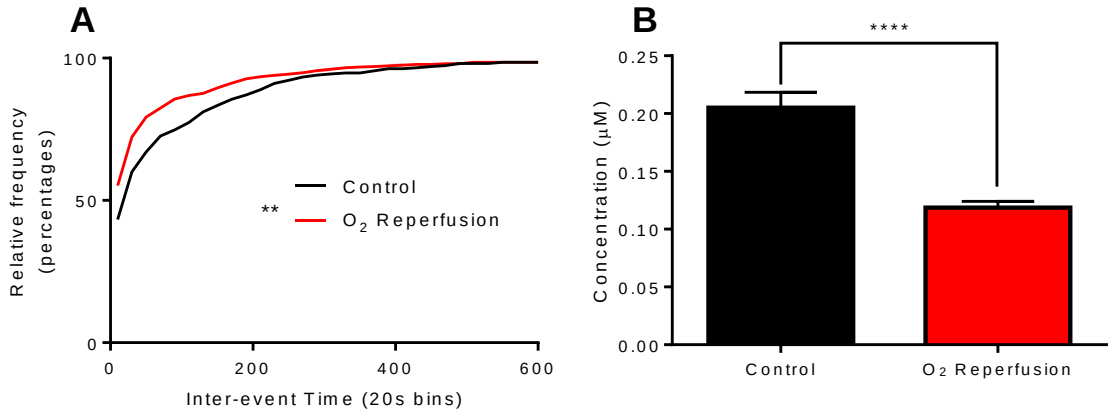

Figure 5.2: Adenosine transients in hippocampal slices during O_2 reperfusion. Reperfusion shows (**A**) a significant difference (KS test, p = 0.0063) in the inter-event time distribution when slices have been oxygen starved for 15 minutes followed by oxygen reperfusion. Frequency is higher in slices with O_2 reperfusion. (**B**) Additionally, the average concentration of adenosine transients decreases (t-test, p < 0.0001) from 205 ± 10 nM to 119 ± 5 nM during reperfusion. (n = 8 Errors are SEM)

simulate hypoxia or ischemia. Measuring adenosine transients during or after the ischemic insult to the slices can tell us how the tissue responds energy deprivation. Preliminary data (**Fig 5.1**) shows that after 30 minutes of oxygen deprivation, the concentration of adenosine transients decreased during reperfusion (t-test, p < 0.0001, n = 8 slices each), but the frequency increased (KS test, p = 0.006, n = 8 slices each).

A thorough investigation into how adenosine transients change during ischemic conditions will give us more information on the role of fast adenosine signaling. This includes measuring transients during hypoxia and during reperfusion as well as measuring transients during oxygen/glucose deprivation (OGD) to simulate ischemia.

Increases in transient adenosine would indicate that the hypoxia or ischemia is triggering pathways to recruit adenosine for its neuroprotective role. On the other hand, decreases in adenosine might indicate that transient adenosine pathway is impaired in these detrimental scenarios. Understanding the neuroprotective function of transient adenosine can give us insight into how different treatment options could help tissue survive ischemic circumstances such as a stroke.

5.4 Final Conclusions

In conclusion, electrochemical detection of spontaneous transient adenosine events has provided us with information about adenosine function in the brain on a more acute time scale. The release profile of spontaneous, transient adenosine varies by brain region, as does the magnitude to which transients self-regulate via A_1 receptors. Moreover, brain slices are a useful tool in the analysis of adenosine transients as its advantages can complement the advantages of research performed *in vivo*. While this work has ruled out activity dependence and PANX1 as the release mode of adenosine transients, the mechanism continues to elude us. We hypothesize that spontaneous adenosine is mostly likely occurring via vesicular release through mEPSPs or mIPSPs, but further work needs to be done to prove these pathways. Once the release mechanism is determined, the function of adenosine transients as a neuromodulator will be easier to investigate as we will understand what controls these events. A more thorough understanding of the function and pathways of transient adenosine will allow

researchers to investigate new therapeutic options that relate to adenosine, particularly in the realm of ischemia.

5.5 References:

(1) Wang, H. L.; O'Malley, R. M.; Fernandez, J. E. *Macromolecules* **1994**, *27* (4), 893–901.

(2) Swamy, B. E. K.; Venton, B. J. *Anal. Chem.* **2007**, *79* (2), 744–750.

(3) Dryhurst, G. *Electrochemistry of Biological Molecules*; 1977.

(4) Chang, S.-Y.; Jay, T.; Muñoz, J.; Kim, I.; Lee, K. H. *Analyst* **2012**, *137* (9), 2158.

(5) Hashemi, P.; Dankoski, E. C.; Wood, K. M.; Ambrose, R. E.; Wightman, R. M. *J. Neurochem.* **2011**, *118* (5), 749–759.

(6) Denno, M. E.; Privman, E.; Borman, R. P.; Wolin, D. C.; Venton, B. J. *ACS Chem. Neurosci.* **2016**, *7* (3), 407–414.

(7) Samaranayake, S.; Abdalla, A.; Robke, R.; Wood, K. M.; Zeqja, A.; Hashemi, P. *Analyst* **2015**, *140* (11), 3759–3765.

(8) Threlfell, S.; Cragg, S. J.; Kallo, I.; Turi, G. F.; Coen, C. W.; Greenfield, S. A. *J. Neurosci.* **2004**, *24* (40), 8704–8710.

(9) Haas, H. L.; Sergeeva, O. A.; Selbach, O. *Physiol. Rev.* **2008**, *88* (3), 1183–1241.

(10) Cunha, R. A. *Neurochem. Int.* **2001**, *38* (2), 107–125.

(11) Von Kügelgen, I.; Allgaier, C.; Schobert, A.; Starke, K. *Neuroscience* **1994**, *61* (2), 199–202.

(12) Pankratov, Y.; Lalo, U.; Verkhratsky, A.; North, R. A. *Pflugers Archiv European Journal of Physiology*. 2006, pp 589–597.

(13) Lalo, U.; Verkhratsky, A.; Burnstock, G.; Pankratov, Y. *Wiley Interdiscip. Rev. Membr. Transp. Signal.* **2012**, *1* (3), 297–309.

(14) Stanimirovic, D. B.; Bertrand, N.; Merkel, N.; Bembry, J.; Spatz, M. *Metab. Brain Dis.* **1994**, *9* (3), 275–289.

(15) Oishi, Y.; Huang, Z.-L.; Fredholm, B. B.; Urade, Y.; Hayaishi, O. *Proc. Natl. Acad. Sci.*

2008, *105* (50), 19992–19997.

(16) Nguyen, M. D.; Lee, S. T.; Ross, A. E.; Ryals, M.; Choudhry, V. I.; Venton, B. J. *PLoS One* **2014**, *9* (1), e87165.

(17) Nguyen, M. D.; Ross, A. E.; Ryals, M.; Lee, S. T.; Venton, B. J. *Pharmacol. Res. Perspect.* **2015**, *3* (6), e00189.

(18) Wang, Y.; Venton, B. J. *J. Neurochem.* **2017**, *140* (1), 13–23.

(19) Nguyen, M. D.; Wang, Y.; Ganesana, M.; Venton, B. J. *ACS Chem. Neurosci.* **2017**, *8* (2), 376–385.

(20) Coney, A. M.; Marshall, J. M. *J. Physiol.* **1998**, *509 (Pt 2* (2), 507–518.

(21) Goodman, R. R.; Snyder, S. H. *J. Neurosci.* **1982**, *2* (9), 1230–1241.

(22) Pajski, M. L.; Venton, B. J. *ACS Chem. Neurosci.* **2010**, *1* (12), 775–787.

(23) Ross, A. E.; Nguyen, M. D.; Privman, E.; Venton, B. J. *J. Neurochem.* **2014**, *130* (1), 50–60.

(24) Jo, Y. H.; Schlichter, R. *Nat. Neurosci.* **1999**, *2* (3), 241–245.

(25) Richardson, P. J.; Brown, S. J. *J. Neurochem.* **1987**, *48* (2), 622–630.

(26) Zhang, J.; Yang, Y.; Li, H.; Cao, J.; Xu, L. *Brain Res.* **2005**, *1050* (1–2), 110–117.

(27) Cummings, D. D.; Wilcox, K. S.; Dichter, M. A. *J. Neurosci.* **1996**, *16* (17), 5312–5323.

(28) Bruzzone, R.; Barbe, M. T.; Jakob, N. J.; Monyer, H. *J. Neurochem.* **2005**, *92* (5), 1033–1043.

(29) Silverman, W.; Locovei, S.; Dahl, G. *AJP Cell Physiol.* **2008**, *295* (3), C761–C767.

(30) Bargiotas, P.; Krenz, A.; Hormuzdi, S. G.; Ridder, D. A.; Herb, A.; Barakat, W.; Penuela, S.; von Engelhardt, J.; Monyer, H.; Schwaninger, M. *Proc. Natl. Acad. Sci.* **2011**, *108* (51), 20772–20777.

(31) Gupte, A.; Buolamwini, J. K. *Bioorganic Med. Chem. Lett.* **2009**, *19* (3), 917–921.

(32) Ross, A. E.; Venton, B. J. *J. Neurochem.* **2015**, *132* (1), 51–60.